nature genetics

Bridging high-throughput genetic and transcriptional data reveals cellular responses to alpha-synuclein toxicity

Esti Yeger-Lotem[1,2,8], Laura Riva[1,8], Linhui Julie Su[2], Aaron D Gitler[2,7], Anil G Cashikar[2,7], Oliver D King[2,7], Pavan K Auluck[2,3], Melissa L Geddie[2], Julie S Valastyan[2,4], David R Karger[5], Susan Lindquist[2,6] & Ernest Fraenkel[1,5]

Cells respond to stimuli by changes in various processes, including signaling pathways and gene expression. Efforts to identify components of these responses increasingly depend on mRNA profiling and genetic library screens. By comparing the results of these two assays across various stimuli, we found that genetic screens tend to identify response regulators, whereas mRNA profiling frequently detects metabolic responses. We developed an integrative approach that bridges the gap between these data using known molecular interactions, thus highlighting major response pathways. We used this approach to reveal cellular pathways responding to the toxicity of alpha-synuclein, a protein implicated in several neurodegenerative disorders including Parkinson's disease. For this we screened an established yeast model to identify genes that when overexpressed alter alpha-synuclein toxicity. Bridging these data and data from mRNA profiling provided functional explanations for many of these genes and identified previously unknown relations between alpha-synuclein toxicity and basic cellular pathways.

The cellular response to perturbations including environmental changes, toxins and mutations is typically complex and comprises signaling and metabolic changes, as well as changes in gene expression. Revealing the molecular mechanisms underlying cellular response to a specific perturbation may determine the nature of the perturbation, thus illuminating disease mechanisms[1] or a drug's mode of action[2,3], and identify points of intervention with potential therapeutic value[4].

High-throughput experimental techniques are commonly used for finding components of these response pathways because they provide a genome- and proteome-wide view of molecular changes. mRNA profiling experiments rapidly identify genes that are differentially expressed following stimuli. Genetic screening, including deletion, overexpression and RNAi library screens, identify genetic 'hits', genes whose individual manipulation alters the phenotype of stimulated cells. However, each technique has obvious limitations for identifying the full nature of cellular responses. mRNA profiling experiments do not target the series of events that led to the differential expression. Genetic screens provide strong evidence that a gene is functionally related to the response process, but this relationship is often indirect and hard to decipher, especially in high-throughput experiments that typically result in scores of relevant genes with various functions.

It has been noted previously in a few specific instances[2,5–9] that genetic screens do not identify the same genes as mRNA assays conducted in the same conditions. Here we show that this discrepancy is, in fact, a general rule. Furthermore, we find a marked bias in each technique. We bridge this gap between the two forms of high-throughput data by using an algorithm that exploits molecular interactions data to reveal the functional context of genetic hits and additional proteins that participate in the response but that were not detected by either the genetic or the mRNA profiling assays themselves.

We applied the algorithm to identify cellular responses to increased expression of alpha-synuclein, a small human protein implicated in Parkinson's disease whose native function and role in the etiology of the disease remain unclear[10]. We screened an established yeast model for alpha-synuclein toxicity[11,12] using an additional set of 3,500 overexpression yeast strains, exposing the multifaceted toxicity of alpha-synuclein. Application of our approach to the genetic hits from the screen and to transcriptional data of the yeast model provides the first cellular map of the proteins and genes responding to alpha-synuclein expression.

[1]Department of Biological Engineering, Massachusetts Institute of Technology, Cambridge, Massachusetts 02139, USA. [2]Whitehead Institute for Biomedical Research, Cambridge, Massachusetts 02142, USA. [3]Departments of Pathology and Neurology, Massachusetts General Hospital, Boston, Massachusetts 02114, and Harvard Medical School, Boston, Massachusetts 02115, USA. [4]Department of Biology, Massachusetts Institute of Technology, Cambridge, Massachusetts 02139, USA. [5]Computer Science and Artificial Intelligence Laboratory, Massachusetts Institute of Technology, Cambridge, Massachusetts 02139, USA. [6]Howard Hughes Medical Institute, Department of Biology, Massachusetts Institute of Technology, Cambridge, Massachusetts 02139, USA. [7]Present addresses: Department of Cell and Developmental Biology, The University of Pennsylvania, Philadelphia, Pennsylvania, USA (A.D.G.), Medical College of Georgia, Augusta, Georgia, USA (A.G.C.) and Boston Biomedical Research Institute, Watertown, Massachusetts, USA (O.D.K.). [8]These authors contributed equally to this work. Correspondence should be addressed to S.L. (lindquist_admin@wi.mit.edu) or E.F. (fraenkel-admin@mit.edu).

Received 7 August 2008; accepted 27 January 2009; published online 22 February 2009; doi:10.1038/ng.337

Table 1 Measured responses to cellular perturbations

Perturbation[a]	Number of differentially expressed genes[b]	Number of genetic hits[c]	Overlap	*P* value
Growth arrest (HU)	59	86	0	1
DNA damage (MMS)	198	1,448	43	0.81
ER stress (tunicamycin)	200	127	5	0.42
Fatty acid metabolism (oleate)	269	103	9	0.041
ATP synthesis block (arsenic)	828	50	9	0.25
Protein biosynthesis (cycloheximide)	20	164	0	1
Gene inactivation, screen complete (24 data sets)[d]	27	130	0	1
Gene inactivation, screen incomplete (149 data sets)[d]	24	12	0	1

[a]See **Supplementary Table 1a** for data sources. [b]Differentially expressed genes were defined as those showing at least a twofold change in expression following the perturbation or as defined in the original papers. [c]Number of genes whose genetic manipulation affects the phenotype of perturbed cells as defined in the original papers. [d]Median results are shown.

RESULTS

Comparing genetic hits and differentially expressed genes

We analyzed published mRNA profiles and genetic hits for 179 distinct perturbations in yeast (Methods). The perturbations included chemical and genetic insults affecting a multitude of cellular processes. Thirty of the genetic screens are complete, typically identifying >100 genetic hits. In almost all cases the overlap was small and statistically insignificant (**Table 1** and **Supplementary Table 1a** online).

We used Gene Ontology (GO) enrichment analysis to check whether each assay may be biased toward distinct aspects of cellular responses (**Supplementary Table 1b** and **Supplementary Fig. 1a** online). The combined genetic hits from all 179 genetic screens were highly enriched for several annotations, among the most frequent of which were biological regulation (23.3%, $P < 10^{-82}$), including transcription (14%, $P < 10^{-44}$) and signal transduction (6.3%, $P < 10^{-31}$). In contrast, the differentially expressed genes from all perturbations were enriched mostly for various metabolic processes (for example, organic acid metabolic process 7.1%, $P < 10^{-18}$) and oxidoreductase activities (7.2%, $P < 10^{-34}$). We observed the same enrichment trends upon focusing only on the 30 perturbations for which complete data were available when analyzed individually or when combined (**Supplementary Tables 1 c,d** and **Supplementary Note** online). Thus, we find that genetic assays tend to probe the regulation of cellular responses, whereas mRNA profiling assays tend to probe the metabolic aspects of cellular responses.

The differences in annotation between genetic hits and differentially expressed genes imply that each gene set alone often provides a limited and biased view of cellular responses. This hypothesis was confirmed in pathways that were well-studied by more classical methods. In the yeast DNA-damage response pathway, for example, a genetic screen[4] detected proteins that sense DNA damage (Mec3, Ddc1, Rad17 and Rad24), whereas mRNA profiling detected repair enzymes such as Rnr4 (ref. 13). Yet core components that had been uncovered by intense investigations over many years, such as the signal transducers Mec1 and Rad53 and the transcription factor Rfx1, remained undetected by either high-throughput assay.

To fully reap the benefits of applying high-throughput methods to new problems and underexplored biological processes, it is essential to find new routes to connect these data and obtain a true picture of the regulation of cellular responses. Judging from characterized pathways such as the DNA-damage response discussed above, we expect that some of the genetic hits, which are enriched for response regulators, will be connected via regulatory pathways to the differentially expressed genes, which are the output of such pathways, via components of the response that are missing from the experimental data (**Fig. 1**).

ResponseNet algorithm for identifying response networks

We devised the ResponseNet algorithm to identify molecular interaction paths connecting genetic hits and differentially expressed genes, including components of the response that are otherwise hidden (**Fig. 1**). The yeast *Saccharomyces cerevisiae* provides a powerful model system for such analysis owing to the extensive molecular interactions data now available (Methods and **Supplementary Table 2a** online). We assembled an integrated network model of the yeast interactome that contains protein–protein interactions, metabolic relations and protein–DNA interactions detected by various methods with different levels of reliability[14]. The resulting interactome relates 5,622 interacting proteins and 5,510 regulated genes, which are represented by network nodes, via 57,955 molecular interactions, which are represented by network edges.

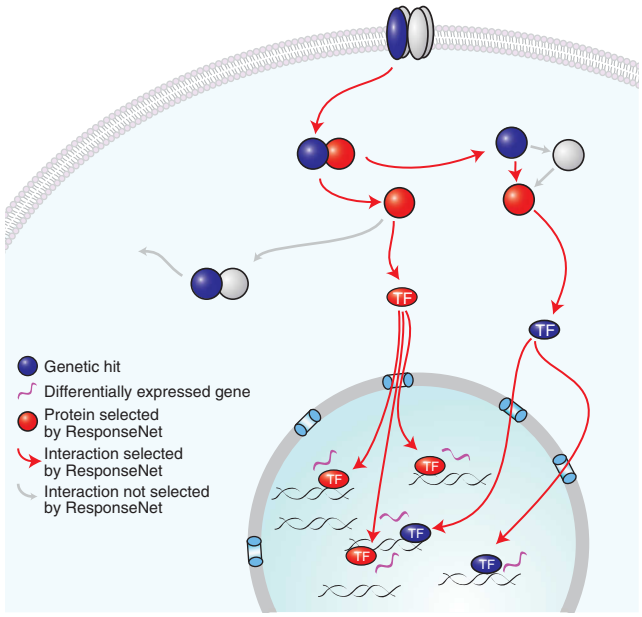

Figure 1 Regulatory relationships between genetic and transcriptional data. Cellular response is depicted through a general signaling pathway, including receptor binding, transcription factor (TF) translocation into the nucleus and gene expression. Genetic screens and mRNA profiling identify only some of these molecular components and often do not identify the same genes, as shown. We find that the proteins products of genes identified in genetic screens (colored blue) tend to be molecules with regulatory roles. We therefore hypothesize that they may directly or indirectly contribute to the regulation of the observed change in gene expression (colored magenta). ResponseNet identifies the likely regulatory pathways and predicts proteins that are part of these pathways even if they are not identified in either screen (colored red).

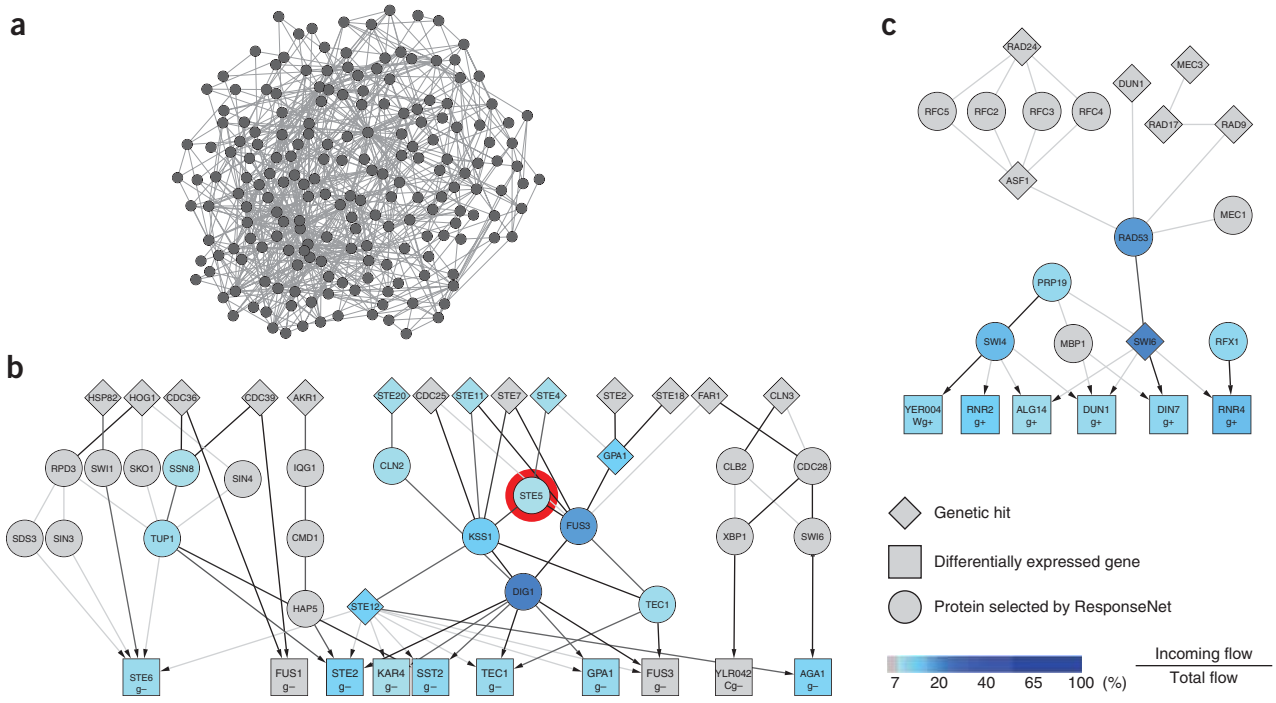

Figure 2 Interactome subnetworks connecting genetic and transcriptional data. (**a**) A network connecting genetic and transcriptional[19] data of *STE5* deletion strain via paths with length of three edges or fewer finds 193 nodes and 778 edges. (**b**) The network created by ResponseNet connects the genetic and transcriptional[19] data of *STE5* deletion strain via 23 intermediary nodes and 96 edges. Higher ranked nodes, as determined by ResponseNet, appear in darker shades of blue and include core components of the pheromone response pathway. Ste5 itself, marked by a red circle, is ranked ninth among the top predicted proteins. (**c**) The highly ranked part of the network created by ResponseNet upon connecting genetic hits[4,20] to DNA-damage signature genes[21] identified in yeast treated with the DNA-damaging agent methyl methanesulfonate (MMS). The highest ranking intermediate nodes predicted by ResponseNet include core components of the DNA-damage–response pathway. The complete network appears in **Supplementary Figure 4** online. Each node represents either a protein or a gene, and edges represent protein–protein, metabolic and protein–DNA interactions. The darkness of an edge increases with the amount of flow it carries. Differentially expressed genes are labeled with a suffix of g+ for upregulation and g– for downregulation. Networks were visualized using Cytoscape.

Our interactome representation has two important features that facilitate identification of pathways relating genetic hits to transcriptional changes. First, we highlighted the transcriptional regulatory role of proteins by representing differentially expressed genes and their protein products as separate gene and protein nodes, respectively. The only connection between protein and gene nodes is through edges representing observed protein–DNA interactions between transcriptional regulators and their target genes. Edges between two protein nodes represent other interaction types. Consequently, pathways connecting genetic hits to differentially expressed genes must pass through transcriptional regulators (**Supplementary Fig. 1b**). Second, because interactions vary in their reliability, each edge was given a weight that represents the probability that the connected nodes interact in a response pathway. Probabilities were computed using a Bayesian method that considers the experimental evidence supporting an interaction, and that favors interactions among proteins acting in a common cellular response pathway (Methods and **Supplementary Table 2b**).

Because of the vast number of edges, a search for all interaction paths connecting the genetic hits to the differentially expressed genes typically results in 'hairball' networks that are very hard to interpret (**Fig. 2a**). Pioneering approaches that searched an interactome for high-probability paths had to limit the output path lengths to three edges for computational complexity issues[15,16]. We aimed for a solution that would (i) pick the subset of genetic hits most likely to modulate the differentially expressed genes without limiting it a priori to known regulatory genes, (ii) identify and rank intermediary proteins that are likely to be part of response pathways but escaped detection by high-throughput methods and (iii) give preference to proteins that lie on high-probability paths connecting the genetic hits to the differentially expressed genes without imposing constraints on the network topology.

These requirements were met with a 'flow algorithm', a computational method used previously to analyze known signaling or metabolic pathways (for example, see ref. 17). Basically, flow goes from a source node to a sink node through the graph edges; edges are associated with a capacity that limits the flow and with a cost. (As a loose analogy, this resembles water finding the path of least resistance through a complex landscape.) To identify response pathways we required that flow pass from genetic hits through interactome edges to differentially expressed genes (**Supplementary Fig. 1b**). We then formulated our goal as a minimum-cost flow optimization problem[18]: Cost was defined as the negative log of the probability of an edge. Hence, minimizing the cost gives preference to high-probability paths (Methods).

The solution to the optimization problem is a relatively sparse network connecting many of the genetic hits to many of the differentially expressed genes through known interactions and intermediary proteins (**Fig. 2b**). Although these intermediary proteins escaped detection by either high-throughput genetic analysis or mRNA profiling, they are predicted by the algorithm to participate in the response. All proteins in the solution are ranked by the amount of flow they

Table 2 Yeast genes that modify α-syn toxicity when overexpressed

Gene class	α-syn toxicity suppressors	α-syn toxicity enhancers
Amino acid transport	*Avt4, Dip5, Lst8*	
Autophagy	*Nvj1*	
Cytoskeleton	*Icy1, Icy2*	
Manganese transport	*Ccc1*	*Pmr1*
Protein phosphorylation	*Cdc5, Gip2, Ime2, Ptp2, Ptc4, Rck1, Yck3*	*Cax4, Ppz1, Ppz2, Sit4*
Transcription or translation	*Cup9, Fzf1, Hap4, Jsn1, Mga2, Stb3, Tif4632, Vhr1*	*MATALPHA1, Mks1, Sut2*
Trehalose biosynthesis	*Nth1, Tps3, Ugp1*	
Ubiquitin-related	*Cdc4, Hrd1, Uip5*	*Ubp7, Ubp11*
Vesicular transport, ER-Golgi	*Bre5, Erv29, Sec21, Sec28, Sft1, Ubp3, Ykt6, Ypt1*	*Bet4, Glo3, Gos1, Gyp8, Sec31, Sly41, Trs120, Yip3*
Other cellular processes	*Isn1, Mum2, Osh2, Osh3, Pde2, Pho80, Pfs1, Qdr3*	*Eps1, Ids2, Izh3, Tpo4*
Unknown function	*YBR030W, YDL121C, YDR374C, YKL063C, YKL088W, YML081W, YML083C, YMR111C, YNR014W, YOR129C, YOR291W (Ypk9)*	

carry. The more flow that passes through a protein, the more important it is in connecting the input sets.

Validation of the ResponseNet algorithm

To determine whether ResponseNet provides valid biological insights, we used it to analyze data from perturbations of well-studied pathways. For example, we used ResponseNet to connect genetic hits associated with Ste5 (from the *Saccharomyces* Genome Database) and differentially expressed genes[19] collected from a strain lacking Ste5, a scaffold protein that coordinates the MAP kinase cascade activated by pheromone (**Fig. 2b**). Nodes selected by ResponseNet were highly enriched for proteins functioning in the pheromone response pathway (46%, $P < 10^{-18}$), thus revealing the perturbed biological process. The highly ranked intermediary proteins included key regulators of the pheromone response including Ste5, the source of perturbation.

ResponseNet also performed well in analyzing the complex cellular response to DNA damage[4,20,21]. Nodes discovered by ResponseNet were highly enriched for the GO categories response to DNA damage stimulus (21%, $P < 10^{-14}$) and DNA repair (19%, $P < 10^{-14}$). The highly ranked part of the network contained core pathway proteins that were uncovered by years of intense investigation but escaped detection by high-throughput screens, including signal transducers (Mec1, Rad53), members of the RFC complex (Rfc2, Rfc3, Rfc4, Rfc5) and the transcriptional regulator Rfx1 (**Fig. 2c**). Statistical evaluation of the performance of ResponseNet on data for less well-characterized pathways is described in the **Supplementary Note**.

Mapping the cellular responses to alpha-synuclein toxicity

Having established the validity of our method to uncover connections between otherwise disparate high-throughput datasets, we applied ResponseNet to investigate the cellular toxicity associated with alpha-synuclein (α-syn). α-Syn is a small lipid-binding protein that is natively unfolded when not bound to lipids and prone to forming toxic oligomers[22]. It has been implicated in several neurodegenerative disorders, particularly Parkinson's disease (PD): it is the main component of Lewy bodies, locus duplication or triplication of α-syn lead to familial forms of PD, and increased expression of α-syn leads to neurodegeneration in several animal models[23]. Despite immense efforts, the cellular pathways by which α-syn leads to cell death are just beginning to emerge.

The yeast *Saccharomyces cerevisiae* provides a powerful system for studying the toxicities of α-syn that result from its intrinsic physical properties. Expression of human α-syn in yeast yields dosage-dependent defects also found in mammalian systems, including cytosolic-lipid-droplet accumulation, reactive-oxygen-species production and ubiquitin-proteasome system impairment[11]. An initial screen for yeast genes that modify α-syn toxicity when overexpressed identified genes involved in ER-to-Golgi vesicle trafficking and led to the observation that α-syn blocks ER-to-Golgi vesicle trafficking[12].

We now report the results of screening 5,500 overexpression yeast strains, thereby covering 85% of the yeast proteome. We identified 55 suppressors and 22 enhancers of α-syn toxicity, many with clear human orthologs, including the homolog of human PD gene *ATP13A2* (also known as *PARK9*; **Table 2** and **Supplementary Table 3a** online). As demonstrated in the accompanying article (Gitler *et al.*[24]), PARK9 and the human homologs of eight other genetic modifiers with diverse functions (Ypt1, Hrd1, Ubp3, Pde2, Cdc5, Yck3, Sit4 and Pmr1) are efficacious in neuronal models, validating the yeast model as meaningful to α-syn toxicity in neurons[12,24]. Major classes of genes that emerged include vesicle-trafficking genes, kinases and phosphatases, ubiquitin-related proteins, transcriptional regulators, manganese transporters and trehalose-biosynthesis genes (**Supplementary Table 3a,b**). Notably, trehalose was recently shown to promote the clearance of misfolded mutant α-syn[25], and manganese exposure has been linked with Parkinson's-like symptoms, albeit with a distinct underlying pathology[26]. The genes identified by the screen point to causal relations between α-syn expression and toxicities previously associated with PD but not specifically linked to α-syn (**Supplementary Note**).

mRNA profiling of the yeast model was determined in a separate study (unpublished data and **Supplementary Table 3b,c**). Upregulated genes prominently included genes with oxidoreductase activities (13%, $P < 10^{-9}$). Downregulated genes included ribosomal genes (28%, $P < 10^{-30}$), as commonly observed under stress[27]. More specific to α-syn toxicity, the downregulated genes were markedly enriched for genes encoding proteins localized to the mitochondria (60%, $P < 10^{-44}$).

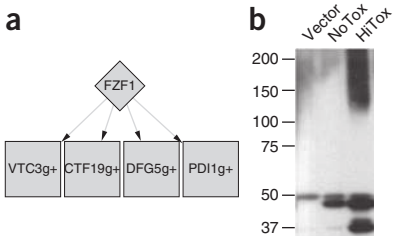

Figure 3 Nitrosative stress response to α-syn expression in yeast. (**a**) The predicted subnetwork containing Fzf1 and its differentially expressed target genes. Graphical representation is similar to **Figure 2**. (**b**) Immunoblotting against S-nitrosocysteine performed on a control strain (vector), on a strain expressing one copy of α-syn (NoTox) and on a high-toxicity strain (HiTox) expressing several copies of α-syn reveals that increasing levels of α-syn increase the amount of S-nitrosylated proteins.

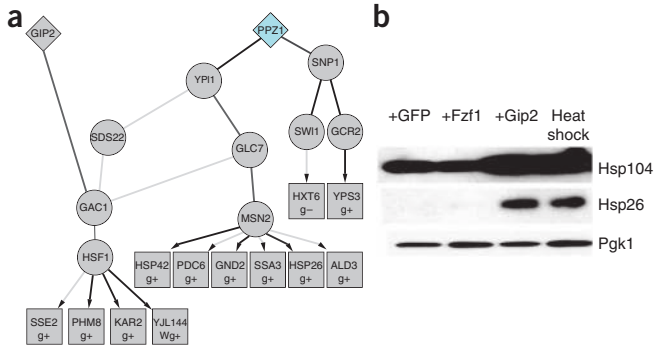

Figure 4 Overexpression of Gip2 causes induced expression of Hsf1 targets. (**a**) The predicted subnetwork links the toxicity suppressor Gip2 and the toxicity enhancer Ppz1 to Hsf1 and Msn2 via components of type 1 protein phosphatase complex (Gac1, Glc7, Ypi1, Sds22). Graphical representation is similar to **Figure 2**. (**b**) Immunoblotting of vector cells overexpressing GFP, Fzf1 or Gip2 with antibodies against Hsp104 and Hsp26. Overexpression of Gip2 is sufficient to activate Hsf1 and induce higher protein levels of both its targets Hsp104 and Hsp26, similar to that of vector cells subjected to heat shock. In contrast, overexpression of another genetic suppressor, Fzf1, does not activate Hsf1. Immunoblotting against Pgk1 was used as a loading control.

The genetic and mRNA profiling data exemplify both the power and the limitations of the current approaches. Although they reveal the wide range of cellular functions altered by α-syn, the precise roles of the identified genes in the cellular response are unclear. For example, we checked whether the ubiquitin-related genetic hits affect α-syn degradation. However, in strains overexpressing these ubiquitin-related genes, we did not detect changes in steady-state α-syn protein concentrations (**Supplementary Fig. 2** online). As with our analyses above, the overlap between the genetic hits and the differentially expressed genes was minor (four genes, $P = 0.96$).

Application of ResponseNet to these disparate datasets gave a more coherent view of the cellular response (**Supplementary Fig. 3a** online). The resulting network provided context to a large portion of the data: 34 (44%) genetic hits and 166 (27%) differentially expressed genes were linked to each other through 106 intermediary proteins. These include two-thirds of the protein kinase, phosphatase and ubiquitin-related genetic hits, illuminating their intricate role in the response to α-syn.

The major cellular pathways identified by ResponseNet included ubiquitin-dependent protein degradation, cell cycle regulation and vesicle-trafficking pathways, all of which have previously been associated with PD (**Supplementary Note** and **Supplementary Fig. 3a**). Four examples illustrate the ability of ResponseNet to clarify aspects of α-syn responses relevant to PD and uncover others whose relationship to α-syn was completely unknown.

Nitrosative stress

Fzf1 was the only genetic hit related to nitrosative stress[28]. However, ResponseNet connected it to four upregulated transcripts, including that encoding Pdi1, a protein disulfide isomerase (PDI) (**Fig. 3a**). Notably, the upregulation of human PDI protects neuronal cells from neurotoxicity associated with ER stress and protein misfolding (both of which are linked to α-syn expression in yeast and neurons), and PDI is one of a small number of specific proteins S-nitrosylated in PD that activate protective pathways, in addition to the generalized nitrosative damage that is a hallmark of the disease[29]. We found that increased expression of α-syn causes both specific and general increases in S-nitrosylation of proteins (**Fig. 3b**). This was highly surprising because the yeast genome does not encode a canonical nitric oxide synthase and, until very recently, yeast were not thought to produce nitric oxide[30]. Our results indicate that the nitrosylation of specific proteins and generalized nitrosylation is a highly conserved and deeply rooted response to cellular perturbations created by α-syn.

Heat shock

The induction of the heat-shock response directly or via chemical inhibition of Hsp90 (ref. 31) suppresses α-syn toxicity in many model systems including yeast, flies, mice and human cells (for example, see refs. 32,33). However, heat-shock–related genes were conspicuously absent among the list of genetic suppressors. Nonetheless, ResponseNet predicted the involvement of two highly conserved heat-shock regulators, the chaperone Hsp90 (isoform Hsp82, **Supplementary Fig. 3a**, panel a) and the heat-shock transcription factor Hsf1 (**Fig. 4a**). Hsf1 appeared downstream of the toxicity suppressor Gip2, a putative regulatory subunit of the Glc7 phosphatase, which interacts with Gac1. Gac1 is a regulatory subunit of the Glc7 complex that is known to activate Hsf1 (ref. 34). These connections suggested that Gip2 overexpression might induce a heat-shock response. Indeed, we found that strains overexpressing Gip2 show elevated concentrations of heat-shock proteins (**Fig. 4b**). ResponseNet therefore provided a mechanistic explanation for the suppression of α-syn toxicity achieved by Gip2 overexpression and identified a new regulator of the highly conserved heat-shock response.

The mevalonate-ergosterol biosynthesis pathway

This pathway, which is targeted by the cholesterol-lowering statin drugs, synthesizes sterols as well as other products with connections to α-syn toxicity, such as farnesyl groups required for vesicle trafficking proteins and ubiquinone required for mitochondrial respiration. ResponseNet ranked highly Hrd1, which regulates the protein target of statins, and the predicted intermediary Hap1, a proposed transcriptional regulator of the pathway[35] (**Supplementary Fig. 3a**, panel a). In addition, the α-syn mRNA profile modestly correlated with the profile of yeast treated with lovastatin ($r = 0.32$, $P < 10^{-93}$, L.J.S. and S.L., unpublished data), and several genetic hits also could be associated with products of the pathway (enzymes Bet4 and Cax4, farnesylated proteins Ypt1 and Ykt6 and putative sterol carriers Sut2, Osh2 and Osh3). We therefore tested the effect of lovastatin, which selectively inhibits the highly conserved HMG-CoA reductase protein in yeast and in mammalian cells, on α-syn toxicity. Addition of 5 μM lovastatin to the media caused a further reduction in growth to strains overexpressing α-syn (**Fig. 5a**), but did not reduce growth of either wild-type controls or of cells expressing another toxic protein, a glutamine-expansion variant of huntingtin exon I[36] (**Supplementary Fig. 3b**). We further tested ubiquinone, a downstream output of this pathway, reasoning that its downregulation through the action of α-syn might increase cellular vulnerability. Indeed, the addition of ubiquinone-2 to the media provided a modest suppression against α-syn toxicity. Ubiquinone is an antioxidant, but this was not a nonspecific antioxidant response, as the antioxidant N-acetylcysteine had no effect (data not shown).

The target of rapamycin (TOR) pathway

ResponseNet identified the TOR pathway proteins Tor1, Tor2 and their target transcription factors as intermediary between the genetic suppressor Lst8, a positive regulator of the TOR pathway, and several upregulated genes involved in spore wall formation (a vectorially directed secretory process in yeast) and vacuolar protein degradation

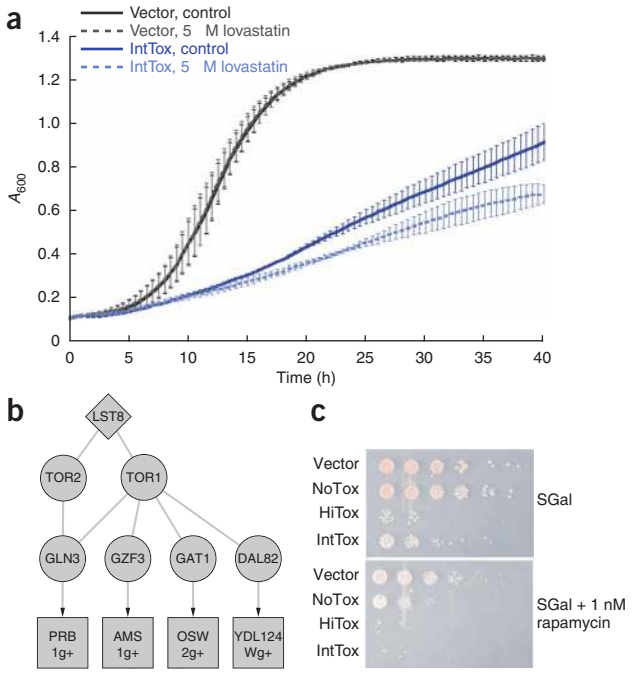

Figure 5 Effects of the small molecules lovastatin and rapamycin on α-syn toxicity. (**a**) Lovastatin inhibits growth of the yeast strain expressing an intermediate level of α-syn. Growth of a control strain (vector) and an intermediate toxicity strain (IntTox) expressing several copies of α-syn was measured in a galactose containing media with and without 5 μM lovastatin. Each growth curve reflects the average of three individual runs, each of which is indicated by a bar. (**b**) The predicted subnetwork containing TOR pathway components includes the predicted proteins Tor1 and Tor2. Graphical representation is similar to **Figure 2c**. (**c**) The effect of rapamycin on growth of different yeast strains. The upper panel shows the growth of a control strain (vector), a strain expressing one copy of α-syn (NoTox), a high-toxicity strain (HiTox) and an intermediate toxicity strain (IntTox) both expressing several copies of α-syn, in a galactose containing media (SGal) that is used to induce expression of α-syn. The lower panel shows the same strains grown in media that also contains 1 nM rapamycin, showing that rapamycin inhibits growth of all α-syn–expressing strains but not the control strain, as observed by the difference in the number of colonies per drop. The different columns correspond to serial dilutions.

(**Fig. 5b**). We found that addition of the TOR-inhibitor rapamycin to the media markedly enhanced the toxicity of α-syn. Indeed, a low dose of α-syn, which is otherwise innocuous, became toxic (**Fig. 5c**). Establishing the specificity of this effect to α-syn, rapamycin did not reduce growth of cells expressing glutamine expansion variants of huntingtin exon I (**Supplementary Fig. 3c**). As other studies have suggested benefits of rapamycin treatment in PD models, these results call for further investigation and suggest a complexity to the response to rapamycin that is potentially due to the vast range of processes affected by TOR activation.

DISCUSSION

We provide a novel framework in which genetic, physical and transcriptional data naturally complement each other in the context of cellular response to biological perturbations. Although the complementary nature of these data has been noted[2,5–9,37], a systematic analysis of the relationship between stimulus-specific genetic modifiers and transcriptional responses has been lacking. By examining over 150 distinct stimuli we find that differentially expressed genes and genetic hits are consistently disparate (**Table 1**); genetic hits are biased toward regulatory proteins, whereas the differentially expressed genes are biased toward metabolic processes. Indeed, each assay has inherent 'blind spots'. Many yeast regulatory proteins are not detected by transcriptional assays because either they are predominantly regulated post-transcriptionally, they have a low transcript concentration[38] or their differential expression is transient, making changes hard to measure. Conversely, the genes that are differentially transcribed are often involved in metabolic processes or redundant functions, which tend to be robust against single mutations[39].

The discordance between genetic hits and differentially expressed genes has implications for the search for therapeutic strategies. In yeast, inactivating a differentially expressed gene is no more likely to affect cell viability than targeting a randomly chosen gene. Bridging the gap between these data using techniques like ResponseNet can potentially reveal intervention points not discovered in the high-throughput assays themselves (**Fig. 2**) that may be targeted by drugs.

Our computational approach is based on a flow algorithm to connect the genetic hits and differentially expressed genes. Unlike studies that link a target gene with its causal transcriptional change[13,15,16,40–43], a flow-based approach allows for a global, efficient and simultaneous solution for multiple target genes that puts no a priori bounds on the structure of the output. Indeed, the predicted output networks have rich structures with half of all paths having a length of three edges or more. The ability of ResponseNet to analyze interactome data containing tens of thousands of nodes and edges make it well suited to analyzing the accumulating data from other species or other techniques.

We applied our approach to a yeast model for α-syn pathobiology implicated in PD. Our unbiased screen identified 77 genes whose overexpression altered α-syn toxicity (**Table 2**). These included genes involved in vesicle trafficking (as previously reported), protein degradation, cell cycle regulation, nitrosative stress, osmolyte biosynthesis and manganese transport. This screen established an interface between α-syn and a large number of cellular and environmental factors previously linked to neuropathology and, in some cases, specifically to parkinsonism, but not specifically linked to α-syn. Many of the genes we identified are highly conserved in humans, where they may exert similar effects. Indeed, eight out of nine toxicity modifiers tested had similar effects on α-syn toxicity in yeast and in neuronal systems[24].

Application of ResponseNet to the α-syn model successfully provided functional context to many of the genetic hits identified in our yeast screen (**Supplementary Fig. 3a**) and pointed to the involvement of several cellular pathways (**Figs. 3–5**). Of these, the mevalonate-ergosterol pathway is of special interest as its perturbation could potentially alter a variety of downstream pathways, including protein farnesylation and ubiquinone biosynthesis, which are closely related to the vesicle trafficking defects and mitochondrial dysfunction observed in the yeast model. Indeed, a link between sterol biosynthesis and the etiology of PD has recently emerged. Individuals with PD have significantly lower concentrations of low-density lipoprotein (LDL) cholesterol than their spouses[44], and low concentrations of LDL preceded the appearance of PD in a group of men of Japanese ancestry[45]. Our work provides a molecular framework for elucidating this connection.

The global picture obtained by integrating high-throughput genetic, transcriptional and physical data demonstrates the power of integrative approaches to illuminate underexplored cellular processes. As high-throughput assays are becoming routine in the study of complex

disease and developmental processes, approaches for deciphering these data based on their underlying characteristics are vital.

METHODS

Genetic and transcriptional datasets. Chemical perturbation data were downloaded from original papers. Genetic hits for gene inactivation included proteins that genetically interact with the inactivated gene according to *Saccharomyces cerevisiae* Genome Databases (SGD). Differentially expressed genes included genes that showed at least a twofold change in expression with a P value ≤ 0.05 (ref. 19), or else as defined according to the original papers. Genetic and mRNA profiling assays for chemical perturbations were paired if the chemical concentrations were comparable.

Interactome data description. The interactome was represented as a graph $G = (V, E)$ where nodes V represent genes and proteins and edges E represent their interactions. Different nodes represent a gene and its corresponding protein.

Bidirectional edges between protein nodes represent physical protein–protein interactions or metabolic interactions between enzymes if the substrate of one is the product of the other.

Directed edges represent regulatory interactions. Outgoing edges connected protein nodes to gene nodes if there was evidence from literature or ChIP-chip assays that the proteins may regulate the genes. Proteins nodes were connected if both proteins were transcriptional regulators and one regulated the other.

The data sources appear in the **Supplementary Note**. **Supplementary Table 2a** lists the number of interacting pairs per interaction type in the interactome.

Weighting scheme for interactome edges. *Interactions between protein nodes.* Each interacting protein pair $p_i p_j$ was associated with an interaction vector $Ip_i p_j$; vector entry $I_k p_i p_j$ is an indicator function for interaction evidence of type k. Interactions are weighted (w_{ij}) to reflect the probability that $p_i p_j$ function in a randomly selected response pathway (denoted $RP_{Pi,Pj} = 1$) as follows:

$$w_{ij} = \mathrm{P}(RP_{p_i p_j} = 1 | I_{p_i p_j}) = \mathrm{P}(I_{p_i p_j} | RP_{p_i p_j} = 1)\mathrm{P}(RP_{p_i p_j} = 1)/\mathrm{P}(I_{p_i p_j}),$$

where

$$\begin{aligned}\mathrm{P}(I_{p_i p_j}) = {} & \mathrm{P}(I_{p_i p_j} | RP_{p_i p_j} = 1)\mathrm{P}(RP_{p_i p_j} = 1) \\ & + \mathrm{P}(I_{p_i p_j} | RP_{p_i p_j} = 0)P(RP_{p_i p_j} = 0)\end{aligned}$$

We assumed conditionally independence between different types of evidence:

$$\mathrm{P}(I_{p_i p_j} | RP_{p_i p_j}) = \prod\nolimits_k \mathrm{P}(I_{kp_i p_j} | RP_{p_i p_j})$$

Interactions between protein and gene nodes. Weights were designed to reflect the reliability of the interaction on the basis of experimental evidence and binding-site conservation.

The scheme for calculating P(RP) and P(I_k| RP) and the weights per interaction type appear in the **Supplementary Note**. Because high edge weights could indicate unusually well-studied proteins[46] or imperfectness of the assumption of conditional independence, all weights were capped to a maximum value of 0.7.

Linear programming formulation. For each perturbation, the input to ResponseNet consisted of the weighted interactome $G = (V, E)$, the genetic hits $Gen \subset V$ and the differentially expressed genes $Tra \subset V$ identified following the perturbation. Each edge $(i, j) \in E$ was characterized by a weight w_{ij} and a capacity $c_{ij} = 1$.

The graph G was updated as follows:

1. $V' = V \cup \{S, T\}$, where S and T are auxiliary nodes representing the source and sink, respectively.

2. $E' = E \cup (S,i)_{\forall i \in Gen} \cup (i,T)_{\forall i \in Tra}$, connecting S to the genetic hits and T to the differentially expressed genes by directed edges.

3.

$$c_{Si} = \frac{|strength_i|}{\sum_{j \in Gen} |strength_j|},$$

$\forall i \in Gen$, where the strength of each genetic hit was measured by the variation it conferred on the number of colonies per drop if available; otherwise, strengths were uniform.

4.

$$c_{iT} = \frac{|\log_2(strength_i)|}{\sum_{j \in Tra} |\log_2(strength_j)|},$$

$\forall i \in Tra$, where the strength was measured by either the relative change in its transcript level or the P value associated with it, depending on their availability.

5. $w_{Si} = c_{Si}\ \forall i \in Gen$ and $w_{iT} = c_{iT}\ \forall i \in Tra$

Letting f_{ij} denote the flow from node i to node j and for any given $\gamma \geq 0$, the following optimization problem was solved using LOQO[47]:

$$\min_f((\sum_{i \in V', j \in V'} -\log(w_{ij}) * f_{ij}) - (\gamma * \sum_{i \in Gen} f_{Si}))$$

Subject to:

$$\sum_{j \in V'} f_{ij} - \sum_{j \in V'} f_{ji} = 0 \quad \forall i \in V' - \{S, T\}$$

$$\sum_{i \in Gen} f_{Si} - \sum_{i \in Tra} f_{iT} = 0$$

$$0 \leq f_{ij} \leq c_{ij} \quad \forall (i,j) \in E'$$

The solution $F = \{f_{ij} > 0\}$ defined the predicted response network. For enrichment analysis only protein nodes were considered, and genetic hits were included only if they received flow from nodes other than the source. Protein nodes were ranked in decreasing order according to the total amount of their incoming flow. Although the solution to the optimization problem is a directed network, this directionality only reflects the way in which the algorithm directed flow from the genetic hits to the differentially expressed genes and does not represent the causal order of events (**Supplementary Fig. 1b**).

Additional information regarding the formulation, space of solutions, setting γ value and ResponseNet performance appear in the **Supplementary Note**. For ResponseNet validation $\gamma = 10$.

Statistical analysis. Probabilities of overlap between genetic hits and differentially expressed genes were calculated using Fisher's exact test, given a total of 6,000 yeast genes. Enrichment analysis was done using the Gene Ontology Term Finder from SGD.

α-Syn toxicity modifier screen The high-throughput yeast transformation protocol appears elsewhere[12].

Immunoblotting. Phosphoglycerate kinase 1(Pgk1) mouse monoclonal antibody was used at 1:5000. Hsp26 rabbit polyclonal antibody (gift from J. Buchner, Center for Integrative Protein Science and Department of Chemistry, Technische Universität München) was used at 1:5000. Hsp104 mouse monoclonal antibody (4B; ref. 48) was used at 1:5000. S-nitosocysteine rabbit polyclonal antibody (Sigma) was used at 1:10,000.

α-Syn ResponseNet analysis. Differentially expressed genes had at least a twofold change in expression with P value ≤ 0.05 (**Supplementary Table 3c**). Capacities of edges connecting the source to genetic hits were relative to the absolute strength of the genetic hits (**Supplementary Table 3a**). Capacities of edges connecting differentially expressed genes to the sink were relative to the absolute log of the change in expression. We repeated the analysis excluding nonspecific stress responses (**Supplementary Note**). ResponseNet was run with $\gamma = 12$.

α-Syn growth in presence of small molecules. For spotting assays, yeast strains were initially grown to saturation in media containing raffinose, normalized for their A_{600} and serially diluted by fivefold before spotting onto appropriate yeast media. Growth curves were monitored using the Bioscreen instrument. Yeast strains were pre-grown in 2% raffinose medium and induced in 2% galactose medium in presence of either the compound or vehicle control (1% DMSO final) with starting A_{600} of 0.1. Cells were grown at 30 °C, with plates shaken

every 30 s to ensure proper aeration and A_{600} measurements taken every half hour over a 2-d period. The resulting data (A_{600} versus time) were plotted using Kaleidagraph. At least three independent runs were conducted for each growth condition.

Note: Supplementary information is available on the Nature Genetics website.

ACKNOWLEDGMENTS

E.Y.-L. has been supported by an EMBO long-term postdoctoral fellowship and by a research grant from the National Parkinson Foundation. L.R. has been supported by Roberto Rocca doctoral fellowship and the CSBi Merck-MIT postdoctoral fellowship. L.J.S. was supported by an American Cancer Society postdoctoral fellowship. A.D.G. was a Lilly Fellow of the Life Sciences Research Foundation. M.L.G is supported by a research grant from the National Parkinson Foundation. S.L. is a founder of and has received consulting fees from FoldRx Pharmaceuticals, a company that investigates drugs to treat protein folding diseases. A.D.G., A.G.C. and S.L. are inventors on patents and patent applications that have been licensed to FoldRx. E.F. is the recipient of the Eugene Bell Career Development Chair. This work was supported in part by HHMI and by MGH/MIT Morris Udall Center of Excellence in PD Research NS38372. We thank M. Taipale, S. Treusch and G. Caraveo Piso for helpful discussions and comments and T. DiCesare for help with figures. L.R. thanks G. Casari and S. Cerutti for support and helpful discussions.

COMPETING INTERESTS STATEMENT

The authors declare competing financial interests: details accompany the full-text HTML version of the paper at http://www.nature.com/naturegenetics/.

Published online at http://www.nature.com/naturegenetics/
Reprints and permissions information is available online at http://npg.nature.com/reprintsandpermissions/

1. Calvano, S.E. *et al.* A network-based analysis of systemic inflammation in humans. *Nature* **437**, 1032–1037 (2005).
2. Haugen, A.C. *et al.* Integrating phenotypic and expression profiles to map arsenic-response networks. *Genome Biol.* **5**, R95 (2004).
3. Parsons, A.B. *et al.* Integration of chemical-genetic and genetic interaction data links bioactive compounds to cellular target pathways. *Nat. Biotechnol.* **22**, 62–69 (2004).
4. Begley, T.J., Rosenbach, A.S., Ideker, T. & Samson, L.D. Hot spots for modulating toxicity identified by genomic phenotyping and localization mapping. *Mol. Cell* **16**, 117–125 (2004).
5. Deutschbauer, A.M., Williams, R.M., Chu, A.M. & Davis, R.W. Parallel phenotypic analysis of sporulation and postgermination growth in *Saccharomyces cerevisiae*. *Proc. Natl. Acad. Sci. USA* **99**, 15530–15535 (2002).
6. Fry, R.C., Begley, T.J. & Samson, L.D. Genome-wide responses to DNA-damaging agents. *Annu. Rev. Microbiol.* **59**, 357–377 (2005).
7. Birrell, G.W. *et al.* Transcriptional response of *Saccharomyces cerevisiae* to DNA-damaging agents does not identify the genes that protect against these agents. *Proc. Natl. Acad. Sci. USA* **99**, 8778–8783 (2002).
8. Winzeler, E.A. *et al.* Functional characterization of the *S. cerevisiae* genome by gene deletion and parallel analysis. *Science* **285**, 901–906 (1999).
9. Smith, J.J. *et al.* Expression and functional profiling reveal distinct gene classes involved in fatty acid metabolism. *Mol. Syst. Biol.* **2**, 2006.0009 (2006.).
10. Schiesling, C., Kieper, N., Seidel, K. & Kruger, R. Review: familial Parkinson's disease–genetics, clinical phenotype and neuropathology in relation to the common sporadic form of the disease. *Neuropathol. Appl. Neurobiol.* **34**, 255–271 (2008).
11. Outeiro, T.F. & Lindquist, S. Yeast cells provide insight into alpha-synuclein biology and pathobiology. *Science* **302**, 1772–1775 (2003).
12. Cooper, A.A. *et al.* Alpha-synuclein blocks ER-Golgi traffic and Rab1 rescues neuron loss in Parkinson's models. *Science* **313**, 324–328 (2006).
13. Workman, C.T. *et al.* A systems approach to mapping DNA damage response pathways. *Science* **312**, 1054–1059 (2006).
14. Beyer, A., Bandyopadhyay, S. & Ideker, T. Integrating physical and genetic maps: from genomes to interaction networks. *Nat. Rev. Genet.* **8**, 699–710 (2007).
15. Yeang, C.H., Ideker, T. & Jaakkola, T. Physical network models. *J. Comput. Biol.* **11**, 243–262 (2004).
16. Ourfali, O., Shlomi, T., Ideker, T., Ruppin, E. & Sharan, R. SPINE: a framework for signaling-regulatory pathway inference from cause-effect experiments. *Bioinformatics* **23**, i359–i366 (2007).
17. Dasika, M.S., Burgard, A. & Maranas, C.D. A computational framework for the topological analysis and targeted disruption of signal transduction networks. *Biophys. J.* **91**, 382–398 (2006).
18. Cormen, T.H., Leiserson, C.E., Rivest, R.L. & Stein, C. *Introduction to Algorithms* (The MIT Press, Cambridge, Massachusetts, 2001).
19. Hughes, T.R. *et al.* Functional discovery via a compendium of expression profiles. *Cell* **102**, 109–126 (2000).
20. Chang, M., Bellaoui, M., Boone, C. & Brown, G.W. A genome-wide screen for methyl methanesulfonate-sensitive mutants reveals genes required for S phase progression in the presence of DNA damage. *Proc. Natl. Acad. Sci. USA* **99**, 16934–16939 (2002).
21. Gasch, A.P. *et al.* Genomic expression responses to DNA-damaging agents and the regulatory role of the yeast ATR homolog Mec1p. *Mol. Biol. Cell* **12**, 2987–3003 (2001).
22. Tofaris, G.K. & Spillantini, M.G. Physiological and pathological properties of alpha-synuclein. *Cell. Mol. Life Sci.* **64**, 2194–2201 (2007).
23. Lee, V.M. & Trojanowski, J.Q. Mechanisms of Parkinson's disease linked to pathological alpha-synuclein: new targets for drug discovery. *Neuron* **52**, 33–38 (2006).
24. Gitler, A.D. *et al.* α-Synuclein is part of a diverse and highly conserved interaction network that includes PARK9 and manganese toxicity. *Nat. Genet.* advance online publication, doi:10.1038/ng.300 (1 February 2009).
25. Sarkar, S., Davies, J.E., Huang, Z., Tunnacliffe, A. & Rubinsztein, D.C. Trehalose, a novel mTOR-independent autophagy enhancer, accelerates the clearance of mutant huntingtin and alpha-synuclein. *J. Biol. Chem.* **282**, 5641–5652 (2007).
26. Olanow, C.W. Manganese-induced parkinsonism and Parkinson's disease. *Ann. NY Acad. Sci.* **1012**, 209–223 (2004).
27. Gasch, A.P. *et al.* Genomic expression programs in the response of yeast cells to environmental changes. *Mol. Biol. Cell* **11**, 4241–4257 (2000).
28. Sarver, A. & DeRisi, J. Fzf1p regulates an inducible response to nitrosative stress in *Saccharomyces cerevisiae*. *Mol. Biol. Cell* **16**, 4781–4791 (2005).
29. Uehara, T. *et al.* S-nitrosylated protein-disulphide isomerase links protein misfolding to neurodegeneration. *Nature* **441**, 513–517 (2006).
30. Almeida, B. *et al.* NO-mediated apoptosis in yeast. *J. Cell Sci.* **120**, 3279–3288 (2007).
31. Zou, J., Guo, Y., Guettouche, T., Smith, D.F. & Voellmy, R. Repression of heat shock transcription factor HSF1 activation by HSP90 (HSP90 complex) that forms a stress-sensitive complex with HSF1. *Cell* **94**, 471–480 (1998).
32. Flower, T.R., Chesnokova, L.S., Froelich, C.A., Dixon, C. & Witt, S.N. Heat shock prevents alpha-synuclein-induced apoptosis in a yeast model of Parkinson's disease. *J. Mol. Biol.* **351**, 1081–1100 (2005).
33. Auluck, P.K., Meulener, M.C. & Bonini, N.M. Mechanisms of Suppression of {alpha}-Synuclein Neurotoxicity by Geldanamycin in *Drosophila*. *J. Biol. Chem.* **280**, 2873–2878 (2005).
34. Lin, J.T. & Lis, J.T. Glycogen synthase phosphatase interacts with heat shock factor to activate CUP1 gene transcription in *Saccharomyces cerevisiae*. *Mol. Cell. Biol.* **19**, 3237–3245 (1999).
35. Hickman, M.J. & Winston, F. Heme levels switch the function of Hap1 of *Saccharomyces cerevisiae* between transcriptional activator and transcriptional repressor. *Mol. Cell. Biol.* **27**, 7414–7424 (2007).
36. Duennwald, M.L., Jagadish, S., Muchowski, P.J. & Lindquist, S. Flanking sequences profoundly alter polyglutamine toxicity in yeast. *Proc. Natl. Acad. Sci. USA* **103**, 11045–11050 (2006).
37. Kelley, R. & Ideker, T. Systematic interpretation of genetic interactions using protein networks. *Nat. Biotechnol.* **23**, 561–566 (2005).
38. Holstege, F.C. *et al.* Dissecting the regulatory circuitry of a eukaryotic genome. *Cell* **95**, 717–728 (1998).
39. Deutscher, D., Meilijson, I., Kupiec, M. & Ruppin, E. Multiple knockout analysis of genetic robustness in the yeast metabolic network. *Nat. Genet.* **38**, 993–998 (2006).
40. Shachar, R., Ungar, L., Kupiec, M., Ruppin, E. & Sharan, R. A systems-level approach to mapping the telomere length maintenance gene circuitry. *Mol. Syst. Biol.* **4**, 172 (2008).
41. Bromberg, K.D., Ma'ayan, A., Neves, S.R. & Iyengar, R. Design logic of a cannabinoid receptor signaling network that triggers neurite outgrowth. *Science* **320**, 903–909 (2008).
42. Tu, Z., Wang, L., Arbeitman, M.N., Chen, T. & Sun, F. An integrative approach for causal gene identification and gene regulatory pathway inference. *Bioinformatics* **22**, e489–e496 (2006).
43. Suthram, S., Beyer, A., Karp, R.M., Eldar, Y. & Ideker, T. eQED: an efficient method for interpreting eQTL associations using protein networks. *Mol. Syst. Biol.* **4**, 162 (2008).
44. Huang, X. *et al.* Lower low-density lipoprotein cholesterol levels are associated with Parkinson's disease. *Mov. Disord.* **22**, 377–381 (2007).
45. Huang, X., Abbott, R.D., Petrovitch, H., Mailman, R.B. & Ross, G.W. Low LDL cholesterol and increased risk of Parkinson's disease: prospective results from Honolulu-Asia Aging Study. *Mov. Disord.* **23**, 1013–1018 (2008).
46. Hoffmann, R. & Valencia, A. Life cycles of successful genes. *Trends Genet.* **19**, 79–81 (2003).
47. Vanderbei, R.J. LOQO User's Manual–Version 3.10. *Optimization Methods and Software* **12**, 485–514 (1999).
48. Cashikar, A.G. *et al.* Defining a pathway of communication from the C-terminal peptide binding domain to the N-terminal ATPase domain in a AAA protein. *Mol. Cell* **9**, 751–760 (2002).

Supplementary Note

Bridging high-throughput genetic and transcriptional data reveals cellular responses to alpha-synuclein toxicity

Esti Yeger-Lotem[1,2,8], Laura Riva[1,8], Linhui Julie Su[2], Aaron D Gitler[2,7], Anil G Cashikar[2,7], Oliver D King[2,7], Pavan K Auluck[2,3], Melissa L Geddie[2], Julie S Valastyan[2,4], David R Karger[5], Susan Lindquist[2,6] & Ernest Fraenkel[1,5]

[1]Department of Biological Engineering, Massachusetts Institute of Technology, Cambridge, Massachusetts 02139, USA.

[2]Whitehead Institute for Biomedical Research, Cambridge, Massachusetts 02142, USA.

[3]Departments of Pathology and Neurology, Massachusetts General Hospital, Boston, Massachusetts 02114, and Harvard Medical School, Boston, Massachusetts 02115, USA.

[4]Department of Biology, Massachusetts Institute of Technology, Cambridge, Massachusetts 02139, USA.

[5]Computer Science and Artificial Intelligence Laboratory, Massachusetts Institute of Technology, Cambridge, Massachusetts 02139, USA.

[6]Howard Hughes Medical Institute, Department of Biology, Massachusetts Institute of Technology, Cambridge, Massachusetts 02139, USA.

[7]Present addresses: Department of Cell and Developmental Biology, The University of Pennsylvania, Philadelphia, Pennsylvania, USA (A.D.G.), Medical College of Georgia,

Nature Genetics: doi:10.1038/ng.337

Augusta, Georgia, USA (A.G.C.) and Boston Biomedical Research Institute, Watertown, Massachusetts, USA (O.D.K.).

[8]These authors contributed equally to this work.

Correspondence should be addressed to S.L. (lindquist_admin@wi.mit.edu) or E.F. (fraenkel-admin@mit.edu).

Table of Contents

Nature Genetics: doi:10.1038/ng.337

The bias in the sets of genetic hits and the sets of differentially expressed genes

Enrichment analyses were carried out using Gene Ontology (GO) term finder from SGD[1] and Genomica[2]. Supplementary Table 1B contains the GO enrichment of the genetic hits and of the differentially expressed genes. To validate that the biases for the pooled hits represent general tendencies, as opposed to being dominated by a handful of large data sets, we repeated the analysis in several ways as detailed below.

Separate analysis of the perturbations with complete genetic screens

We calculated the gene ontology (GO) process or function annotation enrichment separately for each of the perturbations in Table 1 for which complete genetic screens were available. To avoid being biased by a handful of perturbations we required that an annotation be enriched in data of at least 6 perturbations, which is 20% of the datasets. Supplementary Table 1C lists the GO annotations that were statistically significantly enriched ($p<=0.05$, FDR corrected) in at least 20% of the sets of genetic hits or at least 20% of the sets of differentially expressed genes. The table details for each GO annotation the number of sets that were significantly enriched for this annotation and the median p-value for its enrichment.

We identified 146 GO annotations enriched in at least 20% of the sets of genetic hits. The three GO annotations enriched in the largest number of genetic hits sets are 'biological regulation' (23 sets, 77%, median $p<10^{-10}$), 'response to stimulus' (23 sets, 77%, median $p<10^{-8}$) and 'regulation of cellular process' (22 sets, 73%, median $p<10^{-9}$). Other frequently enriched annotations among the sets of genetic hits include cell cycle related processes and other regulatory processes (e.g., regulation of cell cycle, post-

Nature Genetics: doi:10.1038/ng.337

translational protein modification and transcription). Therefore, genetic hits sets are indeed enriched for regulatory processes and functions.

We identified only 10 annotations that were significantly enriched in at least 20% of the sets of differentially expressed genes. Eight of these annotations are for various metabolic processes, and the remaining two annotations are for oxidoreductase activity and cell wall constituents.

Interestingly, none of the enriched annotations was common to both the genetic hits sets and the differentially expressed genes sets, supporting our observation of the distinct nature of these gene sets. The genetic hits were enriched for a few annotations that could be construed as related to metabolism. However, all-but-one of these were DNA or RNA metabolic processes, which are more closely related to cell cycle progression and gene transcription than to metabolism *per se*. The GO annotation "one-carbon compound metabolic process" is exceptional. It is the only category that is clearly related to metabolism but is associated with genetic hits (6 sets, p=0.001). We therefore conclude that the bias is evident when the data sources are analyzed separately.

Combined analysis of the perturbations with complete genetic screens

We created a combined genetic hits set and a combined differentially expressed gene set from the perturbations in Table 1 for which complete genetic screens were available. We then checked the GO process and function annotation enrichment of the two combined sets. The enriched annotations that we list in Supplementary Table 1D were limited to annotations also found to be enriched in at least 20% of the sets when analyzed separately. This analysis of the combined sets resulted in the identification of 124 GO annotations enriched in the combined set of genetic hits, and 10 GO annotations enriched

Nature Genetics: doi:10.1038/ng.337

in the combined set of differentially expressed genes. The results for the combined sets appear in Supplementary Table 1D, which lists for each of these GO annotations its enrichment p-value and the percentage of genes in the corresponding set that are attributed to this annotation.

The analysis of the combined sets with complete genetic screens again supports the bias we reported. We find that biological regulation is among the most significantly enriched and most frequent annotation for the set of genetic hits. The genetic hits are also frequently attributed to various regulatory processes, response pathways, and cell cycle phases. The differentially expressed genes are most frequently attributed to oxidoreductase activity and to organic acid metabolic process.

To enable visualization we further limited the annotations to those annotations attributed to at least 5% of the combined gene set. Supplementary Figure 1A presents each of these 39 GO annotations together with the percentage of genes attributed to this annotation in the enriched set.

Graphical representation of the interactome

The interactome was represented as a graph $G = (V, E)$ that consists of nodes (vertices) V representing genes and proteins, and a set of bidirectional and directed edges E representing their interactions. Different nodes in the network represent a gene and its corresponding protein.

Bidirectional edges between protein nodes in the interactome consisted of:

Nature Genetics: doi:10.1038/ng.337

(i) Physical protein-protein interactions, which were downloaded from [3] and from BioGRID release 2.0.30.

(ii) Interactions between two proteins if they both appeared in the same literature-curated protein complex, downloaded from MIPS [4].

(iii) Metabolic interactions between two enzymes, if the substrate of one was the product of the other, based on the metabolic map of *S. cerevisiae* [5].

Directed edges in the interactome consisted of:

(i) Edges from a protein node to a gene node if there was evidence from either literature or ChIP-chip assays [6-8] that the protein was a probable transcriptional regulator of the gene.

(ii) Edges from one protein node to another if both proteins acted as transcriptional regulators and the first regulated the second.

Supplementary Table 2A lists the number of interacting pairs per interaction type in the interactome.

Weighting scheme for interactome edges

Each edge $(i, j) \in E$ between node *i* and node *j* of the interactome is characterized by a weight w_{ij} calculated as follows:

Interactions between protein nodes: We developed a Bayesian weighting scheme that favors interactions between proteins functioning within a common response pathway (*RP*). Each interacting protein pair p_i,p_j was associated with an interaction vector Ip_i,p_j, where vector entry $I_k\,p_i,p_j$ serves as an indicator function for interaction evidence of type *k*. For example, $I_{\text{"two-hybrid HTP"}}\,p_i,p_j$ was set to 1 if p_i interacted with p_j in a high-

Nature Genetics: doi:10.1038/ng.337

throughput two-hybrid experiment. Each interacting protein pair p_i,p_j was assigned a weight w_{ij} reflecting the probability that p_i,p_j function in a randomly selected response pathway (denoted $RP_{\mathrm{pi,pj}}$=1) based on their interaction evidence vector $I_{pi,pj}$. By Bayes' rule,

$w_{ij} = \mathrm{P}(RP_{p_ip_j} = 1 \mid I_{p_ip_j}) = \mathrm{P}(I_{p_ip_j} \mid RP_{p_ip_j} = 1)\mathrm{P}(RP_{p_ip_j} = 1) / \mathrm{P}(I_{p_ip_j})$, where

$\mathrm{P}(I_{p_ip_j}) = \mathrm{P}(I_{p_ip_j} \mid RP_{p_ip_j} = 1)\mathrm{P}(RP_{p_ip_j} = 1) + \mathrm{P}(I_{p_ip_j} \mid RP_{p_ip_j} = 0)\mathrm{P}(RP_{p_ip_j} = 0)$.

We assumed that different types of evidence are conditionally independent, so that $\mathrm{P}(I_{p_ip_j} \mid RP_{p_ip_j}) = \prod_k \mathrm{P}(I_{kp_ip_j} \mid RP_{p_ip_j})$. To estimate the prior probability P(*RP)* and the conditional probability table associated with each evidence type $\mathrm{P}(I_k \mid RP)$ we compiled the following:

1) A set of response pathways containing 54 response-specific processes according to GO process annotations (e.g., response to osmotic stress GO:0006970).

2) A positive set containing all interacting protein pairs functioning in a common response pathway (see 1 above) based on reliable GO process annotations. To exclude less reliable sources of annotation we used only GO evidence relying on direct assay or expert knowledge (GO evidence codes IC, IDA and TAS).

3) A negative set composed of interacting protein pairs known not be in a common response pathway similar to [9].

Supplementary Table 2B lists the resulting weights associated with individual evidence types.

Some edge weights w_{ij} were close to 1, which was unrealistic biologically and could instead indicate unusually well-studied proteins [10] or imperfectness of the assumption of conditional independence. To prevent such edges from dominating the predicting

Nature Genetics: doi:10.1038/ng.337

response networks, and to place all edges with high enough weights on equal footing, the weights w_{ij} were capped to a maximum value of 0.7. Notably, small changes in this value (0.7±0.1) gave similar results in the subsequent analyses.

Interactions between protein and gene nodes: These weights were designed to reflect the interaction's reliability based on experimental evidence and conservation. "ChIP-chip interactions" refer to interactions discovered by the ChIP-chip method. "ChIP-chip motif interactions" refer to those ChIP-chip interactions for which the gene's upstream sequence contained the binding motif of the specific transcription factor. "Reliable interactions" included those ChIP-chip motif interactions for which the motif occurrence in the gene's upstream sequence was conserved in at least two other *Saccharomyces sensu stricto* species, as well as literature-curated interactions. The weight of reliable interactions was set to 0.7. The weight of remaining ""ChIP-chip motif interactions" was set to the fraction of "ChIP-chip motif interactions" that were also reliable (0.59) , and similarly the weight of remaining ChIP-chip interactions" was set to the fraction of "ChIP-chip interactions" that were also reliable (0.51).

The ResponseNet algorithm

Directionality of ResponseNet output

The flow algorithm we employ provides a directed network. However the directionality of the interactions in the network is determined by the fact that we have connected all genetic hits to the source of flow and all differentially expressed genes to the flow sink. Therefore, except for the interactions between transcription factors and their targets, the flow does not necessarily reflect a causal order of events (Supplementary Figure 1B).

Nature Genetics: doi:10.1038/ng.337

For example, a genetic hit might be downstream of a signaling protein; yet, since the flow algorithm directs flow away from genetic hits, the signaling protein will appear downstream of its target. The reversed direction is not a cause for concern, as we are not trying to reconstruct the direction of pathways. Rather, the goal of our algorithm is to identify pathway components (nodes, not edges) that escaped experimental detection.

Analysis of the space of solutions

The optimization problem may have multiple optimal or suboptimal solutions. To characterize the space of solutions we searched for alternative optimal solutions using the method of [11]. Separately minimizing or maximizing each edge in the reported network while maintaining the same optimization score resulted in very few changes to the network. The median change in flow, the median number of nodes added and the median number of nodes lost from the resulting networks were all zero. Moreover, only 78 out of 504 edges showed a change in flow greater than 10^{-4}.

Since our analysis of the resulting networks focuses on the nodes rather than the flow values, we also examined how many nodes changed in these alternative optimal solutions.

Changes in node number upon maximizing edge flow:

Number of nodes lost	*Number of distinct solutions*
0	479
1	23
2	1
3	1

Nature Genetics: doi:10.1038/ng.337

Number of nodes added	*Number of distinct solutions*
0	499
1	5

Changes in node number upon minimizing edge flow:

Number of nodes lost	*Number of distinct solutions*
0	479
1	25

Number of nodes added	*Number of distinct solutions*
0	500
1	1
2	3

These results demonstrate that, at least for the alpha synuclein network, few alternative solutions exist and that they are very similar to the reported solution.

Assessment of ResponseNet performance on 101 datasets

We tested the ability of ResponseNet to identify cellular response pathways using DNA damage and Ste5 inactivation (main text). To test ResponseNet more broadly, we also evaluated its ability to identify hidden components in the cellular response to over one hundred distinct perturbations corresponding to inactivations of genes. For each such perturbation the genetic hits set consisted of the genetic interactors of the inactivated gene (e.g., synthetic lethals), and the differentially expressed genes were based on mRNA profiling of the inactivated strain [12]. The identity of the inactivated gene was hidden from the algorithm, and was used to evaluate the predicted network.

Nature Genetics: doi:10.1038/ng.337

In most of these cases, the true response pathways are poorly understood. Consequently, there is no perfect way to assess the results. Here we consider ResponseNet successful in revealing the cellular response to the perturbation if the nodes ResponseNet predicted fulfill one of two criteria: (i) they included the inactivated gene that was the source of perturbation, and the inactivated gene ranked significantly well, or (ii) they were significantly enriched for a specific biological process attributed to the inactivated gene. We define a specific biological process as a process annotation attributed to at most 1000 genes, including the inactivated gene, based on reliable sources (evidence codes IC, IDA or TAS).

Ranking and enrichment significance were determined by comparing ResponseNet solutions to solutions based on randomized input. Specifically, for each gene inactivation we created 100 randomized solutions: 50 randomized solutions were created by randomizing the genetic hits data while maintaining the differentially expressed genes, and 50 randomized solutions were created by randomizing the differentially expressed genes while maintaining the genetic hits data. In both cases the interactome was not randomized. Each randomized input set was solved using ResponseNet. For each inactivated gene we then compared the results obtained for the original genetic hits and differentially expressed genes to these 100 randomized-input solutions.

To be considered successful the ResponseNet solution for the original data had to:

1. Contain the inactivated gene with a rank that is better than its rank in at least 95% of the randomized-input solutions, or
2. show enrichment for the annotation of the inactivated gene that is

Nature Genetics: doi:10.1038/ng.337

(1) Significant relative to random selections of the same number of genes from the genome ($p< 0.01$ using Fisher's Exact Test), and

(2) More significant than in at least 95% of randomized-input solutions.

ResponseNet success rates for these stringent success criteria are given in Supplementary Note Table 1 below. In total, ResponseNet predictions were successful in 41% of the cases. This rate of success is relatively high considering that ResponseNet typically selected only 1% of the yeast proteins as relevant for the response, and that for the majority of the cases (85%) genetic hits data were rather limited (a median of 14 genetic hits) and no high-throughput genetic screening data are yet available. Despite the fact that relevant interactions might be missing from our data or have low probability compared with alternative paths, in 25% of the cases the inactivated gene was predicted inside the output network and highly ranked among this small fraction (a median rank of 9 from the top). We found that both success criteria contributed to this overall success. The first criterion, which is based on the prediction and ranking of the inactivated gene resulted in 25 successes. Considering that the inactivated gene was predicted only in 33 cases this is a high success rate of 76%. The second criterion resulted in 28 successes. Interestingly, the success rate for cases based on incomplete genetic hits data was 40%, compared to 47% for complete genetic screens, demonstrating that ResponseNet functions well even when limited genetic hits data are available.

The above randomization scheme verifies that ResponseNet success rates do not stem only from either the genetic hits or the differentially expressed genes data. These success rates therefore stress the benefits of integrating both types of data.

Nature Genetics: doi:10.1038/ng.337

Supplementary Note Table 1: Assessment of the algorithm on 101 genetic perturbations.

Source of genetic hits data	Number of genetic data sets	Median % of input explained[1]		Median size of predicted network	Success in predicting and ranking the inactivated gene		% Successes: Inactivated gene identified or perturbed process recovered (number)
		Genetic hits	Differentially expressed genes		% Mutations Identified (number)	Median rank	
Synthetic genetic arrays (complete screen) [13,14]	15	60%	43%	102	20% (3)	21	47% (7)
Literature (incomplete data) [1]	86	95%	56%	61	26% (22)	4	40% (34)
Synthetic genetic arrays (complete screen) and literature (incomplete data)	101	80%	54%	64	25% (25)	4	41% (41)

Setting γ value

The choice of γ primarily determines the size of the output network. Higher γ values will identify more connections between the genetic hits and the differentially expressed genes, but these connections will be of lower probability and therefore more speculative (Supplementary Note Figure 1). For the datasets with which we worked the effective γ values ranged between 7 and 20.

To identify suitable values for γ, we recommend running ResponseNet with γ values ranging between 5 and 20. For each of the output networks compute the fraction of input,

Nature Genetics: doi:10.1038/ng.337

namely genetic hits and differentially expressed genes, that are incorporated into the network, as well as the percentage of low probability edges (weights ≤ 0.3). The best γ value is the minimal value with which a significant fraction (at least 30%) of the input is incorporated while the percentage of low probability edges remains small.

To asses the performance of the ResponseNet algorithm we set γ to 10 in order to restrict solutions to relatively high-probability sub-networks. To analyze the α-syn data we used a slightly higher value of γ because the size of α-syn input sets is bigger than the median size of the validation set. In fact, the number of predicted proteins for the α-syn data with γ = 12 is 106, which is very close to the median number of predicted proteins for the validation set which was 102 predicted proteins when γ =10.

The effect on the α-syn network of varying γ value between 10 and 19 (for γ<10 the flow value was equal to zero, resulting in no output network) is presented in Supplementary Note Figure 1A, B and C. As shown in Supplementary Note Figure 1A, higher γ values incorporate more genetic hits and differentially expressed genes into the output networks, and the number of intermediary nodes increases. For example, upon setting γ to 19, the output network connects all the genetic hits (70/70, where 70 corresponds to the number of genetic hits in the interactome) and most of the differentially expressed genes (437/441, where 441 corresponds to the number of differentially expressed genes in the interactome) via 225 intermediary proteins. These numbers are about twice the numbers obtained with γ=12. The downside is that as γ increases the percentage of high confidence interactions (weights ≥ 0.7) in the network decreases, while the percentage of low confidence interactions (weights ≤ 0.3) increases as shown in Supplementary Note Figure 1B. For example, with γ=12 only two low probability edges were included in the

Nature Genetics: doi:10.1038/ng.337

output (0.007%). By contrast, with γ=19 there are 38 low confidence edges in the output network (0.05 %). Supplementary Note Figure 1C shows that more than 90% of the network proteins reported in the paper based on γ=12 also appear in networks created upon setting γ to values >12. The selection of γ=12 for the analysis of α-syn data was therefore a good compromise between having a concise network with only 2 low confidence interactions and including a big enough subset of the genetic hits (49% [34/70]) and the differentially expressed genes (38% [166/441]).

Genetic overexpression screen of a yeast model for α-synuclein pathobiology

To explore the nature of α-syn toxicity we conducted an unbiased genome wide screen for genes that when overexpressed modify α-syn toxicity in yeast. The first functional cluster of genes to emerge from that screen consisted of genes that affect ER-to-Golgi vesicle trafficking. One of the genes, Ypt1/Rab1, was tested in neuronal models of PD and was found to rescue dopaminergic neurons from α-syn toxicity [15]. Here we report for the first time the remaining genes identified upon screening an overexpression library of > 5000 yeast genes.

We identified a diverse group of genes including 55 suppressors and 22 enhancers of α-syn toxicity, many with clear human orthologs (Table 2). The major classes of genes that emerged include vesicle-trafficking genes, kinases and phosphatases, ubiquitin related proteins, transcriptional regulators, manganese transporters, and osmolyte biosynthesis genes. Importantly, some of these classes of activity have been associated with PD, yet

Nature Genetics: doi:10.1038/ng.337

were not causally linked to α-syn pathobiology. Below we briefly discuss the gene classes and their relevance to PD.

Vesicle-trafficking genes: In addition to the genes previously reported (YPT1, YKT6, ERV29, GYP8, BRE5, UBP3) we now report 10 additional vesicle-trafficking genes, making vesicle-trafficking the largest class we identified. Following the initial identification of this class we found that α-syn represses ER-to-Golgi transport[15], and inhibits fusion of budded vesicles to Golgi and other target membranes in neuronal models of PD [16]. Through these functions α-syn can influence trafficking at synapses: α-Syn knockout mice have lower pools of synaptic vesicle reserves [17], while neuronal cells overexpressing α-syn show an increase in the pool of docked, but not yet fused, secretory vesicles [18]. Together these findings illustrate the power of the yeast screen to illuminate conserved features of α-syn pathobiology as well as its normal biological function.

Kinases and phosphatases: Four phosphatases, including a catalytic subunit of protein phosphatase 2A (PP2A), strongly enhanced α-syn toxicity while three kinases and three additional phosphatases were potent suppressors. α-Syn directly activates PP2A in dopaminergic cells [19] and the phosphorylation status of α-syn itself has been implicated in modulating aggregation, toxicity and PD pathogenesis [20,21]. Also, a yeast casein kinase, Yck3, was identified in our screen as a suppressor of α-syn toxicity [22]. Since phosphorylation of α-syn on serine129 has been previously linked to inclusion formation in neuronal cells [21,22], we tested for phosphorylation of this residue in yeast. Immunoblotting confirms that α-syn is indeed phosphorylated in yeast cells (Supplementary Note Figure 2), indicating that the machinery to phosphorylate the

Nature Genetics: doi:10.1038/ng.337

protein at this residue has been conserved for over a billion years of evolution from yeast to human.

Ubiquitin-related proteins: Two ubiquitin ligases and five ubiquitin proteases are potent modifiers of α-syn toxicity. These results are consistent with previous data implicating ubiquitin-mediated protein degradation pathways in the pathogenesis of synucleinopathies, including PD. The familial PD genes PARKIN and UCH-L1 encode an E3 ubiquitin ligase and an ubiquitin protease, respectively, and α-Syn itself and other proteins are ubiquitinated in Lewy Bodies [23]. By flow cytometry we did not detect changes in steady-state α-syn protein levels in yeast cells overexpressing any of the ubiquitin-related genes (Supplementary Figure 2). Thus, in keeping with recent work in mammalian systems for PARKIN and UCH-L1 [24-26], our data suggest that these members of the ubiquitin system do no act simply by turning over α-syn.

Transcription/translation regulators: We identified regulators of diverse cellular processes mostly as suppressors of α-syn toxicity. These include Hap4, which regulates respiratory genes; Cup9, which regulates transition metal homeostasis; Fzf1, which regulates nitrosative stress and Mga2, which regulates fatty acid metabolism. Most of the abovementioned processes have been associated with Parkinsonism and α-syn toxicity previously, establishing that the causal relationships between α-syn toxicity and these processes is a fundamental, highly-conserved, feature of cell biology. That α-syn might be related to transition metal homeostasis was previously unknown.

Manganese transporters: Many reports link manganese exposure to PD and Parkinsonism [27]. Strikingly, of the tens of metal transporters we tested we recovered only

Nature Genetics: doi:10.1038/ng.337

three as α-syn modifiers, two of which are Mn^{2+} transporters (Ccc1, Pmr1). Ccc1, a strong toxicity suppressor, is predicted to detoxify Mn^{2+} by shunting it to the vacuole. Pmr1, a strong toxicity enhancer, is required for Mn^{2+} transport into Golgi, where Mn^{2+} is needed for glycosylation of secretory proteins [28].

Trehalose biosynthesis genes: Trehalose is an osmolyte that prevents native proteins from misfolding and denatured proteins from aggregating [29], and has been proposed as a potential therapeutic for polyglutamine diseases [30]. We found that three suppressors of α-syn toxicity are related to trehalose biosynthesis. A recent report has shown the efficacy of trehalose in promoting the clearance of misfolded mutant α-syn [31].

Detailed analysis of cellular pathways perturbed by α-synuclein

The output of ResponseNet consisted of 15 connected components revealing several pathways that underlay the cellular response to α-syn toxicity (Supplementary Figure 3A). Below we focus on the main implicated pathways, and describe the proteins predicted by ResponseNet in the context of their connected component.

Ubiquitin-related pathways

The presence of the ubiquitin-related pathways is in accordance with previous evidence of the pathogenesis of Parkinson Disease (PD). Indeed, two of the familial PD genes are a ubiquitin protein ligase (PARKIN) [32] and a ubiquitin C-terminal hydrolase (UCH-L1) [33]. The algorithm identifies three connected components linked to ubiquitin-related pathways.

Nature Genetics: doi:10.1038/ng.337

1. **Connected component B.** The genetic hits Hrd1 and Cdc4 are ubiquitin-protein ligases, while Ubp7 is an ubiquitin protease. ResponseNet connected these hits to the following ubiquitin-related proteins: (i) Cdc48, an ER ATPase that participates in retrotranslocation of ubiquitinated proteins from the ER to the cytosol for degradation by the proteasome; (ii) Ubi4, the ubiquitin protein; (iii) Hse1, required for sorting of ubiquitinated proteins into vesicles prior to vacuolar degradation; (iv) Tec1, a transcription factor that is regulated by ubiquitination [34]; (v) Spt23, an ER localized transcription factor that is activated by ubiquitin/proteasome-dependent processing followed by nuclear targeting. Ubi4 was also 4-fold up-regulated in response to α-syn, suggesting it may indirectly contribute to positive feedback regulation.
2. **Connected component C.** Ubp3 and Bre5, two suppressors of α-syn toxicity, form a deubiquitination complex that co-regulates anterograde and retrograde transport between ER and Golgi apparatus [35]. ResponseNet identified their interaction, and also connected them to Sir4, suggesting that they may disrupt Sir4 silencing activity [36]. Sir4 was connected to Rap1, which was assigned as regulating the expression of 11 genes: three down- and 8 up-regulated, keeping with the known role of Rap1 as both activator and repressor.
3. **Connected component E.** The regulation of the genetic hits Mga2 and Mks1 involves ubiquitin. Mga2 is closely related to Spt23 (described above), and similarly regulates Ole1 transcription [37]. Like Spt23, Mga2 is an ER localized transcription factor that is activated by ubiquitin/proteasome-dependent processing followed by nuclear targeting [38]. ResponseNet predicted Rsp5, the ubiquitin-protein ligase that activates both Mga2 and Spt23 [39].

Nature Genetics: doi:10.1038/ng.337

The genetic enhancer Mks1 is involved in retrograde mitochondria-to-nucleus signaling. ResponseNet predicted Grr1, a component of the SCF E3 ubiquitin-ligase complex, which regulates Mks1 by its polyubiquitination and degradation [40]. Interestingly, ResponseNet also predicted Rtg2, which regulates both retrograde mitochondria-to-nucleus signaling and the TOR pathway. We validated the involvement of the TOR pathway in the response to α-syn in the main text.

The relations identified by ResponseNet demonstrate the extent at which ubiquitin-related pathways can affect diverse cellular processes.

Vesicle trafficking pathways

α-syn was previously shown to repress ER-to-Golgi transport [15] and to inhibit fusion of budded vesicles to Golgi and other target membranes in neuronal models of PD [16]. Below we describe the two connected components mainly related to vesicle trafficking that were identified by ResponseNet.

1. **Connected component A.** In relation with the v-SNARE protein and genetic suppressor Ykt6 ResponseNet predicted (i) Sed5, a t-SNARE required for ER-to-Golgi vesicle trafficking; (ii) Bet1, a v-SNARE required for ER-to-Golgi vesicle trafficking; (iii)Vam3, functioning in vacuolar protein trafficking; (iv) Nyv1, a v-SNARE component of the vacuolar SNARE complex involved in vesicle fusion; (v) Atg8, a protein required for autophagy that participates in multiple membrane trafficking processes [41]; (vi) Ssa3, a chaperone protein whose over-expression has been shown to be protective towards α-syn toxicity [42]. In relation with the genetic suppressor and ER-to-Golgi Ras-like GTPase Ypt1, ResponseNet predicted Bet3 that acts in targeting and fusion of ER-to-Golgi transport vesicles, and is also a component

Nature Genetics: doi:10.1038/ng.337

of part of transport protein particle (TRAPP) complex. Downstream of Bet3 ResponseNet predicted Hsp82, the molecular chaperone and Hap1, the Hsp82 client transcription factor [43]. Hap1 is responsible for heme-dependent activation of many genes, and also plays a role in sterol metabolism, which we validated to be perturbed by α-syn.

2. **Connected component C:** The suppressor Sec21 and Tif4632 were predicted by ResponseNet to target the same transcriptional response. ResponseNet predicted (i) Arf1, a RAS-like GTPase involved in regulation of coated vesicle formation in Golgi; (ii) Rvs167, an actin-associated protein involved in endocytosis; and (iii) Pab1, a poly(A)-binding protein. The interaction between Pab1 and Arf1, selected by ResponseNet, has been reported to provide an unexpected link between COPI vesicles and mRNA and to suggest that ER-Golgi shuttle might be involved in concentrating mRNA at the ER [44]. This again demonstrates the capability of ResponseNet to identify hidden important connections among genetic hits.

Cell cycle and meiosis

Cell cycle regulation has been suggested to play part in neuronal cell death in PD [45,46]. Many proteins predicted by ResponseNet have important functions in cell cycle processes, including the transcription factors Swi5, Swi6, Mbp1 and Swi4. In particular, ResponseNet identified connected component D and G, which almost exclusively composed of cell cycle and meiosis related proteins:

1. **Connected component D**: The genetic suppressor Cdc5 is a protein kinase that plays an important role in controlling cell-cycle-dependent gene expression during mitosis. Responsenet predicted its substrates Fkh2 and Ndd1, the cell cycle regulators which

Nature Genetics: doi:10.1038/ng.337

form the Mcm1-Fkh2-Ndd1 transcription factor complex [47], and also predicted Mcm1.

The genetic suppressor Ime2 is a serine/threonine protein kinase involved in activation of meiosis. ResponseNet predicted (i) Ime1, the master regulator of meiosis, that is activated by Ime2; (ii) Cdc6, and ATP-binding protein required for DNA replication, which Ime2 is known to stabilize [48]; (iii) Orc2, a subunit of the origin recognition complex which directs DNA replication; (iv) Orc3, another subunit of the origin recognition complex; (v) Abf1, a DNA binding protein that functions in DNA replication, and (vi) Sum1, a transcriptional repressor required for mitotic repression of sporulation-specific genes.

The genetic enhancer Matalpha1 is a transcriptional regulator involved in regulation of mating-type-specific gene expression. ResponseNet connected it to the transcription factor Mcm1, which is its main target.

The genetic suppressor Stb3 is known to interact with Sin3. ResponseNet predicted (i) Sin3, a histone deacetylase that regulates several processes, including meiosis; and (ii) Ume6, a key transcriptional regulator of early meiotic genes that also forms a complex with Ime1, also predicted by ResponseNet (see above).

2. **Connected component G**: The genetic suppressor Mum2 is essential for meiotic DNA replication, and is known to interact with Orc2 (predicted by ResponseNet). ResponseNet predicted (i) Tid3, a kinetochore associated protein involved in chromosome segregation and spindle checkpoint; (ii) Dam1, another kinetochore associated protein that aids in chromosome segregation, and (iii) Cbf1, a kintechore localized transcription factor.

Nature Genetics: doi:10.1038/ng.337

Analysis of cellular pathways perturbed by α-syn, excluding general stress response genes from the transcriptional data

In an effort to exclude non-specific stress response from our predictions, we ran ResponseNet with the complete genetic data, but using only a subset of the transcriptional data from which 111 environmental stress response genes [49] were excluded. This resulted in an almost identical network. The main difference was in the pathway downstream the genetic hit Ykt6. Ykt6 is predicted to interact indirectly with Tlg2 and this interaction is absent in the reference network. Interestingly Tlg2 deletion has previously been identified as an enhancer of α-syn toxicity [50].

The list of all the predicted genes with the associated flow values and their interactors is accessible at http://fraenkel.mit.edu/ResponseNet/ResponseNet_asyn_noESR.php Alpha-synuclein (no ESR).

Yeast Strains and Media

Yeast strains used include W303 with α-syn integrated into *HIS3* and *TRP1* loci (IntTox): *MATa can1-100 his3-11,15 leu2-3,112 trp1-1 ura3-1 ade2-1* pRS303Gal-α-synWTYFPpRS304Gal-α-synWT-YFP; W303 with a-syn integrated into *TRP1* and *URA3* loci (HiTox): *MATa can1-100 his3-11,15 leu2-3,112 trp1-1 ura3-1 ade2-1* pRS304Gal-α-synWT-GFP pRS306Gal-α-synWT-GFP; W303 with one copy of a-syn integrated into *TRP1* locus (1x a-syn): *MATa can1-100 his3-11,15 leu2-3,112 trp1-1 ura3-1 ade2-1* pRS304Gal-α-synWTGFP; W303 with two copies of empty vector integrated into *TRP1* and *URA3* loci (2x vector): *MATa can1-100*

Nature Genetics: doi:10.1038/ng.337

his3-11,15 leu2-3,112 trp1-1 ura3-1 ade2-1 pRS304Gal pRS306Gal; and W303 with YFP integrated into *HIS3* locus: *MATa can1-100 his3-11,15 leu2-3,112 trp1-1 ura3-1 ade2-1* pRS303Gal-YFP. Strains were manipulated and media prepared using standard techniques.

Immunoblotting

Yeast lysates were subjected to SDS/PAGE (4-12% gradient, Invitrogen) and transferred to a PVDF membrane (Invitrogen). Membranes were blocked with 5% nonfat dry milk in PBS for 1 hr at room temperature. Primary antibody incubations were performed overnight at 4°C or at room temperature for 1-2 hours. After washing with PBS, membranes were incubated with a horseradish peroxidase-conjugated secondary antibody for 1 hour at room temperature, followed by washing in PBS+0.1% Tween 20 (PBST). Proteins were detected with SuperSignal West Dura (Pierce). Phosphoglycerate kinase 1 (Pgk1) mouse monoclonal antibody was used at 1:5000. Hsp26 rabbit polyclonal antibody (gift from Dr. Johannes Buchner) was used at 1:5000. Hsp104 mouse monoclonal antibody (4B; [51]) was used at 1:5000. S-nitosocysteine rabbit polyclonal antibody (Sigma) was used at 1:10,000.

Nature Genetics: doi:10.1038/ng.337

References

1. SGD project. "Saccharomyces Genome Database".

2. Genomica software. http://genomica.weizmann.ac.il/

3. Reguly, T. et al. Comprehensive curation and analysis of global interaction networks in Saccharomyces cerevisiae. *J Biol* **5**, 11 (2006).

4. Mewes, H.W. et al. MIPS: a database for genomes and protein sequences. *Nucleic Acids Res* **30**, 31-4 (2002).

5. Dasika, M.S., Burgard, A. & Maranas, C.D. A computational framework for the topological analysis and targeted disruption of signal transduction networks. *Biophys J* **91**, 382-98 (2006).

6. MacIsaac, K.D. et al. An improved map of conserved regulatory sites for Saccharomyces cerevisiae. *BMC Bioinformatics* **7**, 113 (2006).

7. Milo, R. et al. Network motifs: simple building blocks of complex networks. *Science* **298**, 824-7 (2002).

8. Harbison, C.T. et al. Transcriptional regulatory code of a eukaryotic genome. *Nature* **431**, 99-104 (2004).

9. Myers, C.L. et al. Discovery of biological networks from diverse functional genomic data. *Genome Biol* **6**, R114 (2005).

10. Hoffmann, R. & Valencia, A. Life cycles of successful genes. *Trends Genet* **19**, 79-81 (2003).

11. Mahadevan, R. & Schilling, C.H. The effects of alternate optimal solutions in constraint-based genome-scale metabolic models. *Metab Eng* **5**, 264-76 (2003).

12. Hughes, T.R. et al. Functional discovery via a compendium of expression profiles. *Cell* **102**, 109-26 (2000).

13. Tong, A.H. et al. Systematic genetic analysis with ordered arrays of yeast deletion mutants. *Science* **294**, 2364-8 (2001).

14. Tong, A.H. et al. Global mapping of the yeast genetic interaction network. *Science* **303**, 808-13 (2004).

15. Cooper, A.A. et al. Alpha-synuclein blocks ER-Golgi traffic and Rab1 rescues neuron loss in Parkinson's models. *Science* **313**, 324-8 (2006).

16. Gitler, A.D. et al. The Parkinson's disease protein alpha-synuclein disrupts cellular Rab homeostasis. *Proc Natl Acad Sci U S A* **105**, 145-50 (2008).

Nature Genetics: doi:10.1038/ng.337

17. Cabin, D.E. et al. Synaptic vesicle depletion correlates with attenuated synaptic responses to prolonged repetitive stimulation in mice lacking alpha-synuclein. *J Neurosci* **22**, 8797-807 (2002).

18. Larsen, K.E. et al. Alpha-synuclein overexpression in PC12 and chromaffin cells impairs catecholamine release by interfering with a late step in exocytosis. *J Neurosci* **26**, 11915-22 (2006).

19. Peng, X., Tehranian, R., Dietrich, P., Stefanis, L. & Perez, R.G. Alpha-synuclein activation of protein phosphatase 2A reduces tyrosine hydroxylase phosphorylation in dopaminergic cells. *J Cell Sci* **118**, 3523-30 (2005).

20. Chen, L. & Feany, M.B. Alpha-synuclein phosphorylation controls neurotoxicity and inclusion formation in a Drosophila model of Parkinson disease. *Nat Neurosci* **8**, 657-63 (2005).

21. Smith, W.W. et al. Alpha-synuclein phosphorylation enhances eosinophilic cytoplasmic inclusion formation in SH-SY5Y cells. *J Neurosci* **25**, 5544-52 (2005).

22. Lee, G. et al. Casein kinase II-mediated phosphorylation regulates alpha-synuclein/synphilin-1 interaction and inclusion body formation. *J Biol Chem* **279**, 6834-9 (2004).

23. Sampathu, D.M., Giasson, B.I., Pawlyk, A.C., Trojanowski, J.Q. & Lee, V.M. Ubiquitination of alpha-synuclein is not required for formation of pathological inclusions in alpha-synucleinopathies. *Am J Pathol* **163**, 91-100 (2003).

24. Lo Bianco, C. et al. Lentiviral vector delivery of parkin prevents dopaminergic degeneration in an alpha-synuclein rat model of Parkinson's disease. *Proc Natl Acad Sci U S A* **101**, 17510-5 (2004).

25. Miller, D.W. et al. Unaltered alpha-synuclein blood levels in juvenile Parkinsonism with a parkin exon 4 deletion. *Neurosci Lett* **374**, 189-91 (2005).

26. von Coelln, R. et al. Inclusion body formation and neurodegeneration are parkin independent in a mouse model of alpha-synucleinopathy. *J Neurosci* **26**, 3685-96 (2006).

27. Olanow, C.W. Manganese-induced parkinsonism and Parkinson's disease. *Ann N Y Acad Sci* **1012**, 209-23 (2004).

28. Lussier, M., Sdicu, A.M. & Bussey, H. The KTR and MNN1 mannosyltransferase families of Saccharomyces cerevisiae. *Biochim Biophys Acta* **1426**, 323-34 (1999).

29. Singer, M.A. & Lindquist, S. Multiple effects of trehalose on protein folding in vitro and in vivo. *Mol Cell* **1**, 639-48 (1998).

Nature Genetics: doi:10.1038/ng.337

30. Tanaka, M., Machida, Y. & Nukina, N. A novel therapeutic strategy for polyglutamine diseases by stabilizing aggregation-prone proteins with small molecules. *J Mol Med* **83**, 343-52 (2005).

31. Sarkar, S., Davies, J.E., Huang, Z., Tunnacliffe, A. & Rubinsztein, D.C. Trehalose, a novel mTOR-independent autophagy enhancer, accelerates the clearance of mutant huntingtin and alpha-synuclein. *J Biol Chem* **282**, 5641-52 (2007).

32. Kitada, T. et al. Mutations in the parkin gene cause autosomal recessive juvenile parkinsonism. *Nature* **392**, 605-8 (1998).

33. Liu, Y., Fallon, L., Lashuel, H.A., Liu, Z. & Lansbury, P.T., Jr. The UCH-L1 gene encodes two opposing enzymatic activities that affect alpha-synuclein degradation and Parkinson's disease susceptibility. *Cell* **111**, 209-18 (2002).

34. Bao, M.Z., Schwartz, M.A., Cantin, G.T., Yates, J.R., 3rd & Madhani, H.D. Pheromone-dependent destruction of the Tec1 transcription factor is required for MAP kinase signaling specificity in yeast. *Cell* **119**, 991-1000 (2004).

35. Cohen, M., Stutz, F., Belgareh, N., Haguenauer-Tsapis, R. & Dargemont, C. Ubp3 requires a cofactor, Bre5, to specifically de-ubiquitinate the COPII protein, Sec23. *Nat Cell Biol* **5**, 661-7 (2003).

36. Moazed, D. & Johnson, D. A deubiquitinating enzyme interacts with SIR4 and regulates silencing in S. cerevisiae. *Cell* **86**, 667-77 (1996).

37. Chellappa, R. et al. The membrane proteins, Spt23p and Mga2p, play distinct roles in the activation of Saccharomyces cerevisiae OLE1 gene expression. Fatty acid-mediated regulation of Mga2p activity is independent of its proteolytic processing into a soluble transcription activator. *J Biol Chem* **276**, 43548-56 (2001).

38. Shcherbik, N., Zoladek, T., Nickels, J.T. & Haines, D.S. Rsp5p is required for ER bound Mga2p120 polyubiquitination and release of the processed/tethered transactivator Mga2p90. *Curr Biol* **13**, 1227-33 (2003).

39. Bhattacharya, S., Zoladek, T. & Haines, D.S. WW domains 2 and 3 of Rsp5p play overlapping roles in binding to the LPKY motif of Spt23p and Mga2p. *Int J Biochem Cell Biol* **40**, 147-57 (2008).

40. Liu, Z., Spirek, M., Thornton, J. & Butow, R.A. A novel degron-mediated degradation of the RTG pathway regulator, Mks1p, by SCFGrr1. *Mol Biol Cell* **16**, 4893-904 (2005).

41. Legesse-Miller, A., Sagiv, Y., Glozman, R. & Elazar, Z. Aut7p, a soluble autophagic factor, participates in multiple membrane trafficking processes. *J Biol Chem* **275**, 32966-73 (2000).

Nature Genetics: doi:10.1038/ng.337

42. Flower, T.R., Chesnokova, L.S., Froelich, C.A., Dixon, C. & Witt, S.N. Heat shock prevents alpha-synuclein-induced apoptosis in a yeast model of Parkinson's disease. *J Mol Biol* **351**, 1081-100 (2005).

43. Lee, H.C., Hon, T., Lan, C. & Zhang, L. Structural environment dictates the biological significance of heme-responsive motifs and the role of Hsp90 in the activation of the heme activator protein Hap1. *Mol Cell Biol* **23**, 5857-66 (2003).

44. Trautwein, M., Dengjel, J., Schirle, M. & Spang, A. Arf1p provides an unexpected link between COPI vesicles and mRNA in Saccharomyces cerevisiae. *Mol Biol Cell* **15**, 5021-37 (2004).

45. West, A.B., Dawson, V.L. & Dawson, T.M. To die or grow: Parkinson's disease and cancer. *Trends Neurosci* **28**, 348-52 (2005).

46. Hoglinger, G.U. et al. The pRb/E2F cell-cycle pathway mediates cell death in Parkinson's disease. *Proc Natl Acad Sci U S A* **104**, 3585-90 (2007).

47. Darieva, Z. et al. Polo kinase controls cell-cycle-dependent transcription by targeting a coactivator protein. *Nature* **444**, 494-8 (2006).

48. Ofir, Y., Sagee, S., Guttmann-Raviv, N., Pnueli, L. & Kassir, Y. The role and regulation of the preRC component Cdc6 in the initiation of premeiotic DNA replication. *Mol Biol Cell* **15**, 2230-42 (2004).

49. Gasch, A.P. et al. Genomic expression programs in the response of yeast cells to environmental changes. *Mol Biol Cell* **11**, 4241-57 (2000).

50. Willingham, S., Outeiro, T.F., DeVit, M.J., Lindquist, S.L. & Muchowski, P.J. Yeast genes that enhance the toxicity of a mutant huntingtin fragment or alpha-synuclein. *Science* **302**, 1769-72 (2003).

51. Cashikar, A.G. et al. Defining a pathway of communication from the C-terminal peptide binding domain to the N-terminal ATPase domain in a AAA protein. *Mol Cell* **9**, 751-60 (2002).

52. Duennwald, M.L., Jagadish, S., Muchowski, P.J. & Lindquist, S. Flanking sequences profoundly alter polyglutamine toxicity in yeast. *Proc Natl Acad Sci U S A* **103**, 11045-50 (2006).

53. Chang, M., Bellaoui, M., Boone, C. & Brown, G.W. A genome-wide screen for methyl methanesulfonate-sensitive mutants reveals genes required for S phase progression in the presence of DNA damage. *Proc Natl Acad Sci U S A* **99**, 16934-9 (2002).

54. Begley, T.J., Rosenbach, A.S., Ideker, T. & Samson, L.D. Hot spots for modulating toxicity identified by genomic phenotyping and localization mapping. *Mol Cell* **16**, 117-25 (2004).

Nature Genetics: doi:10.1038/ng.337

55. Gasch, A.P. et al. Genomic expression responses to DNA-damaging agents and the regulatory role of the yeast ATR homolog Mec1p. *Mol Biol Cell* **12**, 2987-3003 (2001).

56. Workman, C.T. et al. A systems approach to mapping DNA damage response pathways. *Science* **312**, 1054-9 (2006).

Nature Genetics: doi:10.1038/ng.337

Supplementary Note Figure 1. Characterization of the solutions obtained for the α-syn data upon varying the parameter γ. Values for γ ranged between 10 and 19 with increments of 0.5. For each value of γ the α-syn data was solved using ResponseNet.
A. The relationship between γ and the number of genetic hits, transcriptional data and predicted nodes connected via ResponseNet. Higher γ values incorporate more genetic hits and differentially expressed genes into the output networks, and the number of intermediary nodes increases.
B. The relationship between γ and the frequency of high or low confidence interactions. As γ increases the percentage of high confidence interactions (weights ≥ 0.7) in the network decreases, while the percentage of low confidence interactions (weights ≤ 0.3) increases.
C. The relationship between γ and the sensitivity score. We used our preferred solution for α-syn network (γ=12) as a gold standard to calculate the sensitivity score. The network proteins identified with γ=12 also appear in networks created upon setting γ to values >12.

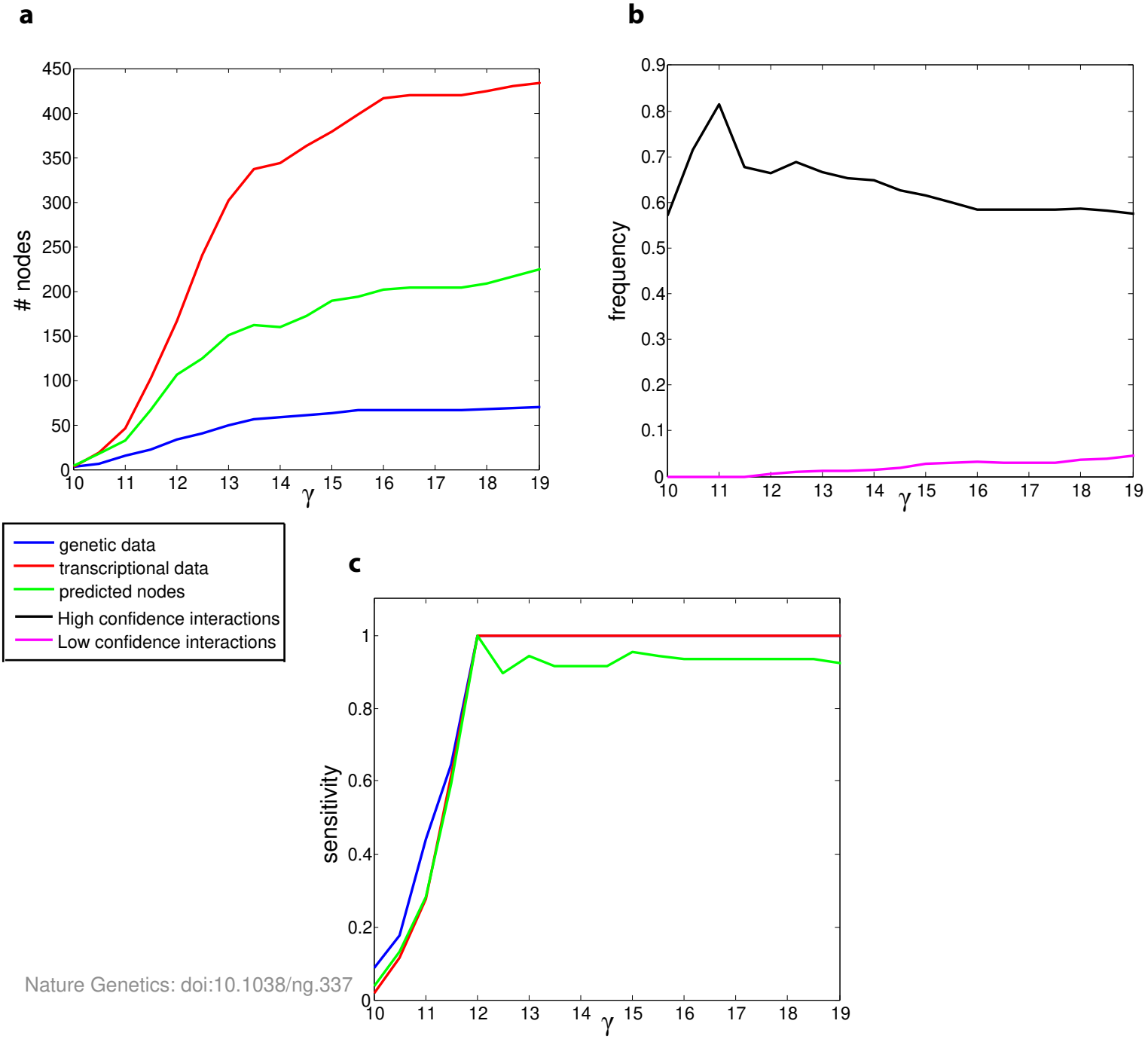

Nature Genetics: doi:10.1038/ng.337

Supplementary Note Figure 2. α-syn is phosphorylated in yeast cells. To check if α-syn is phosphorylated on serine 129 in yeast as it is in neuronal cells, lysates of yeast cells expressing wild-type or S129A mutant α-synuclein were subjected to immunoblotting with antibodies against total α-syn or α-syn phosphorylated at serine 129.

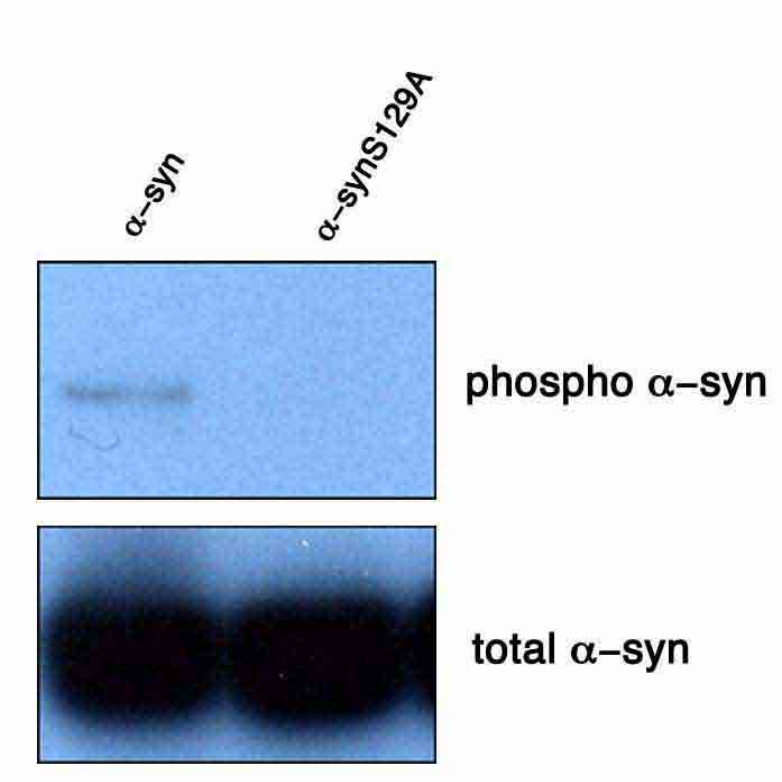

Supplementary Table 1A: Measured response to cellular perturbation.

Perturbation[a]	Transcriptional Data[b]			Genetic data[c]	Overlap			P-value[d]
	Up-regulated	Down-regulated	Total		Up-regulated	Down-regulated	Total	
Growth arrest (HU) [1,2]	51	8	59	86	0	0	0	1
DNA damage (MMS) [3,4]	152	46	198	1448	34	9	43	0.81
ER stress (tunicamycin) [1,5]	157	43	200	127	4	1	5	0.42
Fatty acid metabolism (oleate) [6,7]	-	-	269[e]	103	-	-	9	$4.1*10^{-2}$
ATP synthesis block (arsenic) [8]	-	-	828[e]	50	-	-	9	0.25
Protein biosynthesis (cycloheximide)[1,2]	6	14	20	164	0	0	0	1
Gene inactivation, screen complete (24 data sets [1,9-11])[f]	-	-	27	130	-	-	0	1
Gene inactivation, screen incomplete (149 data sets)[f]	-	-	24	12	-	-	0	1

[a] If no citation given, the transcriptional data is taken from [1] and the genetic data from [9-11].

[b] Number of differentially expressed genes defined as those showing at least a 2-fold change in expression following the perturbation or as defined in original papers.

[c] Number of genes whose genetic manipulation affects the phenotype of perturbed cells relative to wild type.

[d] Hypergeometric p-values are calculated considering 6000 genes.

[e] Signs were absent in the published transcriptional data.

[f] Median values are shown.

Supplementary Table 1B: GO annotation enrichment for combined perturbations.

Set Type	Ontology	GO_term	Cluster frequency	Background frequency	P-value
Differentially Expressed	process	carboxylic acid metabolic process	216, 7.1%	319, 4.4%	8.00E-19
Differentially Expressed	process	organic acid metabolic process	216, 7.1%	319, 4.4%	8.00E-19
Differentially Expressed	process	amino acid and derivative metabolic process	150, 4.9%	206, 2.8%	4.70E-17
Differentially Expressed	process	amino acid metabolic process	138, 4.5%	188, 2.6%	4.81E-16
Differentially Expressed	process	nitrogen compound metabolic process	173, 5.7%	253, 3.5%	2.70E-15
Differentially Expressed	process	amine metabolic process	160, 5.3%	232, 3.2%	1.54E-14
Differentially Expressed	process	amino acid biosynthetic process	85, 2.8%	107, 1.5%	1.28E-12
Differentially Expressed	process	amine biosynthetic process	89, 2.9%	116, 1.6%	1.30E-11
Differentially Expressed	process	nitrogen compound biosynthetic process	89, 2.9%	117, 1.6%	3.26E-11
Differentially Expressed	process	response to chemical stimulus	241, 7.9%	408, 5.6%	2.78E-10
Differentially Expressed	process	sulfur metabolic process	57, 1.9%	68, 0.9%	1.05E-09
Differentially Expressed	process	response to stimulus	419, 13.8%	794, 10.9%	1.59E-08
Differentially Expressed	process	glutamine family amino acid metabolic process	38, 1.2%	42, 0.6%	6.07E-08
Differentially Expressed	process	response to toxin	29, 1.0%	30, 0.4%	2.18E-07
Differentially Expressed	process	vitamin metabolic process	67, 2.2%	93, 1.3%	3.13E-06
Differentially Expressed	process	water-soluble vitamin metabolic process	67, 2.2%	93, 1.3%	3.13E-06
Differentially Expressed	function	oxidoreductase activity	218, 7.2%	276, 3.8%	2.27E-35
Differentially Expressed	function	oxidoreductase activity, acting on CH-OH group of donors	68, 2.2%	78, 1.1%	3.92E-14
Differentially Expressed	function	oxidoreductase activity, acting on the CH-OH group of donors, NAD or NADP as acceptor	62, 2.0%	70, 1.0%	1.73E-13
Differentially Expressed	function	transporter activity	219, 7.2%	379, 5.2%	3.64E-08
Differentially Expressed	function	transmembrane transporter activity	171, 5.6%	285, 3.9%	9.37E-08
Differentially Expressed	component	plasma membrane	173, 5.7%	263, 3.6%	2.85E-13
Differentially Expressed	component	fungal-type cell wall	83, 2.7%	105, 1.4%	1.37E-12
Differentially Expressed	component	external encapsulating structure	89, 2.9%	115, 1.6%	1.45E-12
Differentially Expressed	component	cell wall	89, 2.9%	115, 1.6%	1.45E-12
Differentially Expressed	component	cytosolic part	129, 4.2%	211, 2.9%	2.12E-06
Genetic Hits	process	cellular component organization and biogenesis	1261, 45.9%	2225, 30.5%	7.41E-105
Genetic Hits	process	cellular process	2174, 79.1%	4673, 64.1%	9.82E-99
Genetic Hits	process	chromosome organization and biogenesis	456, 16.6%	578, 7.9%	5.04E-96
Genetic Hits	process	biological regulation	640, 23.3%	958, 13.1%	4.94E-83
Genetic Hits	process	organelle organization and biogenesis	849, 30.9%	1447, 19.8%	6.66E-71
Genetic Hits	process	regulation of biological process	525, 19.1%	777, 10.7%	1.28E-68

Genetic Hits	process	regulation of cellular process	519, 18.9%	766, 10.5%	2.24E-68
Genetic Hits	process	response to stimulus	512, 18.6%	794, 10.9%	2.78E-56
Genetic Hits	process	cell cycle	328, 11.9%	455, 6.2%	1.95E-50
Genetic Hits	process	establishment and/or maintenance of chromatin architecture	210, 7.6%	252, 3.5%	7.38E-49
Genetic Hits	process	cell cycle process	295, 10.7%	401, 5.5%	5.65E-48
Genetic Hits	process	transcription, DNA-dependent	361, 13.1%	532, 7.3%	1.26E-45
Genetic Hits	process	RNA biosynthetic process	362, 13.2%	534, 7.3%	1.31E-45
Genetic Hits	process	transcription	384, 14.0%	577, 7.9%	1.35E-45
Genetic Hits	process	response to DNA damage stimulus	196, 7.1%	238, 3.3%	8.59E-44
Genetic Hits	process	response to endogenous stimulus	204, 7.4%	252, 3.5%	2.13E-43
Genetic Hits	process	telomere organization and biogenesis	221, 8.0%	281, 3.9%	2.69E-43
Genetic Hits	process	telomere maintenance	221, 8.0%	281, 3.9%	2.69E-43
Genetic Hits	process	DNA metabolic process	419, 15.2%	658, 9.0%	1.29E-42
Genetic Hits	process	cell cycle phase	257, 9.4%	348, 4.8%	8.54E-42
Genetic Hits	process	response to stress	335, 12.2%	497, 6.8%	5.49E-41
Genetic Hits	process	chromatin modification	183, 6.7%	222, 3.0%	8.31E-41
Genetic Hits	process	regulation of nucleobase, nucleoside, nucleotide and nucleic acid metabolic process	309, 11.2%	457, 6.3%	6.89E-38
Genetic Hits	process	regulation of cellular metabolic process	349, 12.7%	539, 7.4%	5.84E-37
Genetic Hits	process	regulation of metabolic process	357, 13.0%	557, 7.6%	1.88E-36
Genetic Hits	process	mitotic cell cycle	206, 7.5%	271, 3.7%	4.56E-36
Genetic Hits	process	post-translational protein modification	269, 9.8%	389, 5.3%	3.32E-35
Genetic Hits	process	regulation of transcription	271, 9.9%	398, 5.5%	1.34E-33
Genetic Hits	process	protein modification process	333, 12.1%	521, 7.1%	2.46E-33
Genetic Hits	process	DNA repair	157, 5.7%	193, 2.6%	3.06E-33
Genetic Hits	process	negative regulation of biological process	195, 7.1%	259, 3.6%	5.93E-33
Genetic Hits	process	negative regulation of cellular process	194, 7.1%	258, 3.5%	1.23E-32
Genetic Hits	process	regulation of transcription, DNA-dependent	254, 9.2%	369, 5.1%	1.62E-32
Genetic Hits	process	regulation of RNA metabolic process	268, 9.8%	396, 5.4%	1.83E-32
Genetic Hits	process	transcription from RNA polymerase II promoter	246, 9.0%	354, 4.9%	1.85E-32
Genetic Hits	process	signal transduction	174, 6.3%	225, 3.1%	1.00E-31
Genetic Hits	process	M phase	187, 6.8%	250, 3.4%	7.93E-31
Genetic Hits	process	cell communication	188, 6.8%	252, 3.5%	9.67E-31
Genetic Hits	process	regulation of gene expression	289, 10.5%	444, 6.1%	1.59E-30
Genetic Hits	process	cellular localization	387, 14.1%	651, 8.9%	3.63E-29
Genetic Hits	process	localization	573, 20.9%	1060, 14.5%	6.44E-29
Genetic Hits	process	establishment of cellular localization	365, 13.3%	610, 8.4%	4.50E-28

Genetic Hits	process	vesicle-mediated transport	225, 8.2%	331, 4.5%	3.50E-27
Genetic Hits	process	establishment of localization	544, 19.8%	1010, 13.9%	1.40E-26
Genetic Hits	process	regulation of biological quality	204, 7.4%	294, 4.0%	2.87E-26
Genetic Hits	process	chromatin remodeling	125, 4.5%	154, 2.1%	8.43E-26
Genetic Hits	process	negative regulation of metabolic process	159, 5.8%	213, 2.9%	1.17E-25
Genetic Hits	process	cytoskeleton organization and biogenesis	166, 6.0%	226, 3.1%	1.73E-25
Genetic Hits	process	nucleobase, nucleoside, nucleotide and nucleic acid metabolic process	842, 30.6%	1717, 23.5%	2.04E-25
Genetic Hits	process	negative regulation of cellular metabolic process	158, 5.7%	212, 2.9%	2.41E-25
Genetic Hits	process	regulation of cell cycle	131, 4.8%	165, 2.3%	2.48E-25
Genetic Hits	process	negative regulation of nucleobase, nucleoside, nucleotide and nucleic acid metabolic process	140, 5.1%	181, 2.5%	4.62E-25
Genetic Hits	process	growth	117, 4.3%	143, 2.0%	1.29E-24
Genetic Hits	process	transport	529, 19.3%	990, 13.6%	1.57E-24
Genetic Hits	process	primary metabolic process	1498, 54.5%	3388, 46.5%	2.51E-24
Genetic Hits	process	intracellular signaling cascade	123, 4.5%	155, 2.1%	1.30E-23
Genetic Hits	process	metabolic process	1594, 58.0%	3654, 50.1%	2.37E-23
Genetic Hits	process	intracellular transport	324, 11.8%	551, 7.6%	1.36E-22
Genetic Hits	process	cellular metabolic process	1548, 56.3%	3544, 48.6%	2.61E-22
Genetic Hits	process	developmental process	230, 8.4%	359, 4.9%	3.35E-22
Genetic Hits	process	chromatin assembly or disassembly	99, 3.6%	118, 1.6%	3.53E-22
Genetic Hits	process	regulation of transcription from RNA polymerase II promoter	163, 5.9%	231, 3.2%	9.31E-22
Genetic Hits	process	reproduction	213, 7.8%	328, 4.5%	1.69E-21
Genetic Hits	process	negative regulation of transcription	124, 4.5%	162, 2.2%	3.31E-21
Genetic Hits	process	regulation of cell size	96, 3.5%	115, 1.6%	4.15E-21
Genetic Hits	process	biopolymer metabolic process	1101, 40.1%	2407, 33.0%	1.58E-20
Genetic Hits	process	negative regulation of transcription, DNA-dependent	118, 4.3%	154, 2.1%	3.80E-20
Genetic Hits	process	negative regulation of RNA metabolic process	118, 4.3%	155, 2.1%	1.01E-19
Genetic Hits	process	macromolecule metabolic process	1319, 48.0%	2996, 41.1%	4.90E-18
Genetic Hits	process	secretory pathway	161, 5.9%	240, 3.3%	8.17E-18
Genetic Hits	process	chromatin assembly	85, 3.1%	103, 1.4%	8.62E-18
Genetic Hits	process	secretion by cell	163, 5.9%	246, 3.4%	3.21E-17
Genetic Hits	process	secretion	163, 5.9%	246, 3.4%	3.21E-17
Genetic Hits	process	cellular structure morphogenesis	111, 4.0%	149, 2.0%	3.96E-17
Genetic Hits	process	anatomical structure development	111, 4.0%	149, 2.0%	3.96E-17
Genetic Hits	process	cell morphogenesis	111, 4.0%	149, 2.0%	3.96E-17
Genetic Hits	process	anatomical structure morphogenesis	111, 4.0%	149, 2.0%	3.96E-17
Genetic Hits	process	response to chemical stimulus	242, 8.8%	408, 5.6%	8.36E-17

Genetic Hits	process	mitosis	99, 3.6%	129, 1.8%	1.17E-16
Genetic Hits	process	DNA packaging	89, 3.2%	112, 1.5%	1.39E-16
Genetic Hits	process	M phase of mitotic cell cycle	100, 3.6%	131, 1.8%	1.50E-16
Genetic Hits	process	gene silencing	81, 2.9%	99, 1.4%	2.12E-16
Genetic Hits	process	covalent chromatin modification	76, 2.8%	91, 1.2%	2.61E-16
Genetic Hits	process	histone modification	76, 2.8%	91, 1.2%	2.61E-16
Genetic Hits	process	biopolymer modification	355, 12.9%	656, 9.0%	2.74E-16
Genetic Hits	process	cell growth	72, 2.6%	85, 1.2%	4.66E-16
Genetic Hits	process	establishment and/or maintenance of cell polarity	93, 3.4%	120, 1.6%	4.82E-16
Genetic Hits	process	DNA replication	102, 3.7%	137, 1.9%	1.52E-15
Genetic Hits	process	meiotic cell cycle	103, 3.7%	139, 1.9%	1.84E-15
Genetic Hits	process	M phase of meiotic cell cycle	103, 3.7%	139, 1.9%	1.84E-15
Genetic Hits	process	meiosis	103, 3.7%	139, 1.9%	1.84E-15
Genetic Hits	process	filamentous growth	78, 2.8%	97, 1.3%	7.40E-15
Genetic Hits	process	heterochromatin formation	76, 2.8%	94, 1.3%	1.10E-14
Genetic Hits	process	negative regulation of gene expression, epigenetic	76, 2.8%	94, 1.3%	1.10E-14
Genetic Hits	process	chromatin silencing	76, 2.8%	94, 1.3%	1.10E-14
Genetic Hits	process	regulation of gene expression, epigenetic	78, 2.8%	99, 1.4%	6.90E-14
Genetic Hits	process	asexual reproduction	69, 2.5%	84, 1.2%	7.43E-14
Genetic Hits	process	cell budding	69, 2.5%	84, 1.2%	7.43E-14
Genetic Hits	process	establishment of cell polarity	83, 3.0%	108, 1.5%	1.03E-13
Genetic Hits	process	Golgi vesicle transport	115, 4.2%	168, 2.3%	3.94E-13
Genetic Hits	process	RNA elongation	53, 1.9%	61, 0.8%	2.76E-12
Genetic Hits	process	small GTPase mediated signal transduction	53, 1.9%	61, 0.8%	2.76E-12
Genetic Hits	process	regulation of mitosis	51, 1.9%	58, 0.8%	3.22E-12
Genetic Hits	process	cell cycle checkpoint	48, 1.7%	54, 0.7%	8.47E-12
Genetic Hits	process	actin filament-based process	82, 3.0%	111, 1.5%	8.85E-12
Genetic Hits	process	microtubule-based process	78, 2.8%	104, 1.4%	9.95E-12
Genetic Hits	process	cell division	156, 5.7%	255, 3.5%	1.19E-11
Genetic Hits	process	protein amino acid phosphorylation	76, 2.8%	101, 1.4%	1.63E-11
Genetic Hits	process	interphase	84, 3.1%	116, 1.6%	2.86E-11
Genetic Hits	process	multi-organism process	93, 3.4%	133, 1.8%	3.91E-11
Genetic Hits	process	interphase of mitotic cell cycle	83, 3.0%	115, 1.6%	5.62E-11
Genetic Hits	process	actin cytoskeleton organization and biogenesis	78, 2.8%	106, 1.5%	5.91E-11
Genetic Hits	process	reproduction of a single-celled organism	126, 4.6%	199, 2.7%	1.38E-10
Genetic Hits	process	cellular lipid metabolic process	138, 5.0%	224, 3.1%	2.07E-10
Genetic Hits	process	chromosome segregation	84, 3.1%	119, 1.6%	3.07E-10

Genetic Hits	process	pseudohyphal growth	52, 1.9%	63, 0.9%	3.99E-10
Genetic Hits	process	RNA elongation from RNA polymerase II promoter	47, 1.7%	55, 0.8%	4.34E-10
Genetic Hits	process	biopolymer catabolic process	166, 6.0%	284, 3.9%	5.03E-10
Genetic Hits	process	DNA-dependent DNA replication	76, 2.8%	105, 1.4%	5.36E-10
Genetic Hits	process	sexual reproduction	83, 3.0%	118, 1.6%	5.87E-10
Genetic Hits	process	conjugation	83, 3.0%	118, 1.6%	5.87E-10
Genetic Hits	process	conjugation with cellular fusion	83, 3.0%	118, 1.6%	5.87E-10
Genetic Hits	process	membrane organization and biogenesis	121, 4.4%	192, 2.6%	7.09E-10
Genetic Hits	process	lipid metabolic process	143, 5.2%	237, 3.3%	7.83E-10
Genetic Hits	process	double-strand break repair	48, 1.7%	58, 0.8%	2.79E-09
Genetic Hits	process	macromolecule localization	204, 7.4%	371, 5.1%	3.77E-09
Genetic Hits	process	vacuolar transport	82, 3.0%	119, 1.6%	4.75E-09
Genetic Hits	process	protein amino acid deacetylation	26, 0.9%	26, 0.4%	1.30E-08
Genetic Hits	process	response to abiotic stimulus	81, 2.9%	119, 1.6%	1.76E-08
Genetic Hits	process	telomeric heterochromatin formation	47, 1.7%	58, 0.8%	2.09E-08
Genetic Hits	process	chromatin silencing at telomere	47, 1.7%	58, 0.8%	2.09E-08
Genetic Hits	process	microtubule cytoskeleton organization and biogenesis	60, 2.2%	81, 1.1%	3.41E-08
Genetic Hits	process	sister chromatid segregation	49, 1.8%	62, 0.9%	4.25E-08
Genetic Hits	process	response to drug	85, 3.1%	129, 1.8%	7.77E-08
Genetic Hits	process	actin filament organization	48, 1.7%	61, 0.8%	9.06E-08
Genetic Hits	process	histone deacetylation	24, 0.9%	24, 0.3%	9.35E-08
Genetic Hits	process	non-recombinational repair	29, 1.1%	31, 0.4%	1.29E-07
Genetic Hits	process	response to pheromone	66, 2.4%	94, 1.3%	1.77E-07
Genetic Hits	process	invasive growth in response to glucose limitation	38, 1.4%	45, 0.6%	1.86E-07
Genetic Hits	process	nucleotide-excision repair	38, 1.4%	45, 0.6%	1.86E-07
Genetic Hits	process	vacuole organization and biogenesis	51, 1.9%	67, 0.9%	2.04E-07
Genetic Hits	process	RNA metabolic process	496, 18.0%	1069, 14.7%	2.07E-07
Genetic Hits	process	Ras protein signal transduction	34, 1.2%	39, 0.5%	3.02E-07
Genetic Hits	process	cellular component assembly	244, 8.9%	475, 6.5%	3.13E-07
Genetic Hits	process	reproductive process	113, 4.1%	188, 2.6%	3.23E-07
Genetic Hits	process	mitotic cell cycle checkpoint	28, 1.0%	30, 0.4%	3.25E-07
Genetic Hits	process	meiosis I	54, 2.0%	73, 1.0%	3.79E-07
Genetic Hits	process	mitotic sister chromatid segregation	46, 1.7%	59, 0.8%	4.04E-07
Genetic Hits	process	lipid biosynthetic process	83, 3.0%	128, 1.8%	4.44E-07
Genetic Hits	process	cell surface receptor linked signal transduction	43, 1.6%	54, 0.7%	4.60E-07
Genetic Hits	process	phosphorylation	96, 3.5%	154, 2.1%	4.65E-07
Genetic Hits	process	post-Golgi vesicle-mediated transport	52, 1.9%	70, 1.0%	6.32E-07

Genetic Hits	process	cellular homeostasis	83, 3.0%	129, 1.8%	7.92E-07
Genetic Hits	process	G2/M transition of mitotic cell cycle	31, 1.1%	35, 0.5%	8.31E-07
Genetic Hits	process	cytokinesis	75, 2.7%	114, 1.6%	1.19E-06
Genetic Hits	process	modification-dependent macromolecule catabolic process	96, 3.5%	156, 2.1%	1.28E-06
Genetic Hits	process	phosphorus metabolic process	122, 4.4%	210, 2.9%	1.30E-06
Genetic Hits	process	phosphate metabolic process	122, 4.4%	210, 2.9%	1.30E-06
Genetic Hits	process	endosome transport	40, 1.5%	50, 0.7%	1.51E-06
Genetic Hits	process	spindle organization and biogenesis	38, 1.4%	47, 0.6%	2.27E-06
Genetic Hits	process	homeostatic process	84, 3.1%	133, 1.8%	2.41E-06
Genetic Hits	process	protein localization	170, 6.2%	316, 4.3%	2.68E-06
Genetic Hits	process	protein targeting to vacuole	52, 1.9%	72, 1.0%	3.44E-06
Genetic Hits	process	negative regulation of transcription from RNA polymerase II promoter	47, 1.7%	63, 0.9%	3.50E-06
Genetic Hits	process	protein modification by small protein conjugation	59, 2.1%	85, 1.2%	3.53E-06
Genetic Hits	process	cellular protein catabolic process	97, 3.5%	161, 2.2%	5.27E-06
Genetic Hits	process	modification-dependent protein catabolic process	91, 3.3%	149, 2.0%	6.15E-06
Genetic Hits	process	ubiquitin-dependent protein catabolic process	91, 3.3%	149, 2.0%	6.15E-06
Genetic Hits	process	protein catabolic process	103, 3.7%	174, 2.4%	6.76E-06
Genetic Hits	process	protein targeting	134, 4.9%	240, 3.3%	6.94E-06
Genetic Hits	process	endocytosis	59, 2.1%	86, 1.2%	7.15E-06
Genetic Hits	process	membrane invagination	64, 2.3%	96, 1.3%	9.55E-06
Genetic Hits	process	proteolysis	105, 3.8%	179, 2.5%	9.62E-06
Genetic Hits	process	proteolysis involved in cellular protein catabolic process	92, 3.3%	152, 2.1%	9.67E-06
Genetic Hits	function	transcription regulator activity	207, 7.5%	329, 4.5%	1.19E-18
Genetic Hits	function	DNA binding	161, 5.9%	239, 3.3%	1.84E-18
Genetic Hits	function	nucleoside-triphosphatase activity	163, 5.9%	254, 3.5%	1.71E-15
Genetic Hits	function	pyrophosphatase activity	171, 6.2%	274, 3.8%	1.49E-14
Genetic Hits	function	hydrolase activity, acting on acid anhydrides	171, 6.2%	274, 3.8%	1.49E-14
Genetic Hits	function	hydrolase activity, acting on acid anhydrides, in phosphorus-containing anhydrides	171, 6.2%	274, 3.8%	1.49E-14
Genetic Hits	function	protein binding	316, 11.5%	594, 8.1%	4.14E-13
Genetic Hits	function	enzyme regulator activity	120, 4.4%	188, 2.6%	1.03E-10
Genetic Hits	function	transferase activity	355, 12.9%	703, 9.6%	1.22E-10
Genetic Hits	function	ATPase activity	123, 4.5%	195, 2.7%	1.79E-10
Genetic Hits	function	protein kinase activity	88, 3.2%	129, 1.8%	8.00E-10
Genetic Hits	function	kinase activity	124, 4.5%	202, 2.8%	2.33E-09
Genetic Hits	function	phosphotransferase activity, alcohol group as acceptor	108, 3.9%	171, 2.3%	4.68E-09
Genetic Hits	function	protein deacetylase activity	28, 1.0%	29, 0.4%	1.46E-08

Genetic Hits	function	histone deacetylase activity	28, 1.0%	29, 0.4%	1.46E-08
Genetic Hits	function	ATPase activity, coupled	89, 3.2%	136, 1.9%	2.06E-08
Genetic Hits	function	hydrolase activity	384, 14.0%	800, 11.0%	9.57E-08
Genetic Hits	function	small conjugating protein ligase activity	50, 1.8%	67, 0.9%	4.54E-07
Genetic Hits	function	protein serine/threonine kinase activity	56, 2.0%	78, 1.1%	5.16E-07
Genetic Hits	function	enzyme activator activity	48, 1.7%	64, 0.9%	7.50E-07
Genetic Hits	function	acid-amino acid ligase activity	54, 2.0%	75, 1.0%	8.77E-07
Genetic Hits	function	RNA polymerase II transcription factor activity	81, 2.9%	127, 1.7%	1.03E-06
Genetic Hits	function	deacetylase activity	29, 1.1%	33, 0.5%	2.01E-06
Genetic Hits	function	cytoskeletal protein binding	42, 1.5%	55, 0.8%	3.29E-06
Genetic Hits	function	sequence-specific DNA binding	51, 1.9%	72, 1.0%	6.32E-06
Genetic Hits	function	ubiquitin-protein ligase activity	46, 1.7%	63, 0.9%	7.19E-06
Genetic Hits	function	small protein conjugating enzyme activity	48, 1.7%	67, 0.9%	9.56E-06
Genetic Hits	component	cell part	2438, 88.7%	5505, 75.5%	4.23E-100
Genetic Hits	component	cell	2438, 88.7%	5506, 75.5%	6.30E-100
Genetic Hits	component	intracellular organelle	1930, 70.2%	4033, 55.3%	7.42E-89
Genetic Hits	component	organelle	1930, 70.2%	4034, 55.3%	1.06E-88
Genetic Hits	component	intracellular	2280, 83.0%	5098, 69.9%	5.41E-83
Genetic Hits	component	intracellular part	2262, 82.3%	5065, 69.5%	1.63E-79
Genetic Hits	component	membrane-bound organelle	1777, 64.7%	3694, 50.7%	1.71E-76
Genetic Hits	component	intracellular membrane-bound organelle	1777, 64.7%	3694, 50.7%	1.71E-76
Genetic Hits	component	protein complex	746, 27.1%	1230, 16.9%	9.12E-70
Genetic Hits	component	organelle part	1175, 42.8%	2324, 31.9%	1.60E-51
Genetic Hits	component	intracellular organelle part	1175, 42.8%	2324, 31.9%	1.60E-51
Genetic Hits	component	nucleoplasm part	230, 8.4%	315, 4.3%	3.79E-36
Genetic Hits	component	nucleoplasm	240, 8.7%	337, 4.6%	7.55E-35
Genetic Hits	component	macromolecular complex	875, 31.8%	1724, 23.6%	1.23E-34
Genetic Hits	component	nucleus	962, 35.0%	2007, 27.5%	3.89E-26
Genetic Hits	component	membrane	586, 21.3%	1113, 15.3%	5.62E-26
Genetic Hits	component	membrane part	365, 13.3%	640, 8.8%	7.79E-23
Genetic Hits	component	organelle membrane	358, 13.0%	643, 8.8%	9.14E-20
Genetic Hits	component	endoplasmic reticulum	221, 8.0%	354, 4.9%	1.57E-19
Genetic Hits	component	chromatin remodeling complex	70, 2.5%	79, 1.1%	1.99E-18
Genetic Hits	component	chromosome	162, 5.9%	244, 3.3%	1.05E-17
Genetic Hits	component	cytoplasm	1591, 57.9%	3726, 51.1%	1.62E-17
Genetic Hits	component	cytoskeletal part	131, 4.8%	188, 2.6%	9.39E-17
Genetic Hits	component	chromosomal part	142, 5.2%	211, 2.9%	4.08E-16

Genetic Hits	component	site of polarized growth	112, 4.1%	156, 2.1%	1.12E-15
Genetic Hits	component	cytoskeleton	136, 4.9%	202, 2.8%	2.17E-15
Genetic Hits	component	transcription factor complex	97, 3.5%	131, 1.8%	7.12E-15
Genetic Hits	component	endomembrane system	199, 7.2%	331, 4.5%	9.59E-15
Genetic Hits	component	Golgi apparatus	138, 5.0%	210, 2.9%	3.00E-14
Genetic Hits	component	nuclear envelope-endoplasmic reticulum network	101, 3.7%	141, 1.9%	7.13E-14
Genetic Hits	component	endoplasmic reticulum part	103, 3.7%	145, 2.0%	9.16E-14
Genetic Hits	component	Golgi apparatus part	112, 4.1%	163, 2.2%	2.17E-13
Genetic Hits	component	cellular bud	106, 3.9%	154, 2.1%	1.12E-12
Genetic Hits	component	nuclear chromosome	123, 4.5%	187, 2.6%	1.41E-12
Genetic Hits	component	endoplasmic reticulum membrane	92, 3.3%	130, 1.8%	5.65E-12
Genetic Hits	component	nuclear chromosome part	103, 3.7%	155, 2.1%	1.01E-10
Genetic Hits	component	cytoplasmic part	1179, 42.9%	2748, 37.7%	1.62E-10
Genetic Hits	component	cellular bud neck	82, 3.0%	119, 1.6%	1.62E-09
Genetic Hits	component	nuclear part	527, 19.2%	1129, 15.5%	4.39E-09
Genetic Hits	component	histone deacetylase complex	28, 1.0%	29, 0.4%	1.15E-08
Genetic Hits	component	microtubule cytoskeleton	70, 2.5%	100, 1.4%	2.05E-08
Genetic Hits	component	cell cortex	72, 2.6%	104, 1.4%	2.46E-08
Genetic Hits	component	organelle lumen	398, 14.5%	829, 11.4%	3.07E-08
Genetic Hits	component	endosome	67, 2.4%	95, 1.3%	3.17E-08
Genetic Hits	component	cell cortex part	63, 2.3%	89, 1.2%	9.29E-08
Genetic Hits	component	incipient cellular bud site	35, 1.3%	41, 0.6%	1.91E-07
Genetic Hits	component	nuclear chromatin	38, 1.4%	46, 0.6%	2.32E-07
Genetic Hits	component	nuclear lumen	302, 11.0%	613, 8.4%	2.91E-07
Genetic Hits	component	spindle	61, 2.2%	87, 1.2%	3.37E-07
Genetic Hits	component	chromatin	44, 1.6%	58, 0.8%	1.59E-06
Genetic Hits	component	histone acetyltransferase complex	34, 1.2%	41, 0.6%	1.63E-06
Genetic Hits	component	endosomal part	26, 0.9%	29, 0.4%	4.28E-06
Genetic Hits	component	microtubule organizing center	46, 1.7%	63, 0.9%	5.67E-06
Genetic Hits	component	spindle pole body	46, 1.7%	63, 0.9%	5.67E-06

Supplementary Table 1C: GO process and function annotations enriched in >= 20% of the sets of genetic hits or >= 20% of the sets of differentially expressed genes for the perturbations with complete genetic screens available.

GO annotation	Set type	# of enriched sets	Median enrichment
Amine biosynthetic process	Differentially expressed	8	2.04E-08
Arginine metabolic process	Differentially expressed	8	0.000182
Oxidoreductase activity	Differentially expressed	8	2.09E-05
Arginine biosynthetic process	Differentially expressed	7	9.87E-06
Glutamine family amino acid biosynthetic process	Differentially expressed	7	0.000881
Organic acid metabolic process	Differentially expressed	7	1.38E-06
Structural constituent of cell wall	Differentially expressed	6	6.95E-05
Sulfur compound biosynthetic process	Differentially expressed	6	7.64E-05
Sulfur metabolic process	Differentially expressed	6	2.27E-07
Vitamin biosynthetic process	Differentially expressed	6	2.39E-05
Biological regulation	Genetic Hits	23	1.59E-11
Response to stimulus	Genetic Hits	23	1.73E-09
Regulation of cellular process	Genetic Hits	22	2.69E-10
Response to stress	Genetic Hits	21	7.14E-10
Cell cycle	Genetic Hits	20	2.39E-11
Cell cycle phase	Genetic Hits	20	2.84E-12
Developmental process	Genetic Hits	20	4.85E-07
Mitotic cell cycle	Genetic Hits	20	1.26E-09
M phase	Genetic Hits	19	1.88E-13
Mitosis	Genetic Hits	19	2.26E-08
Regulation of cell cycle	Genetic Hits	19	2.61E-07
DNA metabolic process	Genetic Hits	18	2.31E-27
Sister chromatid segregation	Genetic Hits	18	8.71E-07
Telomere maintenance	Genetic Hits	18	7.59E-14
Chromosome segregation	Genetic Hits	17	3.95E-08
DNA packaging	Genetic Hits	17	1.02E-14
DNA repair	Genetic Hits	17	4.71E-13
Protein binding	Genetic Hits	17	3.31E-07
response to DNA damage stimulus	Genetic Hits	17	1.08E-16
Chromatin remodeling	Genetic Hits	16	3.94E-11
DNA recombination	Genetic Hits	16	3.49E-09
Double-strand break repair	Genetic Hits	16	1.83E-09
Non-recombinational repair	Genetic Hits	16	5.72E-10
Post-translational protein modification	Genetic Hits	16	1.63E-08
Regulation of metabolic process	Genetic Hits	16	3.77E-11
Transcription	Genetic Hits	16	1.75E-09
Cell cycle checkpoint	Genetic Hits	15	2.04E-07
DNA binding	Genetic Hits	15	1.69E-06

Gene silencing	Genetic Hits	15	1.93E-07
Mitotic sister chromatid cohesion	Genetic Hits	15	1.50E-08
Negative regulation of cellular process	Genetic Hits	15	6.70E-10
Chromatin assembly or disassembly	Genetic Hits	14	8.70E-07
Double-strand break repair via nonhomologous end joining	Genetic Hits	14	1.43E-05
Meiosis	Genetic Hits	14	2.31E-08
Negative regulation of transcription	Genetic Hits	14	3.61E-08
Recombinational repair	Genetic Hits	14	1.38E-06
Regulation of transcription	Genetic Hits	14	4.40E-09
Sister chromatid cohesion	Genetic Hits	14	4.95E-08
Cytoskeletal protein binding	Genetic Hits	13	3.04E-08
DNA replication	Genetic Hits	13	3.02E-10
Histone modification	Genetic Hits	13	1.32E-09
Organelle localization	Genetic Hits	13	2.07E-06
regulation of DNA recombination	Genetic Hits	13	2.76E-06
RNA elongation	Genetic Hits	13	7.94E-07
RNA metabolic process	Genetic Hits	13	1.08E-07
Chromatin silencing at silent mating-type cassette	Genetic Hits	12	1.86E-05
DNA-dependent ATPase activity	Genetic Hits	12	1.71E-06
Double-strand break repair via single-strand annealing	Genetic Hits	12	4.11E-08
Double-strand break repair via synthesis-dependent strand an	Genetic Hits	12	1.04E-06
negative regulation of DNA metabolic process	Genetic Hits	12	1.11E-08
negative regulation of DNA recombination	Genetic Hits	12	3.18E-05
regulation of DNA metabolic process	Genetic Hits	12	4.05E-08
transcription from RNA polymerase II promoter	Genetic Hits	12	3.40E-06
Transposition	Genetic Hits	12	3.18E-05
Cell development	Genetic Hits	11	6.61E-05
Chromatin silencing at telomere	Genetic Hits	11	2.10E-06
DNA-dependent DNA replication	Genetic Hits	11	6.28E-09
Histone deacetylation	Genetic Hits	11	1.93E-05
meiosis I	Genetic Hits	11	1.07E-06
Regulation of biological quality	Genetic Hits	11	2.60E-05
Regulation of mitosis	Genetic Hits	11	8.97E-06
Response to chemical stimulus	Genetic Hits	11	9.54E-05
Deacetylase activity	Genetic Hits	10	0.000111
Gene conversion at mating-type locus	Genetic Hits	10	7.74E-05
Heteroduplex formation	Genetic Hits	10	2.23E-05
Histone exchange	Genetic Hits	10	1.77E-09
Meiotic recombination	Genetic Hits	10	9.24E-06
Mitotic recombination	Genetic Hits	10	3.44E-06
negative regulation of DNA replication	Genetic Hits	10	5.26E-05
regulation of transcription from RNA polymerase II promoter	Genetic Hits	10	3.91E-05

Telomere maintenance via recombination	Genetic Hits	10	0.0001
Transcription regulator activity	Genetic Hits	10	6.36E-06
Vesicle-mediated transport	Genetic Hits	10	6.63E-05
Cell morphogenesis	Genetic Hits	9	0.000142
Cellular localization	Genetic Hits	9	1.45E-09
Conjugation	Genetic Hits	9	0.000387
DNA replication checkpoint	Genetic Hits	9	7.95E-06
Double-strand break repair via break-induced replication	Genetic Hits	9	6.41E-06
general RNA polymerase II transcription factor activity	Genetic Hits	9	0.000113
Histone methylation	Genetic Hits	9	2.14E-06
Meiotic chromosome segregation	Genetic Hits	9	1.55E-05
Microtubule motor activity	Genetic Hits	9	8.52E-06
Nucleic acid binding	Genetic Hits	9	0.000165
Postreplication repair	Genetic Hits	9	0.000206
Reproduction	Genetic Hits	9	6.81E-05
Tubulin binding	Genetic Hits	9	2.64E-12
Vacuolar transport	Genetic Hits	9	2.57E-05
Biopolymer catabolic process	Genetic Hits	8	0.000146
DNA integrity checkpoint	Genetic Hits	8	1.62E-06
Establishment of localization	Genetic Hits	8	7.12E-05
Establishment of organelle localization	Genetic Hits	8	5.81E-08
Hydrolase activity, acting on carbon-nitrogen (but not peptide)	Genetic Hits	8	0.000361
Interphase	Genetic Hits	8	1.59E-05
Meiotic gene conversion	Genetic Hits	8	2.25E-05
Microtubule-based process	Genetic Hits	8	1.74E-15
Motor activity	Genetic Hits	8	6.72E-05
Nucleotide-excision repair	Genetic Hits	8	2.50E-07
Protein modification by small protein conjugation	Genetic Hits	8	0.000344
regulation of DNA replication	Genetic Hits	8	6.12E-06
Response to drug	Genetic Hits	8	0.000122
Cell communication	Genetic Hits	7	9.67E-08
Deoxyribonuclease activity	Genetic Hits	7	8.43E-05
DNA replication initiation	Genetic Hits	7	0.000197
DNA strand elongation	Genetic Hits	7	2.61E-07
Lagging strand elongation	Genetic Hits	7	4.68E-05
Methylation	Genetic Hits	7	0.00029
Microtubule-based movement	Genetic Hits	7	1.69E-07
Mismatch repair	Genetic Hits	7	8.37E-05
Nuclear migration	Genetic Hits	7	2.13E-08
Protein amino acid acetylation	Genetic Hits	7	2.42E-05
Protein kinase activity	Genetic Hits	7	0.00061
Pyrophosphatase activity	Genetic Hits	7	0.000231

Response to osmotic stress	Genetic Hits	7	0.000103
sequence-specific DNA binding	Genetic Hits	7	0.000102
Sex determination	Genetic Hits	7	1.86E-05
Signal transducer activity	Genetic Hits	7	1.02E-06
single-stranded DNA binding	Genetic Hits	7	1.29E-05
Spindle localization	Genetic Hits	7	1.14E-07
Aging	Genetic Hits	6	0.000386
chromatin silencing at rDNA	Genetic Hits	6	0.000223
Cyclin-dependent protein kinase activity	Genetic Hits	6	0.00214
DNA topological change	Genetic Hits	6	0.00145
Endocytosis	Genetic Hits	6	0.00082
Establishment of cell polarity	Genetic Hits	6	5.22E-08
Growth	Genetic Hits	6	3.27E-10
Histone acetylation	Genetic Hits	6	0.000902
Hydrolase activity	Genetic Hits	6	2.01E-05
Karyogamy	Genetic Hits	6	1.58E-05
Leading strand elongation	Genetic Hits	6	1.05E-05
Microtubule depolymerization	Genetic Hits	6	0.000849
Microtubule polymerization or depolymerization	Genetic Hits	6	5.88E-05
Nucleosome assembly	Genetic Hits	6	2.24E-05
Nucleotidyltransferase activity	Genetic Hits	6	0.00151
One-carbon compound metabolic process	Genetic Hits	6	0.000991
Organelle fusion	Genetic Hits	6	8.10E-05
Protein amino acid acylation	Genetic Hits	6	0.000131
Protein folding	Genetic Hits	6	0.000726
Protein targeting to vacuole	Genetic Hits	6	0.000278
Replicative cell aging	Genetic Hits	6	0.000342
RNA catabolic process	Genetic Hits	6	0.000746
RNA polymerase II transcription elongation factor activity	Genetic Hits	6	3.72E-05
Secretion	Genetic Hits	6	1.18E-12
Structural constituent of cytoskeleton	Genetic Hits	6	0.00184
structure-specific DNA binding	Genetic Hits	6	2.46E-05

Supplementary Table 1D: GO process and function annotations enriched in the combined perturbations with complete genetic screens available.

These are limited to annotations enriched in at least 20% of the sets when analyzed separately.

GO annotation	Set type	Enrichment p-value	% in set
Oxidoreductase activity	Differentially expressed	6.21E-25	8.28
Organic acid metabolic process	Differentially expressed	6.76E-10	7.37
Amine biosynthetic process	Differentially expressed	2.77E-11	3.53
Sulfur metabolic process	Differentially expressed	1.17E-13	2.57
Vitamin biosynthetic process	Differentially expressed	9.54E-06	1.45
Glutamine family amino acid biosynthetic process	Differentially expressed	0.000287	0.91
Sulfur compound biosynthetic process	Differentially expressed	3.08E-06	0.81
Arginine metabolic process	Differentially expressed	0.000534	0.59
Structural constituent of cell wall	Differentially expressed	0.00336	0.49
Arginine biosynthetic process	Differentially expressed	0.00134	0.43
Biological regulation	Differentially expressed	7.92E-35	20.72
Establishment of localization	Genetic Hits	4.23E-10	18.55
Response to stimulus	Genetic Hits	2.32E-31	17.25
Developmental process	Genetic Hits	1.37E-15	16.43
Regulation of cellular process	Genetic Hits	8.48E-29	16.3
RNA metabolic process	Genetic Hits	0.00147	16.04
DNA metabolic process	Genetic Hits	1.89E-52	14.78
Hydrolase activity	Genetic Hits	6.73E-05	13.44
Cellular localization	Genetic Hits	6.94E-14	12.96
Transcription	Genetic Hits	1.57E-18	12.09
Response to stress	Genetic Hits	3.80E-26	11.83
Regulation of metabolic process	Genetic Hits	1.04E-16	11.31
Cell cycle	Genetic Hits	3.83E-28	11.05
Protein binding	Genetic Hits	2.83E-15	10.1
Post-translational protein modification	Genetic Hits	2.25E-18	9.1
Cell cycle phase	Genetic Hits	1.03E-25	9.02
Cell development	Genetic Hits	0.00021	8.76
Telomere maintenance	Genetic Hits	3.99E-40	8.67
Regulation of transcription	Genetic Hits	4.04E-16	8.58
Vesicle-mediated transport	Genetic Hits	3.67E-14	7.67
Response to chemical stimulus	Genetic Hits	1.21E-08	7.54
DNA packaging	Genetic Hits	6.93E-31	7.46
response to DNA damage stimulus	Genetic Hits	5.08E-32	7.2
transcription from RNA polymerase II promoter	Genetic Hits	3.15E-11	7.11
M phase	Genetic Hits	3.53E-20	6.89
Mitotic cell cycle	Genetic Hits	2.27E-19	6.68
Reproduction	Genetic Hits	8.43E-08	6.63
Cell morphogenesis	Genetic Hits	7.55E-18	6.59
Transcription regulator activity	Genetic Hits	4.35E-05	6.46
Pyrophosphatase activity	Genetic Hits	2.10E-07	6.07
Regulation of biological quality	Genetic Hits	4.13E-11	5.98
Negative regulation of cellular process	Genetic Hits	3.18E-15	5.81
DNA binding	Genetic Hits	2.42E-12	5.64
DNA repair	Genetic Hits	8.42E-23	5.59
Secretion	Genetic Hits	7.95E-09	5.55
Biopolymer catabolic process	Genetic Hits	0.00191	5.16
Cell communication	Genetic Hits	2.63E-08	5.12
regulation of transcription from RNA polymerase II promoter	Genetic Hits		

Chromatin remodeling	Genetic Hits	9.39E-09	4.9
Regulation of cell cycle	Genetic Hits	6.94E-18	4.55
Negative regulation of transcription	Genetic Hits	3.01E-14	4.55
Meiosis	Genetic Hits	6.42E-13	4.12
Chromatin assembly or disassembly	Genetic Hits	3.37E-13	4.03
Growth	Genetic Hits	8.53E-16	3.56
Mitosis	Genetic Hits	9.72E-09	3.56
DNA replication	Genetic Hits	4.94E-10	3.38
Protein kinase activity	Genetic Hits	5.93E-12	3.3
Response to drug	Genetic Hits	5.52E-08	3.3
Establishment of cell polarity	Genetic Hits	9.18E-10	3.25
DNA recombination	Genetic Hits	2.11E-14	3.21
ATPase activity, coupled	Genetic Hits	2.60E-13	3.21
Chromosome segregation	Genetic Hits	1.80E-05	3.17
Vacuolar transport	Genetic Hits	1.57E-08	3.08
Gene silencing	Genetic Hits	6.79E-11	2.95
Microtubule-based process	Genetic Hits	5.09E-12	2.78
Histone modification	Genetic Hits	8.93E-10	2.78
DNA-dependent DNA replication	Genetic Hits	7.58E-14	2.65
Interphase	Genetic Hits	1.60E-09	2.65
Conjugation	Genetic Hits	1.74E-06	2.39
meiosis I	Genetic Hits	0.00302	2.39
Endocytosis	Genetic Hits	5.93E-11	2.21
Response to osmotic stress	Genetic Hits	2.66E-05	2.08
Protein modification by small protein conjugation	Genetic Hits	7.54E-07	1.95
Organelle localization	Genetic Hits	0.000126	1.91
Protein targeting to vacuole	Genetic Hits	2.00E-11	1.87
Double-strand break repair	Genetic Hits	1.93E-07	1.87
Signal transducer activity	Genetic Hits	1.03E-10	1.78
Sister chromatid segregation	Genetic Hits	6.51E-07	1.69
Cell cycle checkpoint	Genetic Hits	2.51E-06	1.69
Cytoskeletal protein binding	Genetic Hits	5.74E-08	1.65
Regulation of mitosis	Genetic Hits	5.74E-08	1.65
Meiotic recombination	Genetic Hits	1.18E-07	1.61
Chromatin silencing at telomere	Genetic Hits	1.03E-07	1.56
DNA-dependent ATPase activity	Genetic Hits	2.20E-06	1.52
RNA elongation	Genetic Hits	8.37E-06	1.48
Hydrolase activity, acting on carbon-nitrogen (but not peptide) bonds, in lin	Genetic Hits	2.12E-08	1.43
Non-recombinational repair	Genetic Hits	1.55E-05	1.39
Protein amino acid acylation	Genetic Hits	1.01E-11	1.3
Deacetylase activity	Genetic Hits	0.00548	1.3
One-carbon compound metabolic process	Genetic Hits	2.45E-09	1.22
Nucleotide-excision repair	Genetic Hits	0.00313	1.22
sequence-specific DNA binding	Genetic Hits	8.28E-07	1.17
Establishment of organelle localization	Genetic Hits	0.000183	1.17
Protein amino acid acetylation	Genetic Hits	7.44E-09	1.09
Histone deacetylation	Genetic Hits	0.00164	1.09
Methylation	Genetic Hits	2.25E-11	1.04
structure-specific DNA binding	Genetic Hits	0.00174	1.04
regulation of DNA metabolic process	Genetic Hits	1.72E-05	1
Chromatin silencing at silent mating-type cassette	Genetic Hits	1.73E-06	0.96
Double-strand break repair via nonhomologous end joining	Genetic Hits	1.45E-05	0.96

Recombinational repair	Genetic Hits	5.32E-08	0.91
DNA strand elongation	Genetic Hits	2.55E-05	0.87
Histone acetylation	Genetic Hits	0.000635	0.87
Mismatch repair	Genetic Hits	0.00353	0.87
Deoxyribonuclease activity	Genetic Hits	2.00E-05	0.83
DNA replication initiation	Genetic Hits	0.000135	0.83
Sister chromatid cohesion	Genetic Hits	0.00217	0.83
Nuclear migration	Genetic Hits	0.00389	0.78
negative regulation of DNA metabolic process	Genetic Hits	2.18E-06	0.74
Histone methylation	Genetic Hits	8.12E-08	0.7
Tubulin binding	Genetic Hits	5.44E-06	0.7
DNA integrity checkpoint	Genetic Hits	5.44E-06	0.7
Lagging strand elongation	Genetic Hits	5.37E-05	0.65
ATP-dependent chromatin remodeling	Genetic Hits	0.000452	0.65
Meiotic gene conversion	Genetic Hits	0.00221	0.65
Meiotic chromosome segregation	Genetic Hits	0.00221	0.65
Microtubule-based movement	Genetic Hits	6.25E-06	0.61
Motor activity	Genetic Hits	6.25E-06	0.61
Postreplication repair	Genetic Hits	0.000125	0.61
Gene conversion at mating-type locus	Genetic Hits	0.000289	0.57
single-stranded DNA binding	Genetic Hits	0.00198	0.57
Double-strand break repair via single-strand annealing	Genetic Hits	0.000197	0.52
regulation of DNA recombination	Genetic Hits	1.34E-05	0.48
Spindle localization	Genetic Hits	0.000108	0.48
regulation of DNA replication	Genetic Hits	3.73E-05	0.44
negative regulation of DNA recombination	Genetic Hits	0.00327	0.44
Transposition	Genetic Hits	0.000104	0.39
Double-strand break repair via synthesis-dependent strand annealing	Genetic Hits	0.000104	0.39
Nucleosome assembly	Genetic Hits	0.00261	0.39
Microtubule motor activity	Genetic Hits	0.00261	0.39
negative regulation of DNA replication	Genetic Hits	0.00176	0.35
Cyclin-dependent protein kinase activity	Genetic Hits	0.000797	0.31
Histone exchange	Genetic Hits	0.00437	0.31
Double-strand break repair via break-induced replication	Genetic Hits	0.00437	0.31
	Genetic Hits	0.00221	0.26

Supplementary Table 2A: Yeast interactome data.

Interaction Type	Number of interacting pairs
Physical	33,765
MIPS Complex	11,014
Metabolic	2,882
Regulatory interactions between transcription factors	207
Protein-DNA interactions	5256 Reliable interactions [a], 3664 ChIP-chip motif interactions [b], 5143 ChIP-chip interactions [c]

[a] Reliable interactions include those ChIP-chip motif interactions for which the motif occurrence in the gene's upstream sequence was conserved in at least two other *Saccharomyces sensu stricto* species, as well as literature-curated interactions.
[b] ChIP-chip motif interactions refer to those ChIP-chip interactions for which the gene's upstream sequence contained the binding motif of the specific transcription factor.
[c] ChIP-chip interactions refer to interactions discovered by the ChIP-chip method.

Supplementary Table 2B: Interaction weights associated with individual types of evidence for protein-protein interaction.

Type of interaction evidence	Probability[1]
Two-hybrid HTP	0.061056
Product-Substrate	0.06908
Affinity Capture-MS HTP	0.216939
Affinity Capture-MS LC	0.255753
Co-purification HTP	0.279417
Affinity Capture-Western HTP	0.312123
Co-fractionation HTP	0.350432
Reconstituted Complex HTP	0.403046
Two-hybrid LC	0.464472
Biochemical Activity LC	0.489647
Biochemical Activity HTP	0.552508
Protein-peptide LC	0.674045
Affinity Capture-Western LC	0.682404
Co-localization LC	0.700851
Transcription Factor -> Transcription Factor	0.71149
Protein-peptide HTP	0.756207
Reconstituted Complex LC	0.789035
MIPS	0.801993
Protein-RNA LC	0.805288
Co-purification LC	0.843226
Co-fractionation LC	0.871346
Co-crystal Structure HTP	0.961121

[1] As described in the Methods section, in our weighting scheme each interaction between two protein nodes p_i, p_j.is associated with a weight w_{ij} such that $w_{ij} = \mathrm{P}(RP_{p_i p_j} = 1 \mid I_{p_i p_j})$ I is a vector of indicator functions such that each function corresponds to a different type of interaction evidence. To estimate the weight w_k associated with interaction evidence type k we assumed an interaction between two proteins was supported by evidence type k alone. We therefore computed w_k based on a vector I_k whose k-th entry was set to 1 and all other entries to 0 and using the formula above.

Supplementary Table 3A: Yeast genes that modify α-syn toxicity when overexpressed.

Yeast Gene	Type	Strength	Human ortholog(s)	Proposed function
Amino Acid Transport				
AVT4	suppressor	3	SLC36A1 SLC36A2 SLC36A3 SLC36A4	Vacuolar transporter; exports large neutral amino acids from the vacuole
DIP5	suppressor	3	SLC7A1 SLC7A14 SLC7A2 SLC7A3 SLC7A4 SLC7A13	Dicarboxylic amino acid permease
LST8	suppressor	3	GBL	Component of the TOR signaling pathway
Autophagy				
NVJ1	suppressor	2		Nuclear envelope protein; functions during piecemeal microautophagy of the nucleus (PMN)
Cytoskeleton				
ICY1	suppressor	4		Protein that interacts with the cytoskeleton
ICY2	suppressor	4		Protein that interacts with the cytoskeleton
Manganese transport				
CCC1	suppressor	4		Putative vacuolar Fe2+/Mn2+ transporter
PMR1	enhancer	-7	ATP2C1 ATP2C2	High affinity Ca2+/Mn2+ P-type ATPase required for Ca2+ and Mn2+ transport into Golgi
Protein phosphorylation				
IME2	suppressor	4	ICK	Serine/threonine protein kinase involved in activation of meiosis
PTP2	suppressor	3	PTPRE, PTPRC, PTPN22, PTPRG	Phosphotyrosine-specific protein phosphatase involved in osmolarity sensing
GIP2	suppressor	3	PPP1R3A PPP1R3B PPP1R3C PPP1R3D PPP1R3E	Putative regulatory subunit of the protein phosphatase Glc7p, involved in glycogen metabolism
YCK3	suppressor	3	CSNK1G1 CSNK1G2 CSNK1G3	Palmitoylated, vacuolar membrane-localized casein kinase I isoform
RCK1	suppressor	3	CAMK1G	Protein kinase involved in the response to oxidative stress
CDC5	suppressor (Cdc5 overexpression is toxic; in presence of a-syn it rescues/rescued)	3	PLK2	Polo-like kinase; found at bud neck, nucleus and SPBs; has multiple functions in mitosis and cytokinesis
PTC4	suppressor	1	PPM1G	Cytoplasmic type 2C protein phosphatase
SIT4	enhancer	-2	PPP6C	Type 2A-related serine-threonine phosphatase.

CAX4	enhancer	-3	DOLPP1	Dolichyl pyrophosphate phosphatase, required for Dol-P-P-linked oligosaccharide intermediate synthesis and protein N-glycosylation.
PPZ2	enhancer	-3	PPP1CC PPP1CB PPP1CA	Serine/threonine protein phosphatase Z
PPZ1	enhancer	-8	PPP1CA PPP1CB PPP1CC	Serine/threonine protein phosphatase Z
Transcription/Translation				
CUP9	suppressor	3	MEIS1 MEIS2 MEIS3 NR_002211.1 PKNOX1 PKNOX2 Q99687-3 TGIF1 TGIF2 TGIF2LX TGIF2LY	Transcriptional repressor involved in copper ion homeostasis
HAP4	suppressor	4		Transcriptional activator and global regulator of respiratory gene expression
FZF1	suppressor	3	KLF15 KLF11 ZNF624	Key transcriptional regulator of cellular response to nitrosative stress
MGA2	suppressor	3	ANKRD1 OSBPL1A	ER membrane protein involved in regulation of OLE1 transcription
MKS1	enhancer	-5		Pleiotropic negative transcriptional regulator involved in Ras-CAMP and lysine biosynthetic pathways and nitrogen regulation; involved in retrograde (RTG) mitochondria-to-nucleus signaling
VHR1	suppressor	3		Transcriptional activator
JSN1	suppressor	2	PUM1	Member of the Puf family of RNA-binding proteins, interacts with mRNAs encoding membrane-associated proteins
SUT2	enhancer	-3		Putative transcription factor; multicopy suppressor of mutations that cause low activity of the cAMP/protein kinase A pathway
TIF4632	suppressor	3	EIF4G1 EIF4G2 EIF4G3	Translation initiation factor eIF4G, subunit of the mRNA cap-binding protein complex (eIF4F)
STB3	suppressor	3		Protein that binds Sin3p in a two-hybrid assay.
MATALPHA1	enhancer	-5		Transcriptional co-activator involved in regulation of mating-type-specific gene expression
Trehalose biosynthesis				
UGP1	suppressor	4	UGP2	UDP-glucose pyrophosphorylase, catalyses the formation of UDP-Glc, a precursor to trehalose
TPS3	suppressor	3		Regulatory subunit of trehalose-6-phosphate synthase/phosphatase complex, which synthesizes trehalose
NTH1	suppressor	2	TREH	Neutral trehalase, degrades trehalose; required for thermotolerance and may mediate resistance to other cellular stresses
Ubiquitin-related				
CDC4	suppressor	4	FBXW7	F-box, associates with Skp1p and Cdc53p to form

				a complex, SCFCdc4, which acts as ubiquitin-protein ligase
UIP5	suppressor	4		Protein of unknown function that interacts with Ulp1p, a Ubl (ubiquitin-like protein)-specific protease
HRD1	suppressor	4	AMFR SYVN1	Ubiquitin-protein ligase required for endoplasmic reticulum-associated degradation (ERAD) of misfolded proteins
UBP11	enhancer	-3	USP21	Ubiquitin-specific protease that cleaves ubiquitin from ubiquitinated proteins.
UBP7	enhancer	-4	USP21	Ubiquitin-specific protease that cleaves ubiquitin-protein fusions.
Vesicular transport, ER-Golgi				
YPT1	suppressor	5	RAB10 RAB13 RAB1A RAB1C RAB8A RAB8B	Ras-like small GTPase, involved in the ER-to-Golgi step of the secretory pathway
YKT6	suppressor	4	YKT6	v-SNARE involved in trafficking to and within the Golgi, endocytic trafficking to the vacuole, and vacuolar fusion
BRE5	suppressor	4	G3BP2	Ubiquitin protease cofactor, forms deubiquitination complex with Ubp3p to regulate ER-Golgi transport
SEC21	suppressor	4	COPG2 COPG	Gamma subunit of coatomer, a heptameric protein complex that together with Arf1p forms the COPI coat
UBP3	suppressor	3	USP10	Ubiquitin-specific protease that interacts with Bre5p to co-regulate anterograde and retrograde transport between ER and Golgi
ERV29	suppressor	3	SURF4	Protein localized to COPII-coated vesicles, involved in vesicle formation and incorporation of specific secretory cargo.
SEC28	suppressor	3	COPE	Epsilon-COP subunit of the coatomer; regulates retrograde Golgi-to-ER protein traffic; stabilizes Cop1p
SFT1	suppressor	2	mouse BET1	Intra-Golgi v-SNARE, required for transport of proteins between an early and a later Golgi compartment.
GLO3	enhancer	-1	ARFGAP3 ZNF289	ADP-ribosylation factor GTPase activating protein (ARF GAP), involved in ER-Golgi transport
TRS120	enhancer	-2	NIBP	One of 10 subunits of the transport protein particle (TRAPP) complex of the cis-Golgi which mediates vesicle docking and fusion
GYP8	enhancer	-2	TBC1D20	GTPase-activating protein for yeast Rab family members; Ypt1p is the preferred in vitro substrate
YIP3	enhancer	-2	RABAC1	Protein localized to COPII vesicles, proposed to be involved in ER to Golgi transport; interacts with Rab GTPases
BET4	enhancer	-3	RABGGTA	Alpha subunit of Type II geranylgeranyltransferase; provides a membrane attachment moiety to Rab-like proteins Ypt1p and Sec4p
SLY41	enhancer	-5	SLC35E1	Protein involved in ER-to-Golgi transport.

GOS1	enhancer	-2	GOSR1	v-SNARE protein involved in Golgi transport, homolog of the mammalian protein GOS-28/GS28
SEC31	enhancer	-2	SEC31A SEC31B	Essential phosphoprotein component (p150) of the COPII coat of secretory pathway vesicles, in complex with Sec13p; required for ER-derived transport vesicle formation
Other cellular processes				
PFS1	suppressor	4		Sporulation protein required for prospore membrane formation at selected spindle poles
PDE2	suppressor	4	PDE10A PDE11A PDE1A PDE1B PDE1C PDE2A PDE3A PDE3B PDE4A PDE4B PDE4C PDE4D PDE5A PDE6A PDE6B PDE6C PDE7A PDE7B PDE8A PDE8B PDE9A	High-affinity cyclic AMP phosphodiesterase, component of the cAMP-dependent protein kinase signaling system
MUM2	suppressor	4		Interacts with Orc2p, which is a component of the origin recognition complex.
OSH3	suppressor	3	OSBPL1A OSBPL2 OSBPL3 OSBPL6 OSBPL7	Member of an oxysterol-binding protein family, functions in sterol metabolism
PHO80	suppressor	3		Cyclin, negatively regulates phosphate metabolism
OSH2	suppressor	3	OSBPL3 OSBP OSBP2	Member of an oxysterol-binding protein family, functions in sterol metabolism
ISN1	suppressor	2		Inosine 5'-monophosphate (IMP)-specific 5'-nucleotidase
EPS1	enhancer	-1		Protein disulfide isomerase-related protein involved in endoplasmic reticulum retention of resident ER proteins.
IDS2	enhancer	-2		Protein involved in modulation of Ime2p activity during meiosis
QDR3	suppressor	4		Multidrug transporter of the major facilitator superfamily, required for resistance to quinidine, barban, cisplatin, and bleomycin
TPO4	enhancer	-3		Polyamine transport protein, recognizes spermine, putrescine, and spermidine; localizes to the plasma membrane; member of the major facilitator superfamily
IZH3	enhancer	-2		Membrane protein involved in zinc metabolism,

				member of the four-protein IZH family, expression induced by zinc deficiency; deletion reduces sensitivity to elevated zinc and shortens lag phase, overexpression reduces Zap1p activity
Unknown Function				
YKL063C	suppressor	4		Uncharacterized, GFP-fusion localizes to the Golgi
YML081W	suppressor	4	EGR3	Uncharacterized, GFP-fusion localizes to the nucleus
YNR014W	suppressor	4		Uncharacterized, expression is cell-cycle regulated and heat-inducible
YKL088W	suppressor	4	PPCDC	Protein required for cell viability. Predicted phosphopantothenoylcysteine decarboxylase
YML083C	suppressor	3		Uncharacterized, strong increase in transcript abundance during anaerobic growth compared to aerobic growth
YDR374C	suppressor	3	YTHDF1 YTHDF2 YTHDF3	Uncharacterized
YOR291W (YPK9)	suppressor	3	ATP13A2 (PARK9) ATP13A3 ATP13A4 ATP13A5	Probable cation-transporting ATPase 2
YDL121C	suppressor	2		Uncharacterized, GFP-fusion localizes to the ER
YBR030W	suppressor	2		Uncharacterized, predicted to function in phospholipid metabolism
YMR111C	suppressor	2		Uncharacterized, GFP-fusion localizes to the nucleus
YOR129C	suppressor	2		Putative component of the outer plaque of the spindle pole body; may be involved in cation homeostasis or multidrug resistance.

Supplemenatry Table 3B: GO annotations for the α-synuclein genetic hits (proteins that modify α-syn toxicity when overexpressed) and genes that are differentially regulated following α-syn expression. Note that this table reports the GO annotations for all the differentially expressed genes, combining the up and down regulated genes. The numbers in the main text differ because they refer to the GO annotations computed separately for the up- and down-regulated genes.

Ontology	Data type	GO_term	P-value
process	Genetic Hits	ER to Golgi vesicle-mediated transport	6.30E-05
process	Genetic Hits	Golgi vesicle transport	6.69E-05
process	Genetic Hits	vesicle-mediated transport	0.00012
process	Genetic Hits	localization	0.00237
process	Genetic Hits	membrane budding	0.00291
process	Genetic Hits	transport	0.01562
process	Genetic Hits	establishment of localization	0.02061
process	Genetic Hits	Golgi vesicle budding	0.02821
process	Genetic Hits	trehalose metabolic process	0.03361
function	Genetic Hits	phosphoric ester hydrolase activity	0.00083
function	Genetic Hits	phosphatase activity	0.00276
function	Genetic Hits	phosphoprotein phosphatase activity	0.00847
function	Genetic Hits	protein serine/threonine phosphatase activity	0.01067
function	Genetic Hits	transcription activator activity	0.0467
component	Genetic Hits	Golgi apparatus	6.79E-06
component	Genetic Hits	Golgi membrane	1.34E-05
component	Genetic Hits	Golgi apparatus part	2.42E-05
component	Genetic Hits	endomembrane system	0.00034
component	Genetic Hits	membrane	0.00347
component	Genetic Hits	COPI vesicle coat	0.0049
component	Genetic Hits	COPI coated vesicle membrane	0.0049
component	Genetic Hits	Golgi-associated vesicle	0.00623
component	Genetic Hits	Golgi-associated vesicle membrane	0.01003
component	Genetic Hits	organelle membrane	0.01656
component	Genetic Hits	coated vesicle	0.01771
component	Genetic Hits	vesicle coat	0.03038
component	Genetic Hits	vesicle membrane	0.03825
component	Genetic Hits	cytoplasmic vesicle membrane	0.03825
component	Genetic Hits	coated vesicle membrane	0.03825
component	Genetic Hits	membrane coat	0.04747
component	Genetic Hits	coated membrane	0.04747
process	Differentially Expressed	mitochondrial translation	5.19E-10
process	Differentially Expressed	mitochondrion organization	8.47E-08
process	Differentially Expressed	generation of precursor metabolites and energy	2.36E-05
process	Differentially Expressed	aerobic respiration	3.09E-05
process	Differentially Expressed	cellular respiration	0.00017
process	Differentially Expressed	acetyl-CoA catabolic process	0.00046
process	Differentially Expressed	tricarboxylic acid cycle	0.00046
process	Differentially Expressed	oxidative phosphorylation	0.0015
process	Differentially Expressed	sulfate assimilation	0.00202
process	Differentially Expressed	sulfur utilization	0.00202
process	Differentially Expressed	acetyl-CoA metabolic process	0.00627

process	Differentially Expressed	coenzyme catabolic process	0.00627
process	Differentially Expressed	energy derivation by oxidation of organic compounds	0.0066
process	Differentially Expressed	cofactor catabolic process	0.01056
process	Differentially Expressed	glutamate metabolic process	0.02155
process	Differentially Expressed	electron transport chain	0.02745
process	Differentially Expressed	respiratory electron transport chain	0.02745
process	Differentially Expressed	ATP synthesis coupled electron transport	0.02745
process	Differentially Expressed	mitochondrial ATP synthesis coupled electron transport	0.02745
process	Differentially Expressed	oxidation reduction	0.02745
process	Differentially Expressed	transposition	0.04596
process	Differentially Expressed	transposition, RNA-mediated	0.04596
function	Differentially Expressed	structural constituent of ribosome	1.61E-11
function	Differentially Expressed	oxidoreductase activity	9.26E-10
function	Differentially Expressed	structural molecule activity	2.49E-08
function	Differentially Expressed	structural constituent of cell wall	0.00055
function	Differentially Expressed	oxidoreductase activity, acting on sulfur group of donors	0.00135
function	Differentially Expressed	copper ion binding	0.00409
component	Differentially Expressed	organellar ribosome	3.90E-12
component	Differentially Expressed	mitochondrial ribosome	3.90E-12
component	Differentially Expressed	mitochondrial part	5.12E-11
component	Differentially Expressed	mitochondrial lumen	2.14E-10
component	Differentially Expressed	mitochondrial matrix	2.14E-10
component	Differentially Expressed	ribosomal subunit	4.16E-10
component	Differentially Expressed	organellar large ribosomal subunit	1.16E-08
component	Differentially Expressed	mitochondrial large ribosomal subunit	1.16E-08
component	Differentially Expressed	cytoplasm	2.32E-08
component	Differentially Expressed	ribosome	5.60E-08
component	Differentially Expressed	fungal-type cell wall	1.19E-07
component	Differentially Expressed	external encapsulating structure	3.61E-07
component	Differentially Expressed	cell wall	3.61E-07
component	Differentially Expressed	mitochondrion	4.25E-06
component	Differentially Expressed	retrotransposon nucleocapsid	5.87E-06
component	Differentially Expressed	large ribosomal subunit	2.69E-05
component	Differentially Expressed	small ribosomal subunit	0.00084
component	Differentially Expressed	mitochondrial inner membrane	0.00085
component	Differentially Expressed	organelle inner membrane	0.00234
component	Differentially Expressed	mitochondrial respiratory chain	0.00472
component	Differentially Expressed	mitochondrial membrane part	0.01315
component	Differentially Expressed	cell	0.01866
component	Differentially Expressed	cell part	0.02746
component	Differentially Expressed	vacuole	0.03438

Supplementary Table 3C: List of the differentially expressed genes identified four hours after induction of α-syn expression. Each Gene ID is associated with the corresponding log2(fold change) and p-value.

Gene ID	log2 (fold change)	P-value
YJR122W	-1.0658	0.000128
YBR284W	1.0594	0.004615
YGL248W	2.5262	0.000114
YMR184W	1.9749	5.40E-05
YGR176W	1.1381	9.20E-05
YLR303W	1.3598	0.000208
YNL208W	2.3106	4.40E-05
YJL012C-A	1.0713	0.000407
YGL236C	-1.1053	0.000235
YNL052W	-1.0725	0.000172
YMR103C	1.0737	0.000125
YLL039C	2.0309	8.50E-05
YGR161W-A	2.5931	7.00E-05
YBR045C	1.7823	0.000125
YML009C	-1.4996	6.70E-05
YDR493W	-1.1733	8.50E-05
YMR169C	1.8537	6.70E-05
YJL104W	-1.1388	0.000276
YOL120C	-1.0333	0.008252
YDR034W-B	4.1468	9.90E-05
YIL098C	-1.2989	8.30E-05
YDL012C	1.0461	0.00055
YPL018W	1.1805	0.000123
YOR356W	-1.3903	7.20E-05
YPL201C	-1.3949	0.000169
YAL034C	1.4535	0.000158
YDL223C	1.7347	5.40E-05
YBL101W-B	1.5501	0.000114
YDR354W	-1.8055	9.80E-05
YGL157W	1.2631	0.000845
YDR178W	-1.1354	0.000148
YCR021C	2.068	5.10E-05
YLL064C	1.3754	7.80E-05
YPL089C	1.0355	0.000159
YGR294W	1.3916	6.80E-05
YDR518W	1.1264	0.000224
YKR091W	1.952	5.40E-05
YPR077C	1.2699	6.00E-04
YDR262W	1.1009	0.000418
YIR028W	1.5881	0.000131
YDR133C	-1.6056	0.000414
YMR245W	-1.187	0.000468
YGL255W	2.1607	0.000174
YBL092W	-1.5886	0.000173
YOR288C	1.264	0.000339
YDR261W-A	2.5098	7.10E-05

Gene ID	log2 (fold change)	P-value
YLL025W	1.3055	7.80E-05
YPL106C	1.0247	0.000622
YOR136W	-1.4178	0.000735
YHR136C	2.4966	0.000176
YDL085C-A	1.5025	0.000123
YLR150W	-1.8644	0.000105
YOR343W-B	2.7193	5.70E-05
YNL217W	1.0037	0.000429
YBR251W	-1.3228	7.30E-05
YNL069C	-1.4775	0.000625
YHR005C-A	-1.0055	0.000517
YNL184C	-1.048	0.000132
YGR037C	1.476	0.000176
YLR155C	1.7544	0.000359
YGL045W	1.4284	0.000927
YPR047W	-1.09	0.00031
YOR264W	-1.1447	0.00019
YBL093C	1.579	0.000531
YGR189C	1.2646	0.000111
YPR158W	1.222	0.000164
YDL010W	1.4647	0.000164
YDR511W	-1.0789	0.000102
YKL104C	2.1744	7.80E-05
YDR342C	-1.8411	0.000698
YNR058W	1.0048	0.000449
YDR298C	-1.23	0.000129
YGR137W	1.0719	0.000128
YDR055W	3.0985	9.50E-05
YDL079C	-1.0582	0.000393
YNL196C	1.1497	9.50E-05
YLL009C	-1.8681	5.40E-05
YMR322C	1.4075	7.80E-05
YPR198W	1.0495	0.000164
YGL156W	2.4129	5.40E-05
YLR410W-B	1.4493	7.80E-05
YGR201C	1.8891	0.000124
YIL070C	-1.7167	5.40E-05
YJR161C	1.2448	7.80E-05
YHR024C	-1.0058	0.00015
YCR003W	-1.334	7.50E-05
YDL227C	-1.9854	0.000398
YGR284C	1.4113	0.000486
YOR306C	2.1626	0.000268
YMR175W	2.1435	8.00E-05
YBR137W	1.1931	0.00024
YDR001C	1.6301	7.80E-05

YNL012W	1.0101	0.000678
YGL006W	1.0596	0.000243
YKL174C	1.0594	0.000201
YKL142W	1.0318	0.000379
YKL107W	1.151	0.000176
YMR157C	-1.1665	0.000333
YML128C	2.675	4.40E-05
YBR287W	1.1058	0.000234
YLR461W	1.4776	6.70E-05
YGL101W	-1.0886	0.000114
YDR393W	-1.0087	0.00019
YIL093C	-1.0605	0.000114
YIL009W	-1.3763	6.40E-05
YHR030C	1.7177	0.000124
YBR072W	5.0806	4.40E-05
YLR107W	1.6543	7.20E-05
YMR187C	1.3805	0.000235
YDR367W	-1.1585	0.000309
YMR122W-A	1.5004	5.40E-05
YKR042W	1.1266	0.000157
YOR348C	-1.6692	0.001265
YDR347W	-2.0823	4.40E-05
YJL034W	3.4918	4.40E-05
YDR494W	-1.1476	0.000139
YOR286W	-1.1778	0.000111
YOR036W	1.5971	0.000295
YBL048W	1.4263	0.000246
YGR032W	2.9502	4.40E-05
YPR079W	1.5435	0.000128
YIL117C	1.424	8.50E-05
YML054C	-1.2275	0.000176
YBL075C	1.771	0.000125
YMR174C	1.3348	0.000235
YKR006C	-1.4399	6.70E-05
YGR161C	3.7462	8.60E-05
YAL061W	1.6676	5.50E-05
YLR092W	1.7457	0.000358
YOR176W	1.4435	0.000114
YKL086W	1.1105	0.000134
YMR081C	-1.2859	0.001584
YBR233W-A	2.8382	0.000114
YGR161W-B	1.2832	0.000137
YML123C	4.6838	5.10E-05
YJL223C	1.5057	0.000114
YKL148C	-1.0311	0.001157
YDL159W-A	2.7848	0.000338
YIR041W	1.2418	0.000174
YLR061W	-1.3411	0.000719
YMR020W	1.2445	0.000405
YER146W	-1.0348	0.000128
YMR012W	-1.2601	0.000339
YCR045C	1.0334	0.000329

YML081C-A	-1.2538	0.000258
YER138W-A	1.3492	0.000131
YPL170W	1.0755	4.00E-04
YGL046W	1.003	0.000172
YLR438W	1.028	0.000588
YBL078C	2.3451	0.000235
YJR107W	1.5751	0.000123
YER045C	1.1873	0.000302
YKR080W	1.6	0.002931
YFL002W-B	2.7463	4.40E-05
YBL045C	-1.0972	0.000302
YEL058W	1.0926	0.000418
YJL155C	1.0719	0.00069
YDL244W	3.0749	5.50E-05
YGL162W	-1.5072	0.000812
YML028W	1.8694	8.30E-05
YIR021W	-1.1546	0.000294
YML120C	-1.0739	0.000467
YPL143W	-1.5393	0.000267
YMR118C	2.1354	4.40E-05
YBR117C	2.3854	6.70E-05
YOL151W	2.21	7.20E-05
YKL065C	1.2737	0.000114
YGR213C	1.4149	7.30E-05
YBL049W	1.3442	0.000249
YGR082W	-1.2733	0.000198
YBR295W	1.5997	9.50E-05
YJL136C	-1.033	0.000863
YMR008C	1.7209	0.000281
YOL164W	1.5895	0.000173
YIL023C	1.6242	5.40E-05
YOR315W	-1.2035	0.002376
YPR002W	-1.763	0.00021
YMR095C	1.8178	0.000176
YFR011C	-1.2138	0.000403
YNR001C	-1.0796	0.000335
YLR295C	-1.539	0.000114
YMR180C	2.0771	7.80E-05
YOL016C	1.2236	0.001568
YPL110C	1.2148	0.000102
YIL158W	-1.7344	0.00032
YDL125C	1.8355	0.000329
YEL025C	-1.1627	9.50E-05
YOL077W-A	-1.1352	0.001012
YPL081W	-1.1939	0.001187
YBR201W	1.5794	0.000408
YDR098C-A	1.206	0.000913
YLL057C	1.548	0.000344
YOL031C	2.38	8.10E-05
YDL024C	1.1257	0.000563
YDR351W	-1.6819	5.40E-05
YGR138C	2.5612	4.40E-05

YIL074C	1.2064	0.000552
YER130C	1.1719	0.000393
YPL088W	2.3649	7.80E-05
YNL332W	3.222	7.80E-05
YMR305C	1.0439	0.000416
YNL277W	1.0835	0.001327
YJL196C	-1.0969	0.00047
YLR054C	2.5078	4.40E-05
YGR008C	2.4242	0.000119
YCR104W	1.3943	7.40E-05
YOR192C-B	1.1038	0.000179
YMR315W	1.149	0.000774
YMR316W	2.0073	0.000794
YLR149C	1.0413	0.000287
YDR384C	-1.0856	0.001517
YDR391C	1.4628	0.000179
YFL031W	1.7173	7.80E-05
YLR058C	1.7323	0.00087
YPL163C	1.0192	0.006448
YHR096C	2.8653	4.90E-05
YJL056C	1.273	0.000147
YKR049C	1.4212	0.000202
YNR034W-A	1.2003	0.000176
YBR296C	1.6555	0.001311
YGR142W	2.6615	0.000175
YGL107C	-1.0175	0.000164
YKL137W	-1.1248	0.000147
YHR038W	-1.0674	0.000131
YOR391C	1.1541	9.80E-05
YGR027W-A	1.0387	0.00347
YMR090W	2.2017	8.50E-05
YJL153C	2.0296	0.000318
YDR149C	-1.12	0.000403
YOR065W	-1.3416	0.000641
YLR292C	1.16	0.000169
YOL064C	1.1554	0.000982
YJL144W	3.4868	6.80E-05
YGL034C	-1.2777	0.000375
YOL055C	2.1735	6.80E-05
YOR343C-B	1.0196	4.00E-04
YCR009C	1.0252	0.000528
YML078W	-1.0425	0.000577
YJL038C	2.9795	8.30E-05
YGR258C	1.0022	0.00047
YDL057W	1.4384	0.000246
YNL044W	1.2732	0.00021
YBL087C	-1.0582	0.00158
YCL044C	1.0366	0.002618
YDR481C	1.3479	0.000306
YJL116C	1.3556	0.000506
YML087C	-1.7512	4.40E-05
YCL024W	-1.0499	0.001208
YLR158C	1.4237	0.000414
YMR291W	1.6313	0.000148
YMR120C	2.6337	0.000157
YHL046C	1.6623	0.000693
YPR156C	1.7516	7.10E-05
YBR021W	-1.9111	9.80E-05
YLR044C	2.0358	7.80E-05
YEL024W	-1.3701	0.000503
YPL173W	-1.0171	0.000128
YBR169C	2.2267	0.000125
YBR071W	1.4768	0.00012
YBR185C	-1.2658	0.000114
YOR234C	-1.0345	0.001216
YGL053W	1.1944	0.000247
YOR173W	1.5126	8.00E-05
YLR287C-A	-1.178	0.000507
YEL071W	1.0289	0.000437
YIL108W	1.9418	7.10E-05
YHR209W	2.477	5.40E-05
YLR189C	-1.243	0.00055
YBL003C	-1.0199	0.000939
YJR137C	1.0944	0.001341
YPL017C	1.5303	0.000319
YPL171C	1.2394	0.000407
YDL114W	1.1076	0.00058
YDR371W	-1.2351	0.000504
YKR011C	1.0391	0.002752
YBR120C	-1.2714	7.30E-05
YHR007C	1.4529	0.000541
YDL222C	1.1619	9.80E-05
YGL184C	2.1507	0.000246
YJL043W	2.6431	5.70E-05
YBR054W	2.0234	0.000534
YGL234W	1.0927	0.000104
YMR242C	-1.1779	0.00071
YGL146C	-1.1732	0.000414
YGR243W	-1.6619	0.000224
YDR059C	1.2306	0.000185
YDR026C	1.0174	0.000124
YGR076C	-1.5248	7.80E-05
YHR128W	-1.3429	0.001976
YLL026W	1.2779	0.000327
YBL030C	-1.8529	0.000114
YCONTRO-L	1.1557	0.000304
YOL161C	1.3519	8.40E-05
YFL020C	1.1495	9.50E-05
YFR026C	5.2337	4.40E-05
YBL107W-A	1.1686	0.000391
YOR096W	-1.0621	0.00032
YLR350W	1.2553	0.00058
YGL159W	-1.1562	0.000516
YKR097W	-1.2272	0.00517

YML116W-A	1.0636	0.000222
YFL014W	4.2413	4.40E-05
YNR076W	1.5881	6.50E-05
YDR350C	-1.7765	5.40E-05
YKL217W	-1.8432	6.00E-04
YOR341W	-1.1933	0.031226
YKR075C	-1.6418	9.50E-05
YDR519W	1.4993	9.80E-05
YNL054W-B	1.6023	0.000468
YBR222C	1.0323	0.000229
YKL109W	-1.1518	0.000229
YPL097W	-1.158	0.000191
YGL028C	-1.3241	0.003464
YBR158W	-1.1815	0.000192
YKL163W	4.5466	4.40E-05
YDR210W-A	2.7187	5.40E-05
YPL262W	-1.1283	0.001001
YGL189C	-1.3005	0.000587
YKL073W	1.3726	0.000112
YDR365W-B	1.0701	0.000155
YCR100C	1.0992	0.000229
YGR268C	1.2322	9.80E-05
YMR303C	-1.1125	0.011794
YDL124W	2.9288	5.80E-05
YML132W	1.2763	0.000164
YBR048W	-1.3159	0.000298
YLR038C	-1.1447	0.00062
YPL019C	1.5419	0.000179
YGR067C	-1.6504	0.000393
YMR173W-A	2.3477	5.10E-05
YER103W	2.1592	0.000119
YGR087C	1.569	0.000715
YLR312W-A	-1.4715	7.10E-05
YJL180C	-1.0238	0.000129
YIL176C	1.4294	0.000114
YDR542W	1.5655	9.20E-05
YAR015W	1.2878	0.000376
YGR088W	1.4151	0.00058
YMR105C	1.1571	0.000198
YKL001C	1.7033	0.000164
YNL252C	-1.1839	9.80E-05
YDR375C	-1.1446	9.90E-05
YER020W	1.2818	0.00021
YFL062W	1.3402	0.000174
YPL014W	1.3944	0.000581
YHR100C	2.5388	4.40E-05
YGR146C	1.2887	0.000128
YPL221W	1.2821	0.000128
YLR142W	2.1985	0.000416
YPL158C	-1.0138	0.000808
YLR126C	1.4567	6.80E-05
YNL241C	1.071	0.000176

YCL030C	1.1372	0.001202
YGR256W	3.1586	4.40E-05
YGR084C	-1.2985	7.80E-05
YDR343C	-2.2602	0.000198
YGL068W	-1.3021	0.000164
YMR230W	-1.3445	0.000426
YMR238W	1.4865	6.70E-05
YHR138C	2.2966	0.000148
YHR143W	-1.369	0.001277
YGL188C	-1.1437	0.000267
YDR077W	2.2193	6.30E-05
YJL181W	-1.0593	0.000714
YBR214W	2.0366	0.000114
YLR390W-A	1.024	0.000243
YIL109C	1.1721	9.20E-05
YLR286C	-1.5682	0.001389
YMR039C	1.24	0.000891
YOL119C	1.2955	0.000209
YDR462W	-1.3977	7.80E-05
YIL040W	1.2976	0.001061
YOL019W	1.3103	0.000164
YMR251W-A	1.3748	0.000685
YPR035W	1.0602	0.001493
YDL020C	1.8543	0.000418
YLR125W	1.5383	6.20E-05
YDR034CC	2.3602	6.20E-05
YNL284C	-1.0366	0.000124
YCL043C	1.8917	5.40E-05
YOR289W	1.0905	0.000185
YML091C	-2.0683	0.000261
YNR009W	-1.1875	0.000318
YBR076W	3.0589	5.40E-05
YLR178C	2.0123	7.20E-05
YHR174W	1.0114	0.000418
YPL247C	1.2919	0.000266
YDR155C	2.0472	0.000112
YOR220W	1.0945	0.001353
YKL164C	1.2635	0.000114
YMR295C	1.7123	7.00E-05
YLR410W-A	2.3634	0.000403
YDL202W	-1.0127	0.000292
YGR165W	-1.0617	0.000176
YFR012W-A	1.5874	0.000298
YNR067C	-1.2236	0.002731
YKL165C	2.3336	5.10E-05
YKR039W	1.0592	0.004605
YKL224C	1.333	7.80E-05
YLR225C	1.3936	0.000114
YJL073W	1.2345	0.000152
YHR001W-A	-1.0343	0.000184
YBR268W	-1.1348	0.000194
YJR028W	1.39	0.000216

YJL017W	1.2919	0.000131
YIL052C	-1.225	0.000363
YOR343W-A	2.6344	8.00E-05
YKR057W	-1.2229	0.000583
YBR182C	1.5046	0.000108
YBR029C	-1.2195	0.000298
YDR171W	2.6268	0.000258
YGL040C	-1.0275	0.000229
YNL327W	-1.2265	0.001576
YNR075W	1.2616	8.00E-05
YCR083W	1.0387	0.000562
YIL157C	-1.021	0.000191
YAL068C	1.5709	7.80E-05
YHR087W	2.8666	0.000114
YDR365C	-1.4443	8.40E-05
YBR294W	3.5866	0.000191
YOR035C	1.179	0.000104
YMR032W	-1.0713	0.000148
YDR210W	1.3388	0.000484
YMR003W	-1.012	0.000268
YDR210CC	1.7628	0.000128
YKL006W	-1.0586	0.000297
YGR043C	1.9962	4.40E-05
YPL134C	-1.161	0.000114
YDR043C	1.1709	0.001204
YDL070W	1.1741	9.70E-05
YPL280W	1.357	7.50E-05
YDR345C	-1.509	0.000174
YHR179W	1.9113	5.40E-05
YCL019W	1.3531	8.30E-05
YBR299W	-1.3182	0.000164
YGR060W	1.0813	0.00018
YOR299W	1.0552	0.000339
YMR320W	1.4491	0.000457
YMR096W	2.4916	0.000185
YDR025W	-1.1479	0.002196
YPL132W	-1.2149	9.90E-05
YAR010C	1.5724	0.000297
YLR430W	1.07	0.000323
YMR271C	1.2167	0.000326
YIL162W	-1.3379	0.000191
YDR346C	-1.0654	0.00015
YMR107W	2.9857	5.40E-05
YAL053W	1.5287	9.50E-05
YMR191W	1.3961	0.00027
YJR156C	3.1044	9.80E-05
YNL142W	1.5452	0.000123
YMR250W	1.4894	6.70E-05
YDR210W-D	1.6705	0.000997
YPL154C	1.0404	0.000122
YNL134C	1.499	0.000143
YFR033C	-1.3405	0.000256
YDR453C	1.4105	7.40E-05
YHR053C	1.4095	0.016953
YML088W	1.1818	0.000416
YLR121C	2.9515	4.40E-05
YBL101W-A	1.6858	6.70E-05
YPL187W	-1.7772	0.000114
YLR423C	1.9177	5.40E-05
YHR104W	1.1853	0.00022
YOR192C-A	2.2182	5.40E-05
YGR038C-A	2.0868	5.40E-05
YBR037C	-1.1632	0.000258
YPR167C	1.4366	0.000416
YIL101C	1.6418	0.00022
YDL234C	1.755	0.000144
YDR411C	1.4934	8.00E-05
YDR007W	1.1237	0.004387
YGL089C	-1.5561	8.40E-05
YJL052W	1.4638	6.20E-05
YPL052W	1.0701	0.000298
YJL191W	-1.2794	0.000114
YER037W	2.9154	4.40E-05
YDL248W	1.6699	8.40E-05
YLR414C	2.1371	6.70E-05
YOL052C-A	2.8185	9.20E-05
YLR124W	1.2016	0.000462
YCL038C	1.2533	0.001826
YOR153W	1.5703	7.70E-05
YGR214W	-1.2568	0.002172
YMR286W	-1.0582	0.000326
YJL016W	1.3855	6.40E-05
YBL101C	1.4721	9.50E-05
YIL072W	1.146	0.000797
YEL040W	-1.2185	0.000967
YHR097C	1.3307	0.000248
YFR022W	1.2008	0.000222
YBL043W	-1.0722	0.000164
YKR085C	-1.2233	0.000283
YNL066W	-1.4982	0.000164
YOR134W	1.5892	0.000153
YNL100W	-1.1392	0.000293
YDR070C	2.5841	0.000105
YFR030W	1.4659	0.000513
YNL315C	-1.1003	0.000172
YPR020W	-1.2197	0.000131
YEL049W	1.0734	0.000114
YKL194C	-1.0063	0.000128
YOR024W	-1.3063	8.90E-05
YJR048W	-2.3465	5.40E-05
YOR298C-A	1.0913	0.002403
YGL126W	2.5723	5.40E-05
YCR034W	-1.0433	0.001507
YNL093W	1.1481	0.001005

YGL261C	1.4973	9.50E-05
YPR154W	1.9199	7.70E-05
YOR099W	1.2365	0.000326
YDL072C	1.3039	0.00046
YPL172C	-1.1559	0.000157
YDR322W	-1.2381	8.50E-05
YCL040W	1.0985	0.000268
YJL108C	1.1142	0.000129
YHR014W	-1.2856	0.000289
YIL154C	1.289	0.000316
YLR264W	-1.2391	0.000899
YJR101W	-1.404	0.000431
YBR033W	-1.0849	0.000774
YPR001W	1.0419	0.000278
YKL170W	-1.0217	0.00024
YOR343C-A	2.8505	4.40E-05
YCL047C	1.0938	0.000148
YOR128C	1.3609	0.000986
YJR078W	3.1325	8.20E-05
YNL157W	1.0773	0.000233
YDR277C	-1.1012	0.000757
YLL041C	-1.2645	0.000237
YKL138C	-1.0383	0.000301
YJL059W	1.0963	0.000975
YNL036W	3.0857	0.000229
YNL192W	1.8865	9.00E-05
YLR168C	-1.5504	5.40E-05
YGL179C	2.1724	6.20E-05
YJR135W-A	-1.0308	0.000315
YNL185C	-1.191	0.000152
YDL083C	-1.1748	0.000685
YER072W	1.0348	0.000419
YNL322C	1.1159	0.000783
YLR109W	1.7113	0.000191
YNL037C	-1.3888	0.000167
YKR093W	-1.1313	0.000737
YER150W	2.3668	5.40E-05
YDR034C-D	1.6024	0.000243
YJR094W-A	-1.0721	0.000741
YGR234W	-1.2913	0.00027
YPL283C	1.036	0.000449
YOR187W	-1.4379	0.000185
YIR017C	1.399	0.000439
YGR204W	1.3337	0.000144
YNR036C	-1.0445	0.000309
YOR232W	-1.3936	0.000202
YJR095W	-1.3732	0.001327
YMR051C	1.3587	0.000298
YHR055C	2.1425	0.001314
YLR214W	1.0731	0.000141
YJL096W	-1.1857	0.000112
YDR533C	1.4607	0.00019

YKL151C	1.7548	0.00025
YHR112C	1.3081	0.000664
YCR007C	1.8227	0.00029
YIL148W	-1.0963	0.001215
YPR166C	-1.0135	0.000125
YLR231C	1.1253	0.000124
YML130C	2.6871	7.80E-05
YFL058W	3.0032	5.40E-05
YJR106W	1.714	6.70E-05
YIR035C	1.3503	7.50E-05
YJL159W	1.3505	8.50E-05
YMR104C	1.1622	0.000112
YLR136C	2.3979	9.20E-05
YLR194C	3.4375	4.40E-05
YGR209C	1.3626	6.00E-04
YEL060C	2.8107	4.40E-05
YMR173W	2.7959	4.40E-05
YDR116C	-1.2933	8.50E-05
YLR069C	-1.151	0.00087
YML052W	-1.5533	0.000153
YLR304C	-1.9623	0.000531
YMR040W	3.5143	8.00E-05
YJR079W	1.783	8.40E-05
YOL045W	1.0688	0.001432
YBR302C	1.4404	0.000172
YGR292W	-1.195	0.000187
YNL040W	1.1889	0.000356
YNL144C	-1.0147	0.002802
YCR098C	2.7102	0.000104
YPL223C	3.1095	4.40E-05
YDR210W-B	2.2518	0.000114
YJL138C	-1.0752	0.000509
YNL336W	1.7849	7.00E-05
YMR267W	-1.3515	0.000164
YGL121C	2.1901	0.000287
YNL160W	1.8915	0.000287
YOR158W	-1.227	7.80E-05
YJR010W	2.0045	0.000343
YPL282C	1.196	0.000114
YJR096W	1.8583	0.000187
YLR120C	2.7988	5.40E-05
YJL171C	1.8037	0.000135
YPR127W	1.6343	5.40E-05
YCL020W	2.3056	8.80E-05
YIR044C	1.2368	8.30E-05
YML025C	-1.2032	7.80E-05
YHL036W	1.0733	0.00074
YLR099C	2.1698	6.10E-05
YOL056W	1.0478	0.000268
YHR057C	1.2352	0.007468
YPR119W	-1.23	0.000693
YJL107C	1.0893	0.000185

References

1. Hughes, T.R. et al. Functional discovery via a compendium of expression profiles. *Cell* **102**, 109-26 (2000).
2. Dudley, A.M., Janse, D.M., Tanay, A., Shamir, R. & Church, G.M. A global view of pleiotropy and phenotypically derived gene function in yeast. *Mol Syst Biol* **1**, 2005 0001 (2005).
3. Workman, C.T. et al. A systems approach to mapping DNA damage response pathways. *Science* **312**, 1054-9 (2006).
4. Begley, T.J., Rosenbach, A.S., Ideker, T. & Samson, L.D. Hot spots for modulating toxicity identified by genomic phenotyping and localization mapping. *Mol Cell* **16**, 117-25 (2004).
5. Parsons, A.B. et al. Integration of chemical-genetic and genetic interaction data links bioactive compounds to cellular target pathways. *Nat Biotechnol* **22**, 62-9 (2004).
6. Koerkamp, M.G. et al. Dissection of transient oxidative stress response in Saccharomyces cerevisiae by using DNA microarrays. *Mol Biol Cell* **13**, 2783-94 (2002).
7. Smith, J.J. et al. Expression and functional profiling reveal distinct gene classes involved in fatty acid metabolism. *Mol Syst Biol* **2**, 2006 0009 (2006).
8. Haugen, A.C. et al. Integrating phenotypic and expression profiles to map arsenic-response networks. *Genome Biol* **5**, R95 (2004).
9. Tong, A.H. et al. Systematic genetic analysis with ordered arrays of yeast deletion mutants. *Science* **294**, 2364-8 (2001).
10. Tong, A.H. et al. Global mapping of the yeast genetic interaction network. *Science* **303**, 808-13 (2004).
11. SGD project. "Saccharomyces Genome Database".

Nature Genetics: doi:10.1038/ng.337

Supplementary Figure 1A. Graphical representation of the gene ontology (GO) annotations enriched in the combined genetic hits set and the combined differentially expressed gene set based on the perturbations in Table 1 for which complete genetic screens were available. The annotations presented are attributed to at least 5% of the genes in the combined datasets and were also found to be enriched in at least 20% of these datasets when they were analyzed separately.

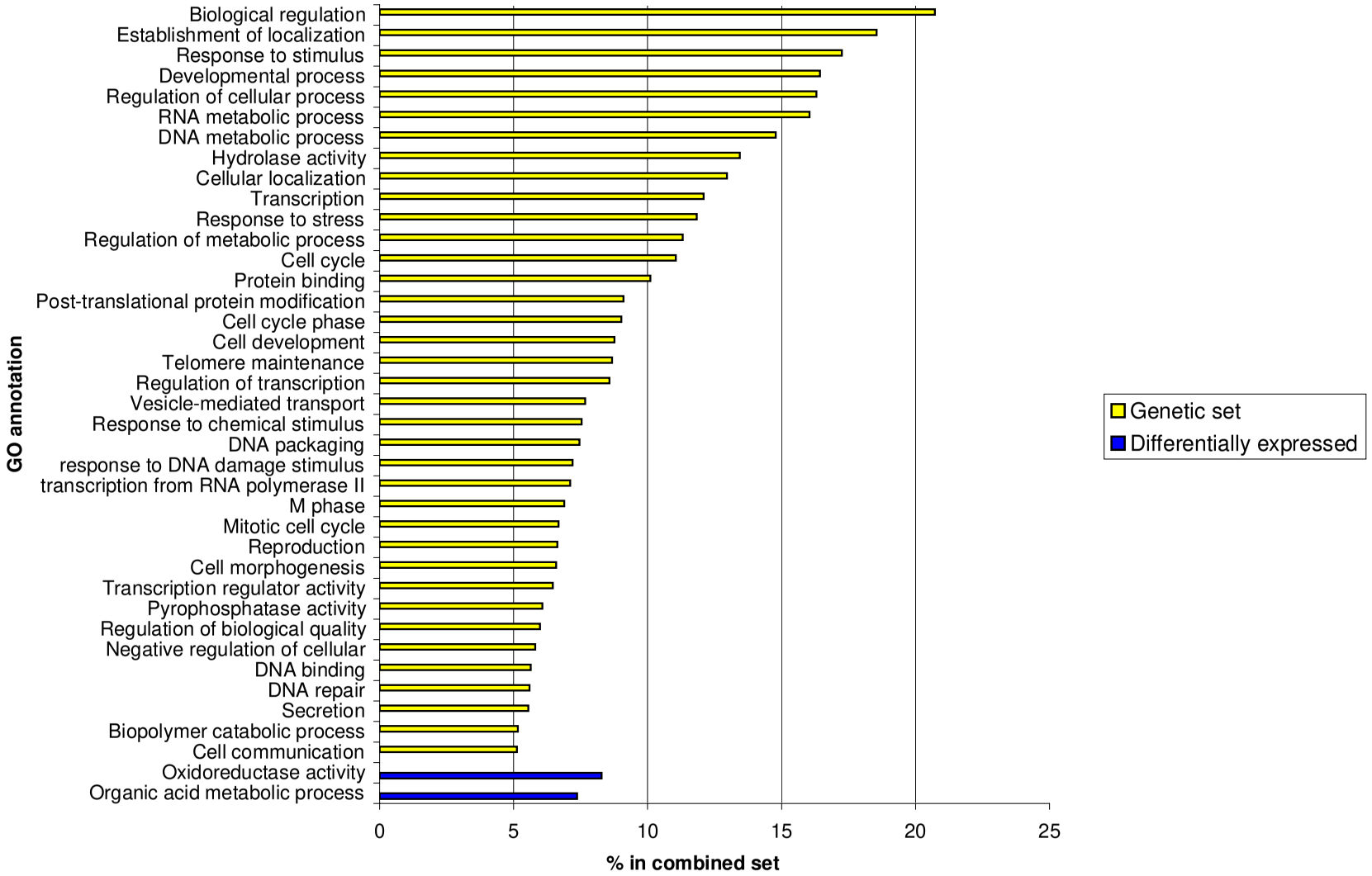

Supplementary Figure 1B. Graphical representation of the relation between genetic and transcriptional profiling data corresponding to a specific perturbation.
Genetic and transcriptional data are integrated with interactome data to find interaction paths through which a subset of the genetic data may regulate the transcriptional response. The regulation may be direct when the transcription factors regulating the response are part of the genetic data, or indirect via intermediate proteins. The ResponseNet algorithm is based on an optimization technique for finding sparse high-probability paths in the interactome that connect the two types of data. The result is a flow diagram (A). The directionality of the protein-protein edges in this flow diagram does not reflect the order of events but was imposed by the ResponseNet algorithm. This directionality and the auxiliary nodes S and T have no biological meaning and can be ignored (B).
Nodes represent proteins and genes, and edges represent their interactions. Diamond shaped nodes represent genetic data, rectangular nodes represent transcriptional data, and circular nodes represent intermediate (hidden) proteins on the paths that link genetic and transcriptional data.

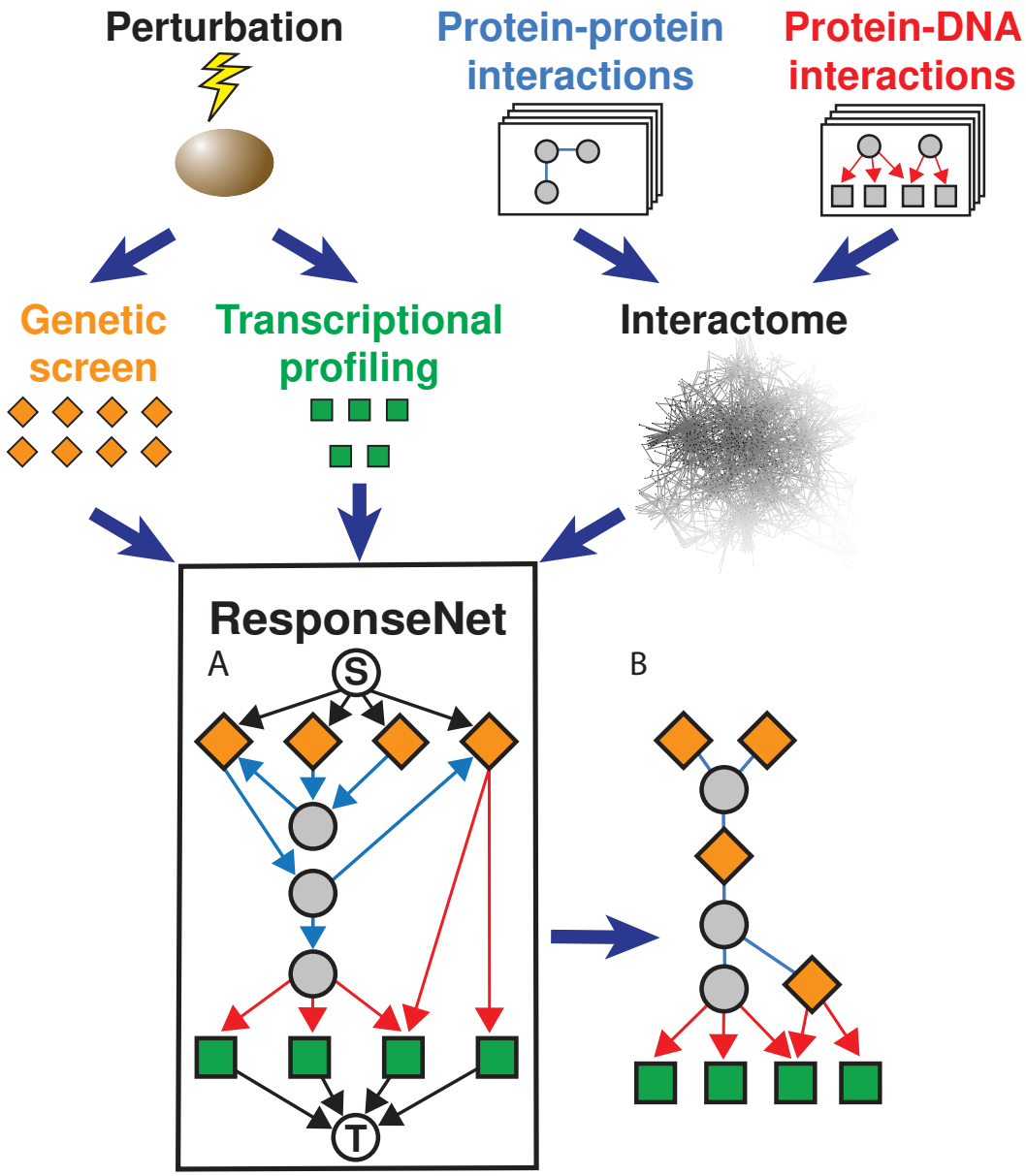

Nature Genetics: doi:10.1038/ng.337

Supplementary Figure 2. Effect of ubiquitin-related hits on alpha-synuclein expression. We performed flow cytometry to analyze if overexpression of ubiquitin-related hits affected levels of α-syn expressed over a ten hour period using a YFP tagged α-syn strain. The only large change is due to overexpression of UIP5. When each of the strains was examined by microscopy, all showed localization similar to the vector control, except for UIP5, which showed a diffuse localization at 6 hours (data not shown). As controls we used a vector strain in which no yeast gene is overexpressed, as well as a strain overexpressing the ubiquitin-protein ligase San1 which has no affect on α-syn toxicity.

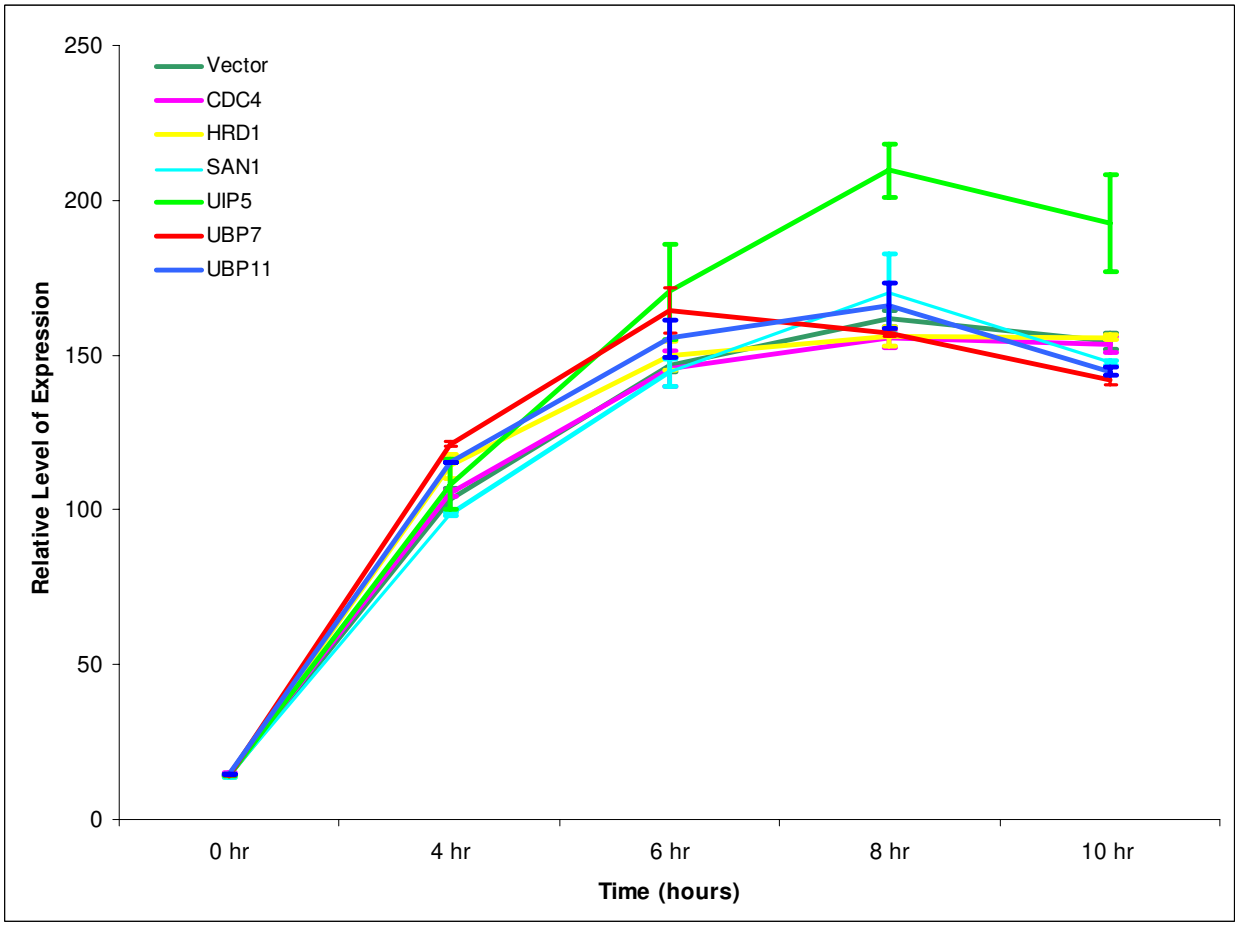

Supplementary Figure 3A. Cellular pathways responding to α-syn toxicity predicted by ResponseNet. The fifteen connected components were revealed by ResponseNet upon integrating the genetic and transcriptional data of the yeast PD model. Nodes represent proteins and genes, and edges represent their interactions. Diamond shaped nodes represent genetic hits (proteins that modify α-syn toxicity when overexpressed); rectangular nodes represent genes that are differentially expressed following α-syn expression; and circular nodes represent proteins predicted by ResponseNet that link genetic hits and differentially expressed genes.
Protein nodes are colored based on their GO process annotation according to the following scheme:

- Ubiquitin-related and protein degradation, colored in orange
- Vesicle trafficking, colored in blue.
- Cell cycle and meiosis, colored in green.
- Phosphate metabolism colored in purple.
- Fatty acid metabolism, colored in pink.
- Response to oxidative stress, colored in light blue.

Differentially expressed genes are labeled with a suffix of g+ for up-regulation and g- for down-regulation.

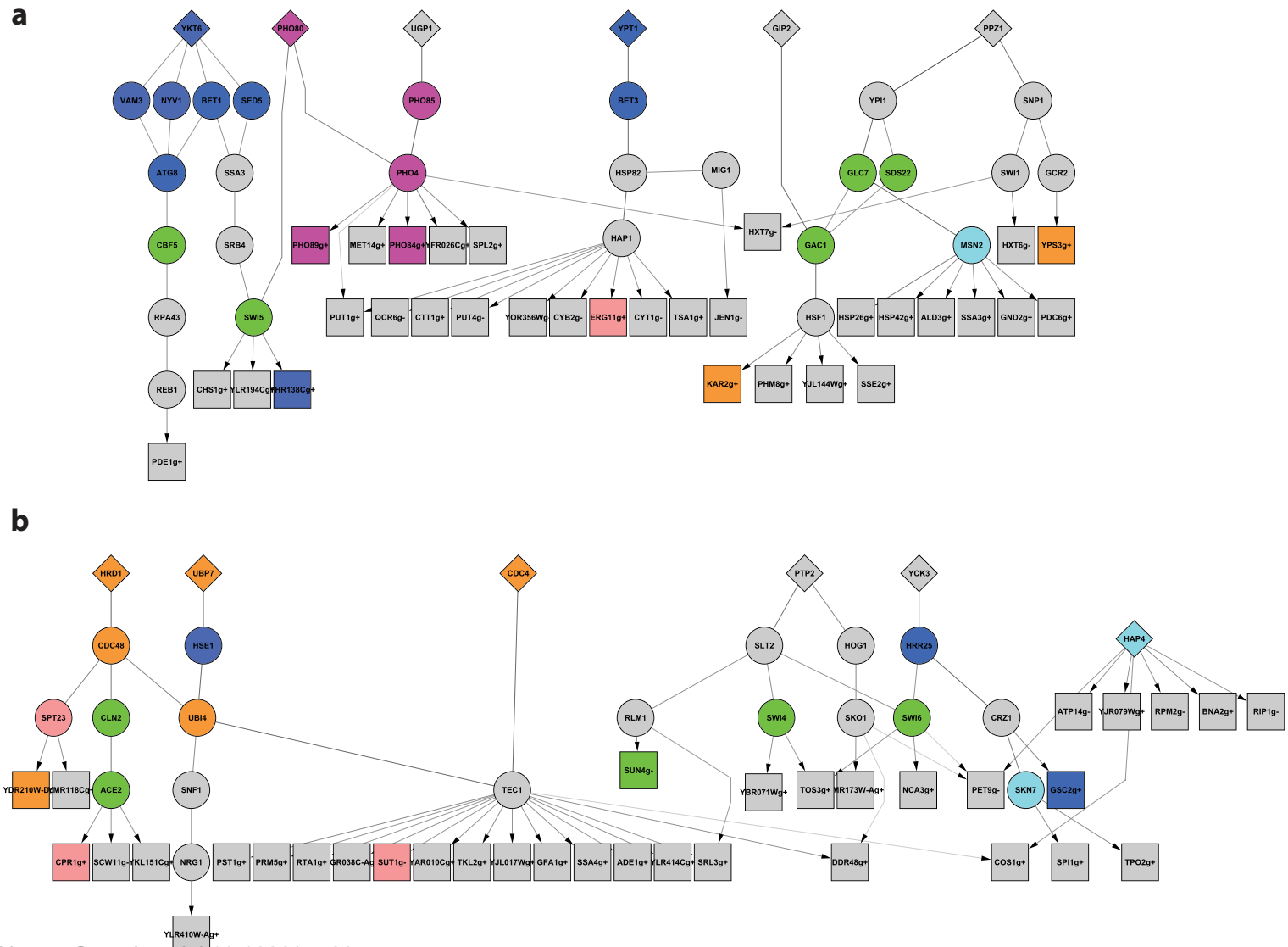

Nature Genetics: doi:10.1038/ng.337

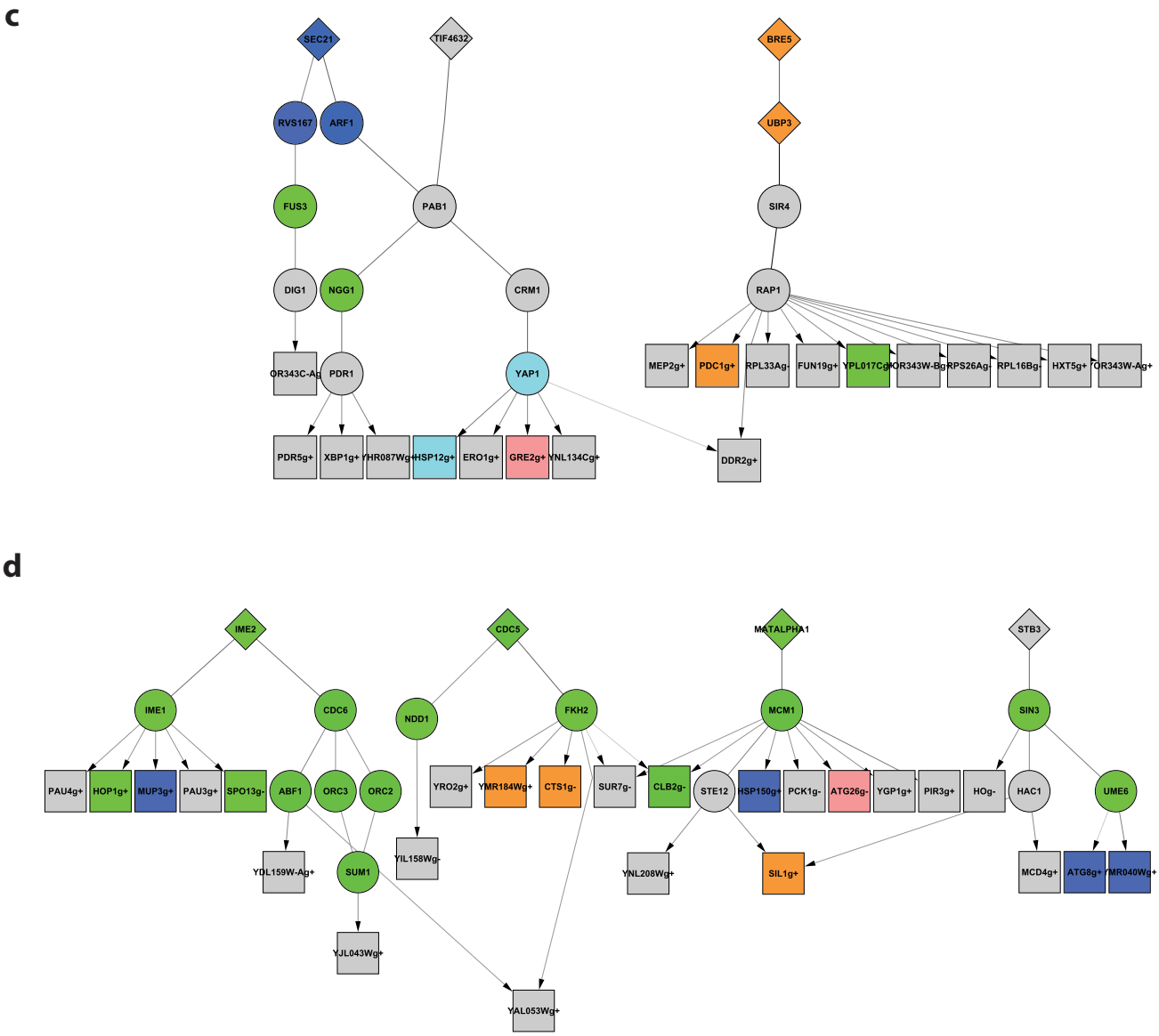
c
SEC21
TIF4632
RVS167
ARF1
FUS3
PAB1
DIG1
NGG1
CRM1
OR343C-Ag
PDR1
YAP1
PDR5g+
XBP1g+
YHR087Wg+
HSP12g+
ERO1g+
GRE2g+
YNL134Cg+
BRE5
UBP3
SIR4
RAP1
MEP2g+
PDC1g+
RPL33Ag-
FUN19g+
YPL017Cg+
OR343W-Bg
RPS26Ag-
RPL16Bg-
HXT5g+
OR343W-Ag+
DDR2g+
d
IME2
CDC5
MATALPHA1
STB3
IME1
CDC6
NDD1
FKH2
MCM1
SIN3
PAU4g+
HOP1g+
MUP3g+
PAU3g+
SPO13g-
ABF1
ORC3
ORC2
YRO2g+
YMR184Wg+
CTS1g-
SUR7g-
CLB2g-
STE12
HSP150g+
PCK1g-
ATG26g-
YGP1g+
PIR3g+
HOg-
HAC1
UME6
YDL159W-Ag+
SUM1
YIL158Wg-
YNL208Wg+
SIL1g+
MCD4g+
ATG8g+
YMR040Wg+
YJL043Wg+
YAL053Wg+
e
MGA2
MKS1
RSP5
RTG2
GRR1
RPO21
SPT7
IDH2g-
CIT1g-
ACO1g-
MTH1
GAL4
GCN4
RGT1
HXT3g-
FUR4g-
SNZ1g+
GR161W-Ag
RTS3g+
SNO1g+
MET16g+
STR3g+
SHM2g+
YKR075Cg-
f
PFS1
NAS2
RPN4
BTN2g+
YJL038Cg+
UBI4g+
PET123g-
AFT2
YPS1g+
g
MUM2
TID3
DAM1
CBF1
RPN4g+
MET3g+
SUL2g+
STM1g-

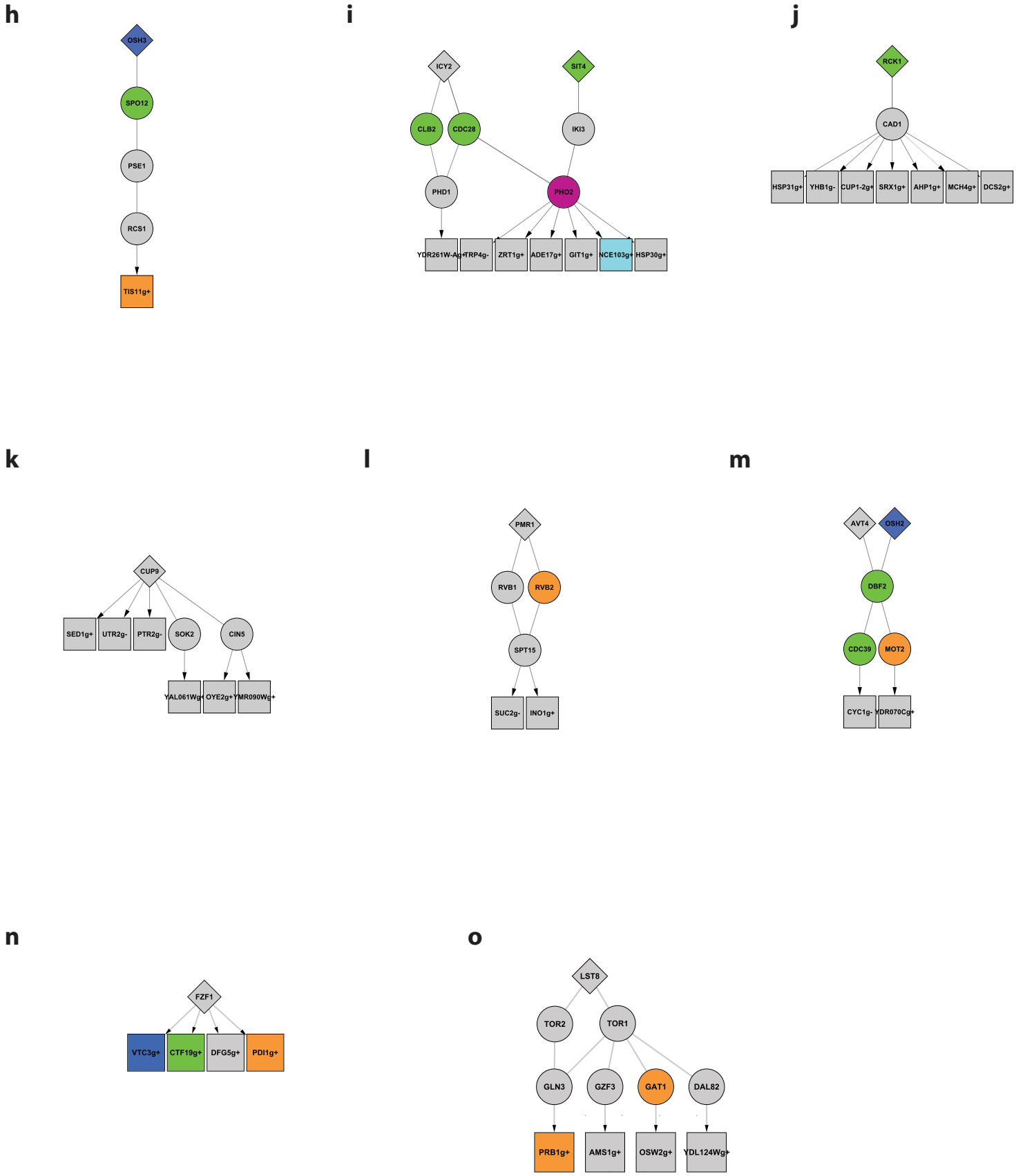

Nature Genetics: doi:10.1038/ng.337

Supplementary Figure 3B. Lovastatin inhibits growth of the yeast strain expressing several copies of α-syn but has no effect on growth of a related yeast model. Growth of a control strain (vector), a strain expressing one copy of α-syn (NoTox), and an intermediate toxicity strain (IntTox) expressing several copies of α-syn was measured in a galactose containing media with and without 5μM lovastatin. As an additional control we tested the effect of lovastatin on growth of a related yeast model in which fragments of the human Huntingtin protein are expressed [1]. Lovastatin had no effect on the growth of either the strain expressing a slightly toxic fragment of Huntingtin containing a 25Q repeat or the strain expressing a toxic fragment of Huntingtin containing a 72Q repeat. Each growth curve reflects average of 3 individual runs marked by bars.

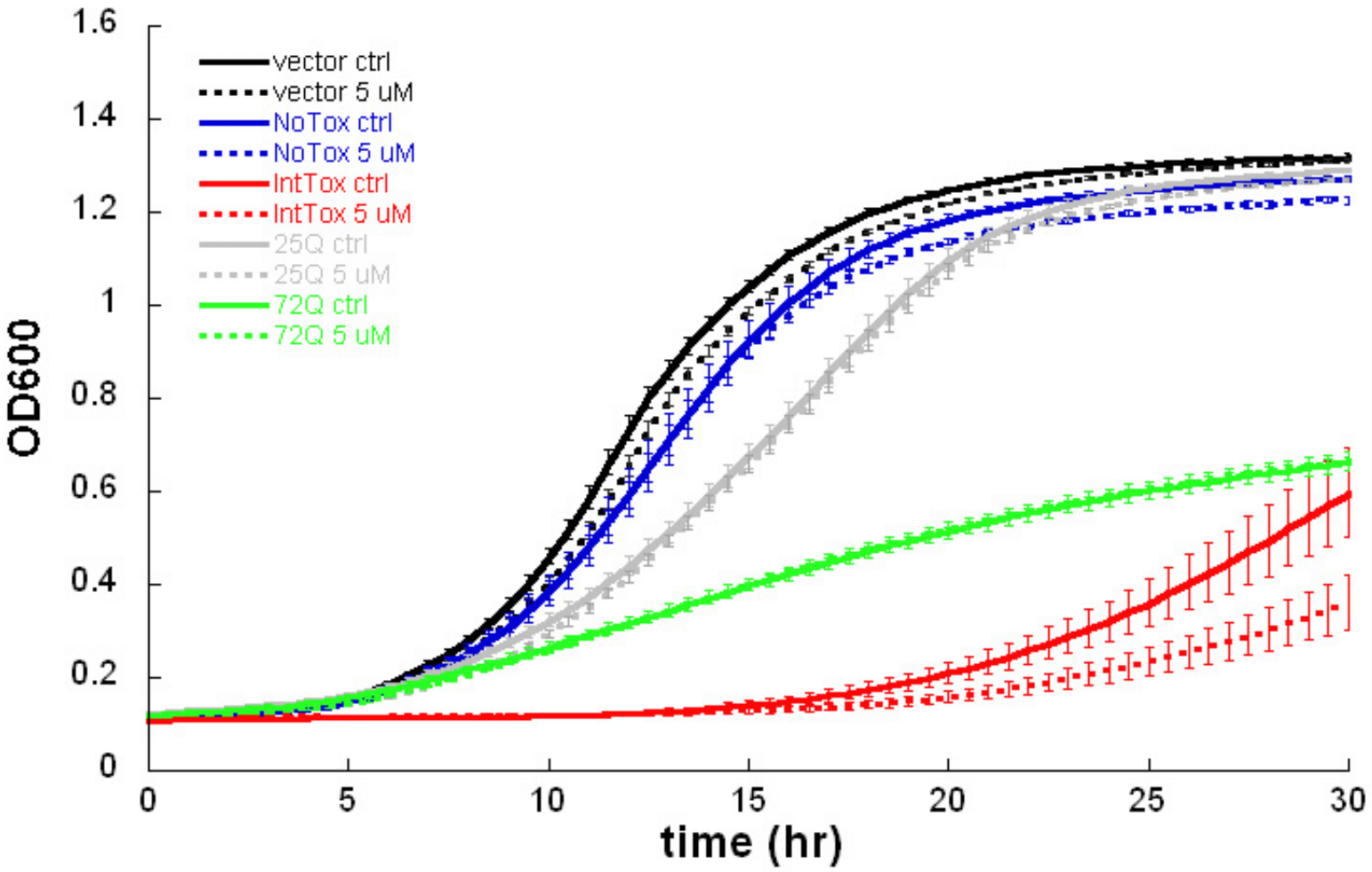

Nature Genetics: doi:10.1038/ng.337

Supplementary Figure 3C. Rapamycin inhibits growth of yeast strains expressing even 1-copy α-syn but has almost no effect on growth of a related yeast model. Growth of a control strain (vector), a strain expressing one copy of α-syn (NoTox), and an intermediate toxicity strain (IntTox) expressing several copies of α-syn was measured in a galactose containing media with and without 1nM rapamycin. As an additional control we tested the effect of rapamycin on growth of a related yeast model in which fragments of the human Huntingtin protein are expressed [1]. Rapamycin had only a slight effect on the growth of both the strain expressing a slightly toxic fragment containing a 25Q repeat, and the strain expressing a toxic fragment containing a 72Q repeat. Each growth curve reflects average of 3 individual runs marked by bars.

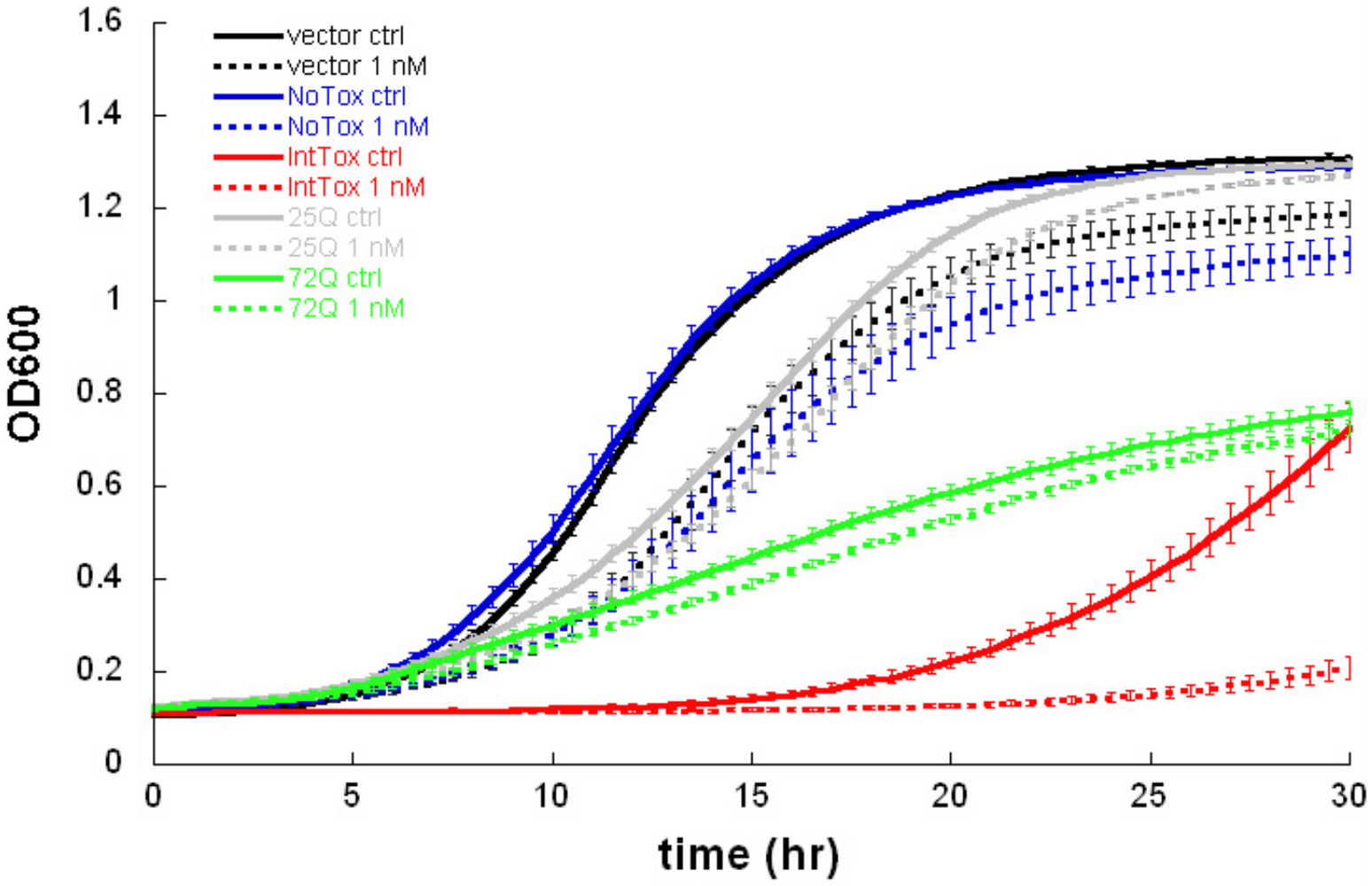

1. Duennwald, M.L., Jagadish, S., Muchowski, P.J. & Lindquist, S. Flanking sequences profoundly alter polyglutamine toxicity in yeast. *Proc Natl Acad Sci U S A* **103**, 11045-50 (2006).

Supplementary Figure 4. Cellular response to the DNA damaging agent Methyl Methanesulfonate (MMS). The predicted network connects 91 genetic hits whose deletion was found to be toxic in two independent screens [1,2] and nine differentially expressed genes defined as "DNA damage signature" genes[3]. MMS specific protein-DNA interactions were included in the input [4]. Due to the size of the input, the output is also considerably larger than the other networks we consider. The flow diagram contains 361 edges between 258 proteins. The predicted network contains 166 intermediate proteins and is highly enriched for response to DNA damage stimulus ($p<10^{-14}$) and DNA repair ($p<10^{-14}$). The node coloring implies the proteins importance in the response as determined by the algorithm, with increasing importance from grey to dark blue. Mec1, Rad53, Rfc2, Rfc3, Rfc4 and Rfc5 are essential genes and therefore could not have been detected via genetic screening of the deletion library.

1 Chang, M., Bellaoui, M., Boone, C. & Brown, G.W. A genome-wide screen for methyl methanesulfonate-sensitive mutants reveals genes required for S phase progression in the presence of DNA damage. *Proc Natl Acad Sci U S A* **99**, 16934-9 (2002).

2 Begley, T.J., Rosenbach, A.S., Ideker, T. & Samson, L.D. Hot spots for modulating toxicity identified by genomic phenotyping and localization mapping. *Mol Cell* **16**, 117-25 (2004).

3 Gasch, A.P. et al. Genomic expression responses to DNA-damaging agents and the regulatory role of the yeast ATR homolog Mec1p. *Mol Biol Cell* **12**, 2987-3003 (2001).

4 Workman, C.T. et al. A systems approach to mapping DNA damage response pathways. *Science* **312**, 1054-9 (2006).

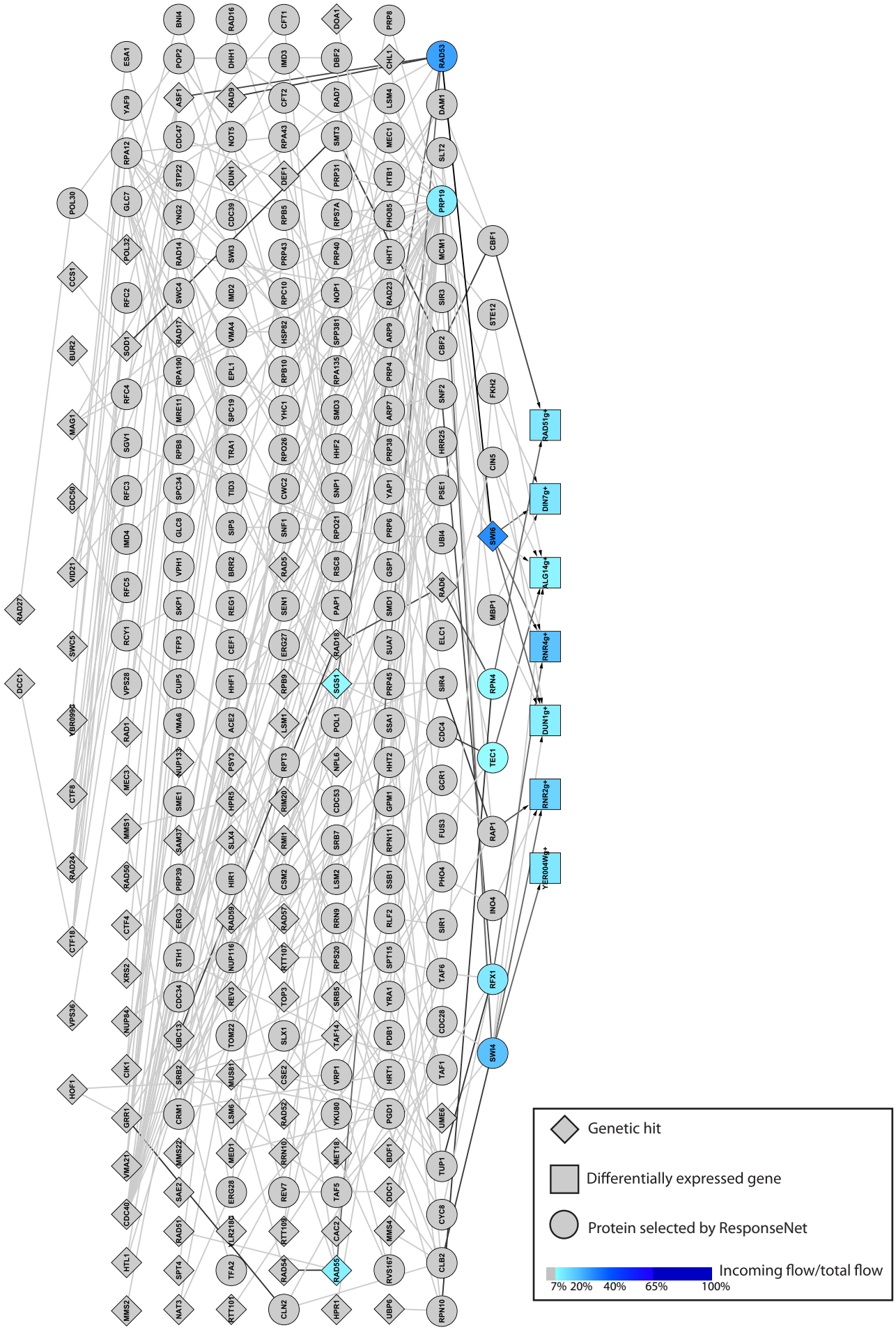

Nature Genetics: doi:10.1038/ng.337